ALTERATIONS IN TRIBOLOGIC BEHAVIOR OF CARTILAGE DURING TISSUE DEGENERATION AND REPAIR

A Dissertation

Presented to the Faculty of the Graduate School

of Cornell University

In Partial Fulfillment of the Requirements for the Degree of

Doctor of Philosophy

by

Natalie Katrina Galley

January 2012

EFFECT OF INJURY AND LUBRICATION ON NATIVE AND REPLACEMENT CARTILAGINOUS TISSUES

Natalie Katrina Galley, Ph.D.

Cornell University 2012

Osteoarthritis is the leading cause of disability in the United States, associated with joint pain and loss of mobility of an increasing proportion of the population. The disease erodes and disrupts the articular surface, which when healthy provides a low-friction, load-bearing, wear-resistant surface for articulation in joints. Osteoarthritis is most frequently idiopathic, but also results from traumatic joint injury. An understanding of the link between joint injury and the degeneration of articular cartilage and potential for protecting the articular surface depends on an understanding of both the biological and mechanical responsiveness of articular cartilage to injury. This thesis investigates this link, exploring the frictional behavior of articular cartilage and how it responds to mechanical and biochemical damage.

BIOGRAPHICAL SKETCH

Natalie was born and raised in Montreal, Quebec, Canada along with her twin sister Nikisha. She received a Bachelor of Engineering degree with distinction in Mechanical Engineering with an Arts minor in Sociology and Economics from McGill University in Montreal. She then completed a two-year Master of Applied Science degree in Aerospace Engineering from the University of Toronto's Institute for Aerospace Engineering in Toronto, Canada. Her experimental research focused on the flame structure of weakly turbulent premixed propane-air and methane-air flames.

In 2006 Natalie started her Ph.D. at Cornell University with the intention of continuing her experimental combustion studies. In her first semester she was convinced by her future academic adviser Larry Bonassar, Ph.D., that the field of Biomechanics was much more interesting and immediately applicable to the world around her and to making a scientific difference, and she continued her graduate research in the Musculoskeletal Tissue Engineering Lab. As a graduate student Natalie dedicated herself to the betterment of the Cornell community, acting as Vice President of the Sibley Graduates in Mechanical and Aerospace Engineering student organization, a trainer for the College of Engineering's Teaching Assistant Training Program, and as an active member of the Diversity Programs in Engineering program.

To my mom.

ACKNOWLEDGEMENTS

I would like to thank my mentor and advisor, Lawrence Bonassar, Ph.D., for his teaching and encouragement throughout my Ph.D. I am continually impressed by Larry's energy and love of science. Before meeting him, I had my future mapped out as aerospace engineer working for the Canadian Space Agency, or NASA. I certainly had no plans to do dissections or visit the vet school necropsy lab, but during the course of this degree I have grown in terms of knowledge, scientific insight, and lab ability, thanks to him. It's been an honor to learn from someone who is so excited and passionate about research.

I would also like to thank the other members of my advisory committee: Suzanne Maher, Ph.D. and Lara Estroff, Ph.D. Their expertise, advice, and wisdom solidified the research presented in this dissertation. I am very grateful for their time and enthusiasm.

I also had the opportunity to expand my scientific horizons by participating in scientific collaborations. Thank you to Alan Grodzinksy, Carl Flannery, Tim Wright, and Steve Doty. In particular I wish to acknowledge my co-authors Carl Flannery, Ph.D. and Alan Grodzinsky, Ph.D. who provided valuable insights and support during this research work. Thank you to also Vince Siu and Jenny Lin who as undergraduate researchers provided valuable input to this work.

I would also like to thank the other members of my lab with whom I've had the pleasure of working, both the old guard who of which I am the last to graduate, and the new generation who will continue on in the Bonassar lab. Thank you for all the help, and for the laughter. A big thank you to all the wonderful fellow engineers who I've met and befriended at Cornell; you know who you are and you know my experience here without you is something I wouldn't wish to contemplate.

Thank you Sri Puranam, for all your support and assistance. Completing our dissertations on opposite coasts has been hugely difficult, but for me impossible without you.

Thank you to my family, who has encouraged and supported me during this phase of my career, and through every step leading up to this. Special thanks to my mom: this is for you.

This research was primarily funded by the Quebec foundation for technological and scientific research, the Canadian National Science and Engineering Research Council, and the Coleman Foundation. Additional funding was provided by Wyeth and Pfizer Research, and Cornell University.

TABLE OF CONTENTS

LIST OF FIGURES

LIST OF TABLES

LIST OF ABBREVIATIONS

AFM	atomic force microscopy
ANOVA	analysis of variance
CACP	camptodactyly-Arthropathy-Coxa vara-Pericarditis syndrome
DMEM	Dulbecco's Modified Eagle's Medium
EC_{50}	half maximal effective concentration
ECM	extracellular matrix
ESEM	environmental scanning electron microscopy
ESF	equine synovial fluid
GAG	glycosaminoglycans
HA	hyaluronic acid
IL-1	interleukin-1
IL-6	interleukin-6
M	molar
μg/ml	microgram per milliliter
μm	micrometer
MMPs	matrix metalloproteinases
MPa	megapascal
OA	osteoarthritis
PBS	phosphate buffered saline
PRG4	proteoglycan 4
rh	recombinant human
SAPL	surface-active phospholipid
SF	synovial fluid
SZP	superficial zone protein
TNF-α	tumor necrosis factor alpha

LIST OF SYMBOLS

Symbol	Variable	Dimensions
°C degrees	Celsius	$L^2 M T^{-2}$
ε_N	compressive normal strain	---
E_Y	Young's modulus	$M L^{-1} T^{-2}$
H	Hersey number	---
H_A	aggregate modulus	$M L^{-1} T^{-2}$
k	hydraulic permeability	$L^3 T M^{-1}$
F_N	normal force	$M L T^{-2}$
F_t	shear force	$M L T^{-2}$
μ	friction coefficient	---
$\mu(t)$	instantaneous friction coefficient	---
μ_0	initial μ, $\mu(t \rightarrow 0)$	---
μ_{min}	minimum μ	---
μ_{eq}	equilibrium μ, $\mu(t \rightarrow \infty)$	---
P	mean pressure	$M L^{-1} T^{-2}$
Sa	average surface roughness	L
τ	relaxation time constant	T
σ	stress	$M L^{-1} T^{-2}$
σ_{eq}	equilibrium stress	$M L^{-1} T^{-2}$
v	surface speed	$L T^{-1}$
VN	load cell normal channel voltage	$M L T^{-2}$
VS	load cell shear channel voltage	$M L T^{-2}$

CHAPTER 1

1 INTRODUCTION

1.1 Articular Cartilage

Structure and function

Articular cartilage is a remarkably resilient tissue found at the articulating ends of long bones. The primary physiological function of cartilage is to provide a low friction interface that distributes compressive loads across joints. Ideally cartilage is able to withstand millions of cycles a year and a lifetime of use; however factors such as low cell density, a dense ECM, and limited vascularisation limit the tissue's regenerative capabilities.

Articular cartilage is characterized by a highly differentiated structural anisotropy; making up this structure are chondrocytes and a complex network of primarily collagen and proteoglycans that comprise the extracellular matrix (ECM). The tissue is highly hydrated and is composed of approximately 70% water, 25% ECM and 5% cells. By dry tissue weight the ECM is mainly proteoglycans and collagen, with aggrecan and type II collagen the most abundant components of each type, respectively. Proteoglycans consist of a large core protein with covalently bonded, sulfated glycosoaminoglycan (GAG) chains. Fibrils of type II collagen, the second most abundant ECM constituent, are covalently cross-linked by type IX collagen forming a collagen network within the tissue.

Adult articular cartilage consists of several zones: superficial, transitional, middle/deep and calcified (Figure 1.1). The properties of the superficial zone (typically 200-1000 nm thick) are of great importance for the weight bearing function of cartilage and its morphology and components influences the wear and lubrication mechanism[82] operating between the joint

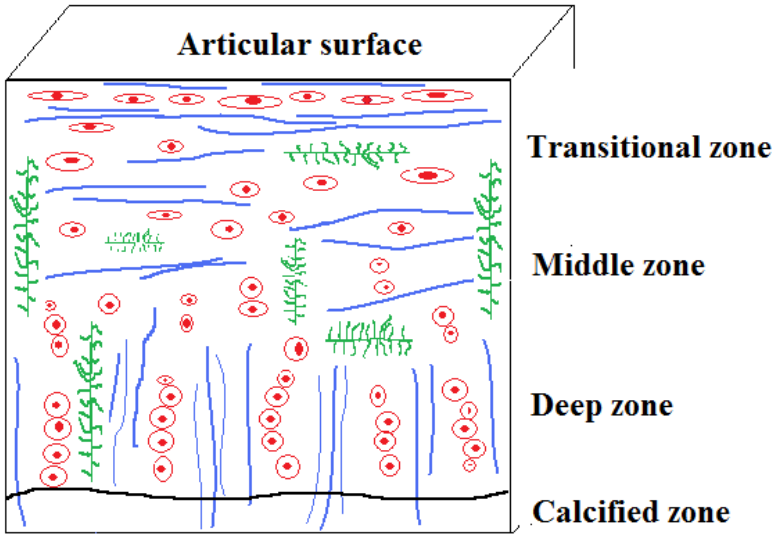

Figure 1.1 Schematic of cartilage structure. Note that components are not to scale; chondrocytes depicted in red, GAG in green and collagen fibers in blue.

surfaces. The chondrocytes found in the superficial zone produce fewer ECM macromolecules compared to deeper cells (which vary in organization and phenotype with depth from the articular surface[27]) but do produce lubricin, a protein which impacts the boundary lubrication properties of the cartilage[124].

Compression of the tissue causes pressurization of the interstitial fluid within the ECM. This pressure is dissipated as the fluid is exuded from the tissue, and reaches equilibrium on the order of 45 minutes[44], depending on sample size, health and magnitude of the applied compression. The hydraulic permeability, which describes the ease with which a pressure gradient can drive fluid through the tissue, governs the shift between fluid load support and matrix load support as fluid motion occurs, and governs resistance to compressive loads. The GAG chains in the ECM play a large role in controlling the tissue's compressive behavior. Electrostatic repulsion from the charged GAG chains reduces compaction of the tissue[15], and in the absence of a compressive force the chains produce an osmotoic pressure that helps rehydrate the tissue[29]. GAGs also provide the majority of resistance to flow and the ability of the tissue to pressurize. This interplay of pressurization and fluid flow affects the frictional response of the tissue, with a low initial coefficient of friction upon loading that increases as support from the pressurized fluid decreases[80].

Cartilage injury and disease

Osteoarthritis (OA) is the leading cause of disability in the United States according to the Centers for Disease Control and Prevention, associated with joint pain and loss of mobility of an increasing proportion of the population. The disease erodes and disrupts the articular surface, affecting its low-friction and wear-resistant function in joints. Osteoarthritis is most frequently idiopathic, initiated by unknown causes, but it may also result from traumatic joint injury. An

understanding of the link between joint injury and the degeneration of articular cartilage and potential for protecting the articular surface depends on an understanding of both the biological and mechanical responsiveness of articular cartilage to injury.

Numerous experiments have shown that joint injuries cause joint degeneration and posttraumatic OA,[13] but the mechanisms responsible for progressive loss of normal articular surfaces after joint injuries are not fully understood. Both in vivo and in vitro studies have examined the response of healthy cartilage to injurious compression. Biochemical changes that have been noted are drops in lubricin levels[30], proteoglycan synthesis[133], and cell viability[107] and increases in GAG loss[89]. Other changes include collagen denaturation[21, 132], increased water content[83], decreased stiffness[90] and cell apoptosis[132]. Acute joint trauma stimulates a release of cytokines including MMPs, IL-1, IL-6, and TNF-α[31, 87], which all influence chondrocyte metabolism.

Changes in cartilage's mechanical properties also occur due to injurious compression. These are due either to direct mechanical failure of the extracellular matrix, or to damage of the chondrocytes, whose subsequent response degrades the matrix over time. Mechanical changes studied to date are primarily variations in compressive and shear moduli[84].

The response of the articular surface in particular to impact loading is not clear. Recent evidence suggests that impact loading of healthy cartilage alone is not enough to cause surface damage[73], and that both injurious impact and subsequent articulating motion are necessary to create measurable roughening of the surface layer.

1.2 Friction of articular joints

Tribology

Friction is a force resisting the relative motion of solid surfaces and fluid layers, which acts opposite in direction to the relative tangential motion of the two surfaces and is modulated by their interactions. The frictional property of an interface is quantitatively measured by the friction coefficient μ, which defines the ratio of the resisting shear friction force to the normal force ($\mu = F_f / F_N$). This number is not a material property but rather depends on several variables in the specific interaction, including the surface materials, the lubricant used, and the operating conditions. Originally based on bearing friction experiments, the classic Stribeck curve shown as a representative sketch here, (Figure 1.2) provides a method for mapping out the various lubrication modes of a rotating journal bearing, relating μ to the Hersey number H, a non-dimensional number relating the lubricant viscosity η and shaft rotation speed ω to the mean pressure P[58]. This relationship is also applicable to the lubrication that occurs in synovial joints[48].

The boundary lubrication regime is characterized by a high degree of contact between the two surfaces and their asperities. The hydrodynamic effects of interposed lubricant do not significantly influence tribological characteristics and interactions in the contact between friction surfaces and between friction surfaces and the lubricant dominate tribological characteristics. Between these two opposing regimes is the mixed lubrication regime. It is characterized by partial contact between the asperities on the two surfaces and the applied load is supported by both direct asperity contact and the hydrodynamic pressure forces in the lubricant film. As the Hersey number increases, μ in fact decreases. Any of this range of lubrication mechanisms may operate in a healthy joint.

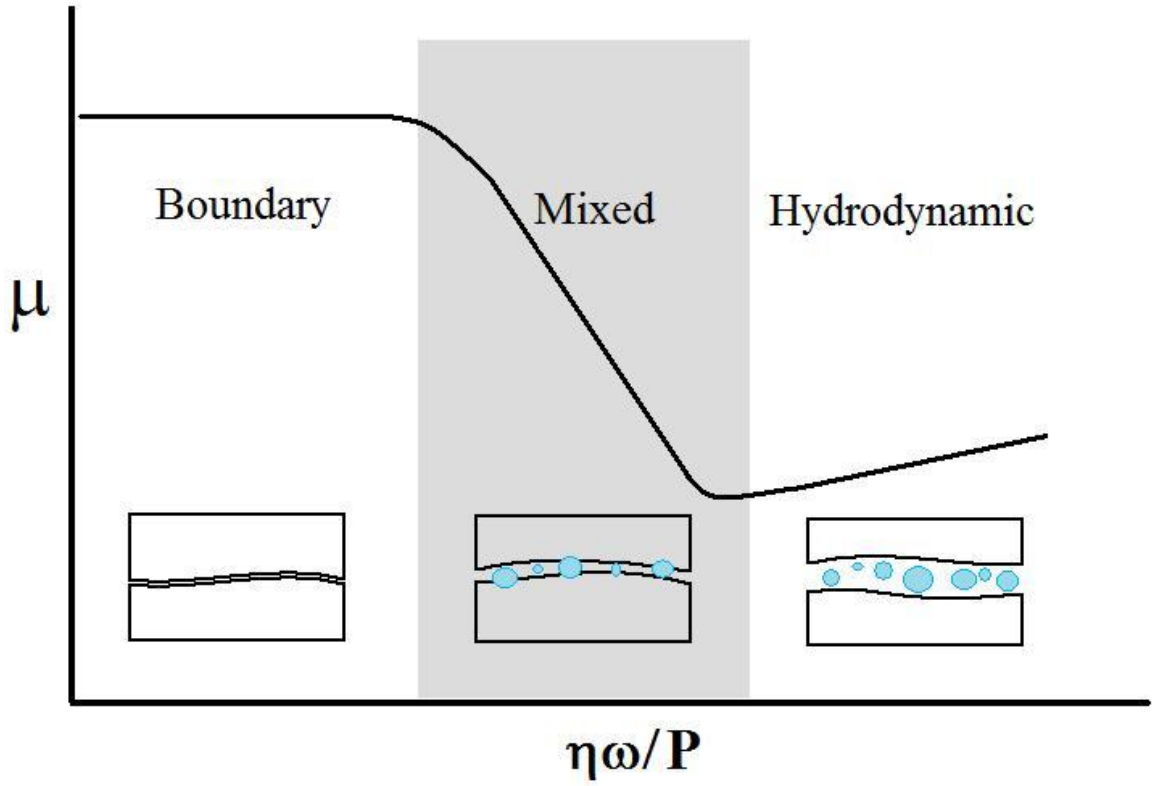

Figure 1.2 Stribeck curve sketch relating friction coefficient μ behavior to the Hersey number, a non-dimensional expression of viscosity η, speed ω, and mean contact pressure (P). The three lubrication modes, boundary, mixed, and hydrodynamic, are related to the asperity-asperity interaction and fluid separation of the two surfaces.

Joint lubrication

Articular cartilage undergoes biphasic lubrication due to fluid pressurization which has a time-history[44] and a strain rate dependence. Immediately following load application lubrication is dominated by tissue pressurization with little variation in μ. Under a constant load fluid leaks from the porous tissue, causing a gradual increase in μ with time that reaches an equilibrium maximum value (μeq) when the fluid motion has stopped. When relaxation of fluid pressurization occurs, lubrication mode is more sensitive to the operating parameters with alterations to strain or speed modulating μ differently.

The superficial zone is responsible for articular cartilage's low coefficient of friction (μ)[53]. There is little agreement on the value of μ for healthy cartilage with reported measurements that vary from 0.003[82] up to 0.3[48].

Cartilage friction measurements, like measurements of traditional tribological surfaces, are complicated by being load and velocity-dependent, as well as being time-dependent[48]. Classic tribology theory divides lubricated surface friction into three distinct lubrication modes where each regime is characterized by the degree of contact between the two solid surfaces.

Boundary vs. hydrodynamic lubrication

When slow speeds and high contact forces exist, the result is boundary mode friction, in which μ and thus potential for damage and wear are highest. Boundary lubricants are substances that lubricate tribological systems during boundary mode friction by lowering the friction coefficient. Boundary mode friction is a type of friction that occurs in both artificial and biological lubrication systems and is primarily characterized by three elements: the articulating surfaces are in contact at asperities, tribological characteristics are not significantly affected by the bulk hydrodynamic effects of the interposed lubricating fluid, and tribological characteristics

are dominated by interactions between the articulating surfaces and between the articulating surfaces and the lubricant.

In boundary lubrication any fluid film between the friction surfaces that is thinner than the substrates' surface roughness and solid-solid contact occurs across the surface. The surfaces contact each other over discontinuous asperities, and the load is supported by this small area. If a lubricant is present, frictional properties are determined by lubricant surface molecules.

In fluid-mediated hydrostatic lubrication mode the interstitial fluid within cartilage becomes pressurized due to the biphasic nature of the tissue. Fluid may also be forced into the asperities between articular surfaces through the porous tissue. Pressurized interstitial fluid and trapped lubricant pools may therefore contribute significantly to the bearing of normal load with little resistance to shear force, facilitating a very low μ.

In boundary friction, fluid support is dissipated and the bulk properties of the fluid no longer play a role. Boundary mode interaction produces the highest μ of any mode of lubrication[109], for example in one study boundary μ of bovine cartilage was up to triple the values for μ for mixed mode[48]. High μ indicates the maximum potential to cause wear and transfer high shear stresses to the articular cartilage and so is associated with greater wear and degradation.

Since articular cartilage only comes into contact over about 10% of the surfaces, solid to solid contact is quite critical in determining friction forces. Boundary lubricants act by adhering to the solid surfaces and repelling them to reduce boundary μ. This effect can be quite marked; values of $\mu \sim 0.3$ in the absence of a boundary lubricant drop to $\mu < 0.05$ under the same conditions when lubricated by synovial fluid[48].

Boundary mode-producing conditions

Boundary mode lubrication is indicated by values of μ during motion being invariant with factors that influence formation of a fluid film, such as relative sliding velocity and axial load. This invariability is visible in Figure 1.2; the flat region of maximal μ occurs over a range of cartilage strains and relative surface speeds as it does for other tribological surfaces. Additionally, as time under load increases, μ increases[44] as the hydrostatic pressure of boundary lubricant-coated surfaces dissipates and the surfaces bear an increasingly higher portion of the load relative to pressurized fluid. Boundary lubrication therefore occurs as decreased resistance both to steady motion and the start-up of motion, which in vivo corresponds to load bearing articulating surfaces after prolonged compressive loading during sitting or standing. Experimentally, boundary mode μ can be measured after the compressed tissue has reached equilibrium, μeq.

The operative lubrication modes occurring in synovial joints depend on the normal and tangential forces on the articulating tissues, on the relative rate of tangential motion between these surfaces, and on the time history of both loading and motion[44, 45]. Determining which conditions result in boundary mode friction is obfuscated by the complexity and number of the variables involved. Time under loading, species, tissue type and disease state create a large sample space to be tested. Furthermore for true boundary mode lubrication to occur, fluid equilibrium within the tissue is a necessary but not sufficient condition. In Figure 1.2, the region marked “Mixed” indicates μ values measured at equilibrium conditions with zero net fluid flow, yet is in the mixed lubrication regime. Invariant μ values over several conditions is necessary to ensure boundary mode conditions.

Pinpointing boundary mode producing conditions is further complicated by the variety of friction testing devices currently in use. These systems vary in basic structure, including whole joint and explanted sample systems, motion type (rotational, linearly oscillating, linearly translating), surfaces used (cartilage on cartilage, cartilage on idealized substrate) and lubricants and species tested in addition to tunable operating parameters such as velocity and contact pressure. As a result the reported values of boundary mode friction coefficient can vary widely and may or may not indeed be true boundary mode friction values. Some of μeq values reported in the current literature are reported in Table 1.

The μ value of whole knee joints is determined in the Jay group by centering the excised joint as the fulcrum of a pendulum with tibial end supported at 45° and the femoral end supporting a hanging pendulum. The pendulum is manually deflected to an angle then released while a camera records the motion of the joint until motions stops. The amplitude deflected by the pendulum is plotted and μ calculated by measuring deceleration of the pendulum from the images. This is a very different approach from the Guilak group where friction is measured by AFM, tracking the lateral deflection signal of the AFM probe as it scans over the surface in contact mode. In the Sah group, a cartilage-on-cartilage system is used. A sample core and annulus are placed in apposition, compressed axially, and subjected to relative rotation in an EnduraTEC machine with customizable parts including internal sensors for axial displacement, axial load (N) and torque (t). Testing is rotational in one direction and then the other.

Several sliding instruments are currently is use. In the Ateshian group sliding motion is provided by a translation stage while normal and frictional loads were measured with a multi-axial load cell. The friction measurements are performed in unconfined compression with continuous reciprocal sliding of 4 mm with the surfaces immersed in lubricant at room

Reference	Contact surfaces	Lubricant	μeq
Schmidt et al.[114]	Cartilage-cartilage	PBS	0.1-0.4
Schmidt et al.[114]	Cartilage-cartilage	Bovine SF	0.01-0.19
Basalo et al.[5]	Cartilage-glass	PBS	0.12
Forster and Fisher[44]	Cartilage-metal	Bovine SF	0.3
Elsaid et al.[34]	Whole joint	Human SF	0.01
Elsaid et al.[34]	Whole joint	Saline	0.09
Coles et al.[23]	Cartilage-AFM tip	N/A	0.25
Gleghorn and Bonassar[48]	Cartilage-glass	PBS	0.28
Gleghorn and Bonassar[48]	Cartilage-glass	Equine SF	0.10

Table 1 Example equilibrium friction coefficient values of various triobometers currently in use.

temperature. Measurements taken at near equilibrium approximately 2,500 seconds after loading. In the Fisher group friction is measured on a sliding-friction machine using a flat metal counterface in a bath of lubricant which is slid in one direction at a constant speed. The cartilage specimen is loaded on to the counterface while secured to one end of a balanced loading arm, pivoted at a fulcrum on an air bearing on the other end of which a piezoelectric force transducer records the frictional force (N). Displacement of the metal counterface is monitored by a linear variable differential transducer to give μ.

The sliding friction instrument of the Bonassar group used in the studies in this thesis provides sliding motion by a translation stage while normal and frictional loads were measured with a load cell. Normal strain imposed on cartilage plug which is against a smooth glass counterface. The friction measurements are performed in unconfined compression with continuous reciprocal sliding over multiples of the cartilage diameter with the surfaces immersed in lubricant at room temperature. The components of this tribometer include: A translational stage: which holds liquid wells containing lubricating fluid and provides controlled relative motion between the surfaces; multi axial load cells that apply strain to the cartilage samples and read the resulting voltage in shear and normal channels; a signal conditioning unit that inputs the excitation voltage and processes and interprets the difference in the resulting signal, and a computer that drives the translational stage, reads the voltage output from the signal conditioning unit, and records the voltage data that in transformed into forces in post-processing. This instrument is shown in Figure 1.3.

Figure 1.3 Bonassar lab tribometer used in these studies, described in detail in Gleghorn et al. 2006[50].

1.3 Naturally occurring synovial lubricants

Synovial fluid

Synovial fluid (SF) is a viscous boundary lubricant used as a positive control in many experiments and is the most effective natural substance for lowering boundary μ in synovial joints. Two key lubricating components of SF are hyaluronic acid (HA) and lubricin. The viscosity of SF is several orders of magnitude higher than that of water under high shear[3] which is thought to play a large role in its lubricating abilities.

The source of boundary lubrication of articular cartilage has long been debated. The presence of hyaluronic acid, alias hyaluronan, in synovial fluid in comparatively high concentrations (2–4 mg/ml and molecular weight 6–7 X 10^6 Da in normal human fluid[26]) gave rise to the belief that HA plays a major role in boundary lubrication[93]. Earlier models considered HA as the predominant articular boundary lubricant but subsequent studies showed that HA affected the viscosity of the synovial fluid but showed insignificant cartilage boundary lubrication[66].

A form of therapy using HA, viscosupplementation, has been used to treat OA of the knee. It involves the replenishment of the synovial fluid via intra-articular injections of HA. Altered properties of synovial fluid in injured joints contribute to the progression of joint destruction and the aim of HA supplementation is to generate increases in the molecular weight and concentration of endogenous HA, thereby increasing the viscosity of the synovial fluid and improving joint function. This treatment has not met with success; although patients receiving this treatment had reduced pain, the effect was no greater than that of a placebo[10].

High molecular weight HA is viscoelastic, i.e., it behaves as a viscous liquid at low shear rates and as an elastic solid at high shear rates. In OA, the concentration and molecular weight of SF HA are reduced and the viscoelastic properties of the fluid are compromised[26]. A larger

molecular weight HA in synovial fluid increases its bulk viscosity which enhances hydrodynamic modes of lubrication. Thus the rationale for use of intra-articular injection of HA in treatment of OA developed; healthy HA presumably supplements the activities of the endogenous HA by increasing its molecular weight and quantity, and thus restores the viscoelasticy of the synovial fluid and reduces joint pain in patients.

Various HA-based viscosupplements have been developed and used clinically to augment the diminished biologic and mechanical properties of diseased synovial fluid. For example Healon (Pharmacia & Upjohn, Kalamazoo, MI) was used in equine and briefly in human arthritic treatments, followed by various other preparations with higher molecular weight designed to increase the residence time in the joint. These treatments did not prove to be clinically useful, however. Although several clinical trials indicated that intra-articular injection of HA resulted in relief of joint pain lasting up to several months in patients with knee OA, similar results were seen with joint aspiration and even a simple needle prick[9, 77]. HA treatments are still available commercially.

Lubricin

The synovial fluid constituent responsible for articular cartilage's boundary lubrication properties is lubricin[122]. Lubricin is a glycoprotein, first isolated by Swann in the 1970s[124]. It appears in the body in a wide range of tissues including in synovial membrane[116], meniscus[117], ligament[120], tendon[105], IVD[118], lung, liver, heart, and bone[59]. Lubricin has also been observed to lubricate a variety of bearings in the boundary mode regime as effectively as synovial fluid, from latex–glass to cartilage–cartilage[69, 108, 113, 121, 123, 138]. In addition to its boundary lubricating ability, lubricin also inhibits synovial cell overgrowth[108], and integrative cartilage repair[35], and prevents cartilage wear and cell adhesion[108].

In articular cartilage, lubricin is synthesized and secreted by chondrocytes within the superficial layer[41, 115] and by synoviocytes[39, 61]. Lubricin is secreted into and abundant within synovial fluid, and is largely localized to the articular surface[52] which contrasts with other large cartilage matrix molecules (e.g. collagen) that are retained throughout the cartilage extracellular matrix; lubricin fails to bind to cartilage deeper than the superficial zone.

Lubricin was originally isolated from synovial fluid[123, 124] and is encoded by the gene proteoglycan 4 (PRG4)[41, 59]. By comparing lubricin with megakaryocyte stimulating factor (MSF), lubricin was found to be a product of MSF gene expression by human synovial fibroblasts[63]. Lubricin was also shown to be homologous with superficial zone protein (SZP), which is specifically synthesized by superficial zone chondrocytes[115]. Failure to secrete lubricin causes camptodactyly-arthropathy-coxa vara-pericarditis syndrome (CACP)[92]. These various products, PRG4, MSF, CACP protein and SZP are collectively referred to as lubricin. The various physical and biological abilities of lubricin result from its multiple functional domains, Figure 1.4. Human lubricin has a molecular weight of 280 kDa and is composed of globular cysteine-rich protein domains occurring at the vitronectin-like N terminal and the hemopexin-like C terminal with a long central mucin-like domain that is extensively glycosylated by O-linked β(1–3)Gal-GalNAc oligosaccharides[67]. The N terminal is believed to play a role in aggregation, and the C terminal in surface binding[41, 72]. This characteristic is a critical property of a boundary lubricant[121], when the contacting surfaces are under high force yet must remain adhered to the surface. The central hydrophilic mucin-like domain carries most of the negative charges of the protein. In composition lubricin is similar to that of mucins that lubricate and protect many surfaces in the human body, including teeth, eyelids, and the gastrointestinal tract.

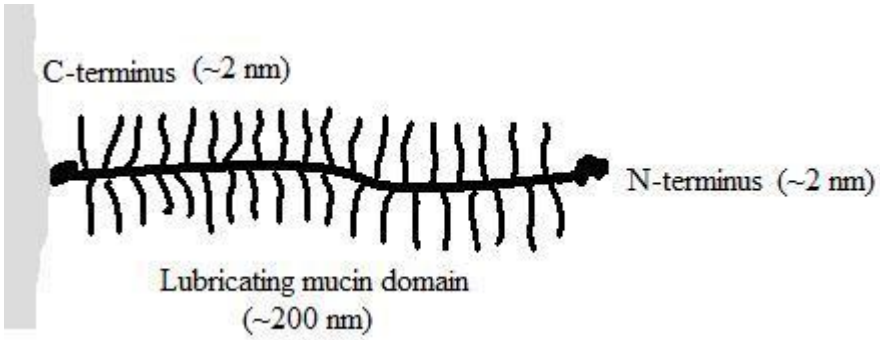

Figure 1.4 Schematic of lubricin structure (not to scale) with functional lubricating and binding domains shown.

The central mucin domain is responsible for the boundary lubrication properties of the protein[67]. The repulsive force the proteins exert between the solid surfaces is due to the charged brush form of the molecule that is cleaved to the substrate at one end. This force is mainly steric[138]; the flexible proteins tend to coil randomly when brought into contact the adsorbed brush layers entropically repel each other by resisting the confinement that reduces the number of conformations. The presence of a long, flexible, and hydrated portion in the structure of this molecule plays a central role in determining its lubricating capability. Its efficiency as a boundary lubricant is due to this and other varied physical and chemical interactions. Lubricin's ability to bind to substrates is strong[138] and it must be to ensure stable adsorption and to prevent the molecules from becoming detached and squeezed out from between the substrates or cartilage surfaces by compression and shear forces. This trait is not true of HA; HA is quickly expelled from solid surfaces under modest pressures and shear forces[125]. As a result, HA fails to lubricate under the conditions where lubricin acts as a good lubricant.

The engineering of an effective therapeutic agent for the treatment of cartilage deterioration in OA is a major unmet medical challenge. After the failure of HA as an intra-articular injection agent, research has now turned to lubricin as a potential curative.

Although HA alone is not an effective boundary lubricant, recent reports indicate a beneficial synergy between lubricin and HA with respect to boundary lubrication. In a cartilage on cartilage friction testing system Schmidt et al. found that lubricin and HA in combination produced a greater boundary-lubricating effect than either constituent alone[113], Jay et al[69] demonstrated that lubricin can interact with SF HA to enhance its chondroprotective properties by dissipating of shear-induced energy and Wong et al. determined that HA supplementation of SF can modulate

cartilage shear after acute injury[137]. Further evaluation of the therapeutic potential of lubricin and HA in a combined formulation may therefore be warranted.

Regulators of boundary lubricants

Boundary lubricants are influenced by both biochemical and physical factors. Various biological factors involved in maintaining fluid film and boundary lubrication characteristics include morphogenic proteins, growth factors, and cytokines.

Bone morphogenetic proteins (BMPs) are a family of morphogens that promote, initiate, and maintain new cartilage and bone growth[104]. Studies have shown that BMP-7 and other growth factors can synergistically promote increased survival and matrix synthesis by normal and osteoarthritic human articular chondrocytes. In particular, BMP-7 stimulates the accumulation of lubricin in explant cultures of bovine superficial zone cartilage[20].

Other growth factors, such as transforming growth factor-β (TGF-β), basic fibroblast growth factor, insulin-like growth factor, and platelet-derived growth factor, have all been shown to be anabolic for cartilage and chondrocytes. TGF-β enhances accumulation of SZP in bovine cartilage and is dose dependent and biphasic[99] and results in a decrease in μeq[51]. SZP expression can be down-regulated by treatment with interleukin-1α[41] and IL-1β increases the equilibrium boundary mode friction value[51]. IL-1α promotes cartilage matrix degradation by enhancing the expression of matrix metalloproteinases (MMPs). IL-1α co-localizes with MMPs in the superficial layer of arthritic cartilage, illustrating the key role of this layer in the development of disease[129].

Interestingly, the boundary-lubricating effect of surface-bound lubricin is independent of compositional ECM changes resulting from short-term exposure to TGFβ, IL-1β, or OSM, and synovial fluid is able to recover and enhance boundary lubrication of cytokine treated cartilage[51].

Mechanical factors play an important role in regulating boundary lubricants as well. Compressive cartilage injury is a well known precursor to osteoarthritis; injurious cartilage compression induces GAG loss[90], decreases proteoglycan synthesis[132] and cell viability[106], upregulates MMP-3, ADAMTS-5, and TIMP-1, and reduces biosynthesis[83, 87].

Injury is also a regulator of boundary lubrication ability. Following injury lubricin is lost from the articular surface corresponding to an increase in boundary μ[70]. Also, cartilage injury is known to damage the cartilage surface and induce tissue fibrillation,[83] which is the initial degenerative changes in osteoarthritis.

The extent of mechanical injury has been shown to depend on several loading variables, including peak stress[101], peak strain[83], and strain rate[83, 101]. In vitro, surface damage depends on both compressive impact loading and subsequent sliding motion; these factors together contribute to cartilage surface degradation[70].

Chondroprotection of injured cartilage is currently being investigated. Either the presence of synovial fluid or lubricin are effective at protecting injured cartilage surface from degradation, while saline is not. There are mixed results on whether HA can provide any chondroprotection through interaction with lubricin. In an in vitro model, HA plus lubricin did not lessen damage to the cartilage surface[46] while in an in vivo rat model it did[126].

Changes in synovial joints following injury

Injury is a regulator of boundary lubrication ability, compromising the ability of lubricin to act effectively. Following injury there is loss of lubricin from the articular surface and a corresponding increase in boundary μ[70]. This has been shown in both animal and clinical studies. In a rabbit model where the anterior and posterior cruciate ligaments were transected investigators determined a significant decrease in both lubricin concentration and lubricating

ability of aspirated synovial fluid at two and three weeks following injury[34]. At three weeks lubricin had dropped precipitously from a nominal 280 μg/ml to 20-110 μg/ml.

In this same study synovial fluid aspirates from emergency room patients was tested for lubricating ability. The SF from injured patients exhibited a large variation in lubricating ability compared with SF from normal patients and its overall friction value was significantly higher than for the healthy control group. This reflects the results of another emergency room observational study where only 1 in 5 injured patients possessed synovial fluid that lubricated normally[64].

Application of boundary lubricants to injured joints

Understanding the mechanical implications of lubricin in boundary mode friction is an important consideration for both creating functional tissue engineered cartilage with appropriate low friction, low wear properties and to develop potential therapeutic interventions to recreate the low friction properties of articular cartilage.

Another avenue of therapeutically relevant research is engineering cartilaginous tissue replacements. Efforts to regenerate or engineer joint tissues have traditionally focused on producing constructs with similar compressive or tensile properties[40, 78, 86] with only recent attempts to construct tissues with proper frictional properties. These studies focus on the production and localization of boundary lubricants to the engineered surface[70], although the mechanisms by which this occurs is still largely unknown.

One such engineering research avenue is a biomimetic approach, manipulating subpopulations of chondrocytes to fabricate constructs that exhibit stratified features of normal articular cartilage[79]. In addition to replicating the heterogeneous organization of native tissue, this type of engineered tissue can be manipulated to show phenotypic zonal characteristics of

articular cartilage, such as lubrication at the surface. Sah et al. showed that cartilaginous constructs formed from superficial zone chondrocytes exhibited less matrix growth and lower compressive properties than constructs from middle zone chondrocytes, with the stratified superficial-middle constructs exhibiting intermediate properties. Expression of lubricin was highest at the construct surfaces, with the localization of lubricin in superficial-middle constructs being concentrated at the superficial surface.

Jay et al. investigated whether cartilage degeneration was prevented or minimized following intra-articular injections of lubricin derived from human synoviocytes in culture, recombinant human lubricin, or human SF in a rat model of unilateral anterior cruciate ligament injury[65]. Intra-articular injections of 200 g/ml were given twice weekly beginning a week after injury for three and a half weeks total.

After treatment with any of the three types of lubricin, a reduction in cartilage damage following ACL transection was evident by significantly lowered OARSI scores for cartilage degeneration compared with no treatment or PBS treatment. This effect indicates that intra-articular lubricin injection following an ACL injury may be beneficial in retarding the degeneration of cartilage and the development of posttraumatic OA.

Similarly encouraging results are reported by Flannery et al., where injections of recombinant human lubricin inhibited development of mechanically induced lesions in a different model[40]. In this rat model the medial collateral ligament and medial meniscus were transected. Intra-articular treatment again was initiated one week after surgery, with a 500 mg/ml dose three times a week for 4 consecutive weeks. Several chondroprotective effects were seen during the disease progression, quantified by decreases in measured lesion size and other reduced cartilage degeneration and structural damage measures.

These independent studies demonstrate that local administration of lubricin is therapeutically effective in preventing cartilage degeneration during the progression of OA. Several questions remain about the dosing, efficacy, and mechanism of intra-articular lubricin injection and are currently active areas of research.

1.4 Research Objectives

The exact pathway by which injured cartilage develops osteoarthritis is still largely unknown, as is the potential and mechanism by which healthy lubricin can prevent this degeneration. Patients experiencing traumatic joint injury have damaged cartilage that eventually loses its tribological function. One of the critical pathologies that occurs in the affected joint is the synovial fluid has lost its boundary lubricating properties, key to chondroprotection. Restoration of this ability by reintroduction of lubricin may be crucial in preventing this loss of function. What our current understanding of cartilage lubrication lacks is a clear link between the mechanical structure of injured cartilage and its lubrication.

The overall objective of this dissertation therefore is to investigate lubricin as a mediator of healthy and damaged articular cartilage boundary mode frictional properties. The central hypothesis of this dissertation is that changes to the articular surface, particularly damage caused by mechanical injury, has a deleterious effect on surface integrity and friction coefficient and this effect can be palliated by the presence of lubricin. Testing this hypothesis begins with an in vitro study wherein we examined the necessary mechanical loading that causes changes in articular cartilage surface integrity and lubrication. We then looked at the effect of exogenous lubricin on preventing these changes. Once we established the efficacy of lubricin in vitro we examined the effect on the same parameters of its introduction to an injured joint in vivo. We then investigated the effect of chemical damage on friction behavior and how this would affect the frictional

performance of injured joints, and finally the frictional performance of an engineered implant designed to repair injured tissue.

Specific Aims

SPECIFIC AIM 1 (CHAPTER 2)

To test the hypothesis that injurious compression initiates mechanical, degradative surface damage to articular cartilage that can be modified by lubricin in vitro.

We determined that varying the strain rate of mechanical injury affected the friction coefficient and surface roughness of articular cartilage by injuring neonatal bovine cartilage explants and varying the strain rate of applied unconfined injurious compression. The injured tissue was then friction tested in four different lubricant baths of either phosphate buffered saline (zero added boundary lubricant), recombinant human lubricin, commercially available hyaluronic acid and equine synovial fluid. ESEM and profilometry subsequently showed focal macroscopic damage to the injured cartilage surfaces that increased with strain rate. These increases were prevented by the presence of lubricin, but not HA, and did so in a lubricin dose-dependent manner. This aim showed that the combination of cartilage impact joined with articulating motion in the absence of a boundary lubricant together are necessary to start cartilage surface fibrillation and subsequently the development of OA, a purely mechanical and a short time-range phenomenon. This damage response has a threshold of impact dependant on strain rate and could be mitigated by the presence of lubricin but not HA.

SPECIFIC AIM 2 (CHAPTER 3)

To test the hypothesis that joint injury initiates mechanical, degradative surface damage to articular cartilage that can be modified by lubricin in vivo.

In this aim we extended our in vitro study of cartilage injury to an in vivo rat model. We determined that the cartilage damage initiated by joint injury can be modified by intra-articular lubricin injection. The right knees of Lewis rats were injured by transecting the medial collateral ligament and medial meniscus. Animals that received thrice weekly injections of a lubricin mutant, LUB:1, for two weeks following a week of post-operative recovery had cartilage with boundary friction values on par with that of healthy cartilage. This effect contrasted to untreated animals that had much higher coefficients of friction at one and three weeks following the surgery. LUB:1 injection also had a chondroprotective effect, reducing the incidence of roughened areas of cartilage occurring in the treated joints to a third those of untreated. In this aim we determined that intra-articular injection of lubricin was chondroprotective in an in vivo rat model

SPECIFIC AIM 3 (CHAPTER 4)

To determine if cartilage friction behavior is affected by the mechanical and biochemical changes caused to the surface layer of damaged cartilage.

We used enzymatic digestion to simulate biochemical damage to the surface layer of cartilage that follows joint injury and is part of OA progress. We extracted lubricin from the surface of healthy cartilage, and then exposed the surfaces to trypsin solution in order to digest GAG from the top down. Increased trypsin exposure caused greater GAG depletion, which had

an increasing effect on friction behavior. This effect was not to shift the value of the maximum friction coefficient, but rather the fraction of time that cartilage experiencing physiologically relevant tribological conditions will be in the boundary mode. A depleted surface layer of approximately 100 μm corresponded to a large shift in the size of the cartilage boundary mode. We propose that this shift is due to the increased permeability of the damaged surface layer which makes it harder for the cartilage to support a protective fluid surface layer and hence more easy to transition into boundary mode. This aim focused on linking a biochemically caused alteration in cartilage to a fundamental shift in its functional tribological behavior.

SPECIFIC AIM 4 (CHAPTER 5)

To test whether the presence of lubricin in an injured tissue repair model can improve frictional properties of an engineered meniscal tissue over time.

The frictional behavior of an engineered meniscal tissue was characterized in vivo. Porous polyurethane scaffolds were implanted into surgically created defects in ovine menisci and then evaluated for frictional and mechanical properties over the course of a year. Both boundary and mixed mode friction behavior changed with implantation time, dropping from high values to the lower ones of native tissue. This effect corresponded to increasing tissue ingrowth with time which also corresponded to increases in modulus and decreases in permeability as the implanted scaffold became more meniscus-like. We propose that the friction changes are due to improved mechanical properties of the scaffold which more easily support a protective hydrodynamic surface fluid layer, and to the ability of the meniscal surface to localize coefficient of friction lowering lubricin.

CHAPTER 2

2 IDENTIFICATION OF A NOVEL MECHANICAL MECHANISM OF ARTICULAR CARTILAGE SURFACE DAMAGE AND ITS INHIBITION BY BOUNDARY LUBRICANTS[1]

2.1 ABSTRACT

Traumatic injury inevitably predisposes the affected joint to the development of osteoarthritis within fifteen years. The pathway leading from mechanical insult to disease state is complicated, multifactorial, and includes biochemical and mechanical changes. A classic hallmark of arthritis is fibrillation of collagen at the articular surface, although it is unclear whether such fibrillation results from mechanical disruption, enzymatic activity or a combination of both. Here we present a strictly mechanical mechanism of cartilage fibrillation and osteoarthritis initiation following joint injury. We show that cartilage fibrillation requires a combination of three distinct mechanical events: impact loading at high strain rates, subsequent sliding motion, and the lack of boundary lubricant, all of which are present after traumatic joint injury. Loading at strain rates greater than 50%/s increased the friction coefficient and induced surface roughening. These changes were inhibited by the presence of lubricin or healthy synovial

[1] To be submitted to the Proceedings of the National Academy of Science with author list: NK Galley (Cornell), S Chen (MIT), EH Frank (MIT), CR Flannery (Pfizer Research), AJ Grodzinsky (MIT), LJ Bonassar (Cornell)

fluid during testing. Our results also suggest that any chondroprotective effect of hyaluronic acid requires interaction with lubricin. The identification of a purely mechanical mechanism for induction of cartilage fibrillation has implications both for the design of physical therapy regimens and the therapeutic use of boundary lubricants to inhibit the initiation and progression of arthritis in the aftermath of traumatic joint injury.

2.2 INTRODUCTION

The complex disease pathway of osteoarthritis (OA) involves multiple biochemical and biomechanical factors[83, 90, 106, 132] whose effects and interactions are not fully understood. OA is characterized by the degeneration of articular cartilage and subsequent matrix fibrillation, lesions and cartilage erosion. One known initiating mechanical factor is joint injury; traumatic insult to an otherwise healthy joint results in an increased risk of OA development in the following fifteen years[110]. The events immediately following such a joint injury are crucial, as surgical interventions to restore joint stability do not reduce the risk of developing post-traumatic OA[38].

The many changes following joint injury are both short-term and long-term in nature. Short-term, injurious loading causes a number of biochemical changes including glycosoaminoglycan loss[28, 102], collagen denaturation[21, 132], increased water content[83], decreased stiffness[90], cell apoptosis[132], upregulation of various cytokines[31, 87] and a lack of lubrication[32]. Changes in joint alignment cause long-term alterations in loading patterns[88, 111], and damage markers in the form of proteoglycan and collagen fragments can persist at elevated concentrations in synovial fluid for decades following the injury [91].

To explore the link between traumatic joint injury and OA in vitro applications of injurious compression have been developed[85]. These models cover a range of loading conditions and include both single loading events[83, 101, 102, 132] as well as cyclic loading[21] and have shown that

cartilage injurious compression causes a number of biochemical changes that include glycosaminoglycan (GAG) loss[102], collagen denaturation[21], and cell death by apoptosis and necrosis[21, 90, 132]. The pattern of loading modulates injury, including peak stress[37], peak strain[83], and strain rate[83, 101]. Mechanically, a single injurious impact decreases stiffness[83] and increases the friction coefficient,[70] which is a property that largely depends on surface characteristics. The surface of healthy articular cartilage has a smooth, well-lubricated appearance and gives the tissue an extremely low coefficient of friction, which is crucial for its long-wearing capabilities. Normal joints exhibit very little friction even when highly loaded; five times body weight has been measured across the human hip joint[95].

Lubrication of synovial joints under high load with near-zero sliding speed (boundary mode lubrication) requires lubricants to lower the adhesion energy between apposed semi-flattened cartilage asperities. The synovial fluid component responsible for this is lubricin, a multidomain glycoprotein that is a product of the PRG4 gene. Lubricin is expressed and secreted by superficial zone chondrocytes and synoviocytes[41, 115] and is homologous to molecules also referred to as superficial zone protein, megakaryocyte-stimulating factor precursor, camptodactyly-arthropathy–coxa vara–pericarditis (CACP) protein, and PRG4[41, 59, 68, 92, 115]. Lubricin can lubricate both biological and non-biological surfaces and has been localized to the surface of multiple tissues, including meniscus, ligament, tendon and the IVD[105, 117, 118, 120] where it acts as a boundary lubricant and deters cellular adhesion[108]. Immediately following injurious impact lubricin synthesis is upregulate[70], although anomalously levels of lubricin in synovial fluid decline after injury[136]. In multiple rat OA models of injury by soft tissue transection intra-articular lubricin injection has prevented cartilage degeneration measured histologically and by degeneration scores[40, 128].

Hyaluronic acid (HA), another primary synovial fluid component, has been prescribed for more than twenty years as a therapeutic intra-articularly injected lubricant in the treatment of OA. Viscosupplementation by various HA products have been used for the treatment of knee OA-related pain for patients, but there is considerable debate as to its effectiveness[134]. This ineffectiveness is due at least in part to its tribological properties; HA contributes to the elastic properties that characterize the bulk behavior of cartilage under pressure, but unlike lubricin, is not a boundary lubricant[40]. Because surface lubrication under high load becomes independent of synovial fluid's bulk viscous property, unless physically bound to the articular surface HA alone cannot provide boundary lubrication and so is not effective at protecting cartilage during maximally damaging boundary lubrication conditions. Although not directly responsible for synovial fluid's boundary lubricating ability, recent investigations suggest a synergistic interaction between the two molecules. In a recent study a mechanism was proposed between lubricin and HA[55] in which HA complexes with lubricin to act as an enhanced lubricant system. At present there are results both in support of and against this synergy[18, 55, 113, 128].

Despite the importance of mechanical injury on the OA initiation response, the effect of varied injury conditions on the friction coefficient of articular cartilage has not been studied. Here we show that the combination of joint impact joined with articulating motion in the absence of a boundary lubricant together are necessary to start cartilage surface fibrillation and subsequently the cascade into OA. This effect is purely a mechanical and a short-term phenomenon. This damage response has a threshold of impact dependant on strain rate and that is mitigated by the presence of boundary lubricants in the form of lubricin but not HA during cartilage-glass articulation.

2.3 RESULTS

Identification of threshold for initiating cartilage fibrillation

To understand the necessary impact profile necessary to initiate cartilage fibrillation a series of friction testing experiments (see Materials and Methods) measured the equilibrium coefficient of friction (μ_{eq}) as a function of strain rate. Previous studies have identified strain rate and peak stress thresholds for damage, and both approaches were investigated here. μ_{eq} was near nominal values for cartilage injured at low strain rates, but increased with strain rate, regardless of whether strain rate or peak stress was held constant at approximately 18 MPa (Figure 2.1). This increase was much more pronounced (slope = $9.65 \text{ X } 10^{-4}$ vs. $3.47 \text{ X } 10^{-4}$) when samples were injured with peak stress held constant compared to peak stress varied.

Combination of injury and sliding induces focal cartilage fibrillation

To characterize the effect of injurious compression on cartilage we analyzed the surfaces with environmental scanning electron microscopy (ESEM) and profilometry. Both techniques showed large changes to the cartilage surfaces following injury and shear induced from sliding, but not either force independently. ESEM of cartilage surfaces showed striking macroscopic damage to the injured cartilage surfaces (Figure 2.2). The bottom panel shows gross articular

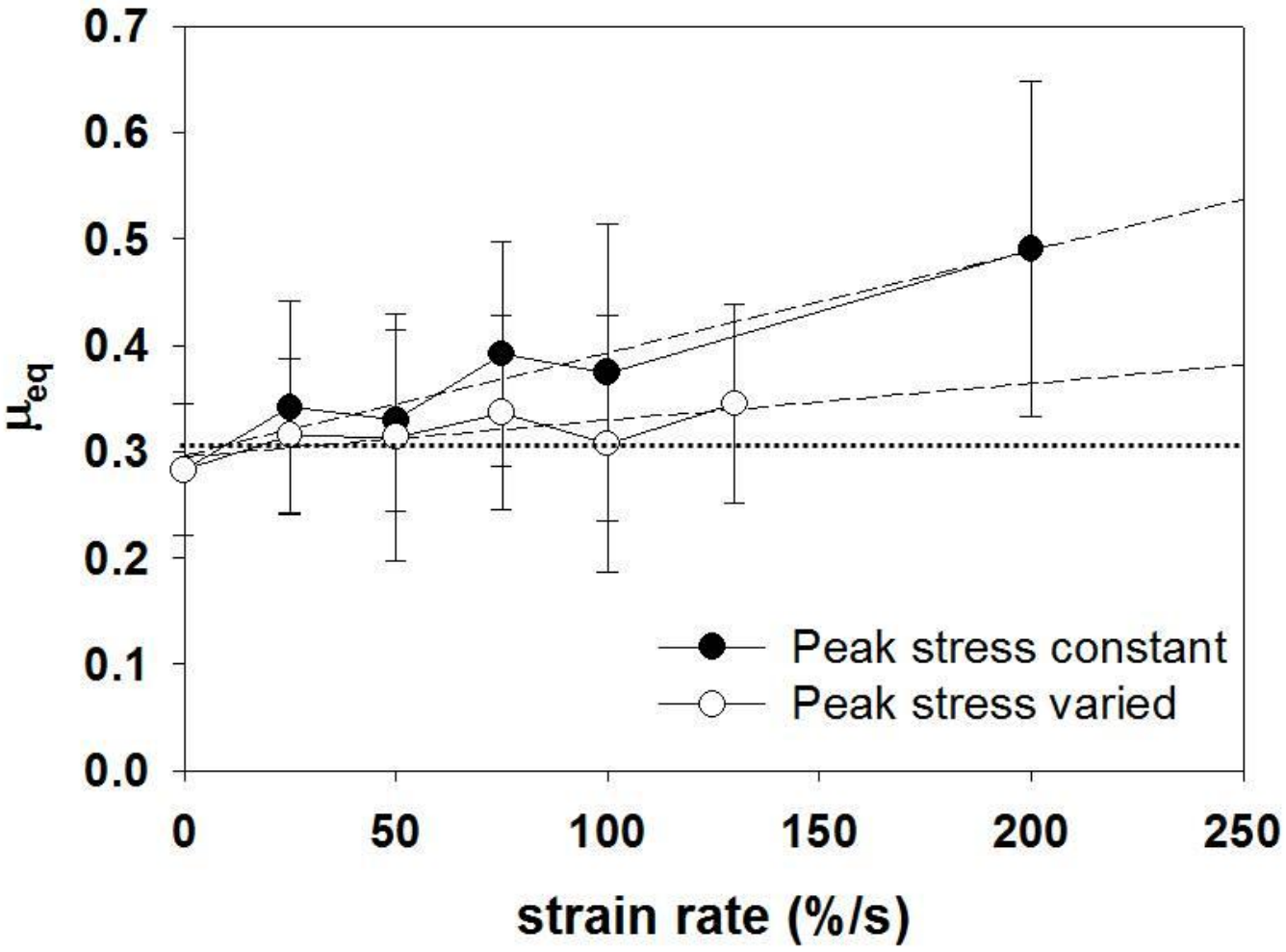

Figure 2.1 μeq increased with strain rate for both samples injured with peak stress constant at approximately 18 MPa and with peak stress varied (between 2 and 20 MPa). Dotted line indicates coefficient of friction of uninjured cartilage with lubricin extracted, and peak stress constant samples increase well above it at high strains. Peak stress constant: $r^2 = 0.931$, y = 9.65e-4 + 0.299 , peak stress varied $r^2 = 0.571$, y = 3.47e-4x + 0295.

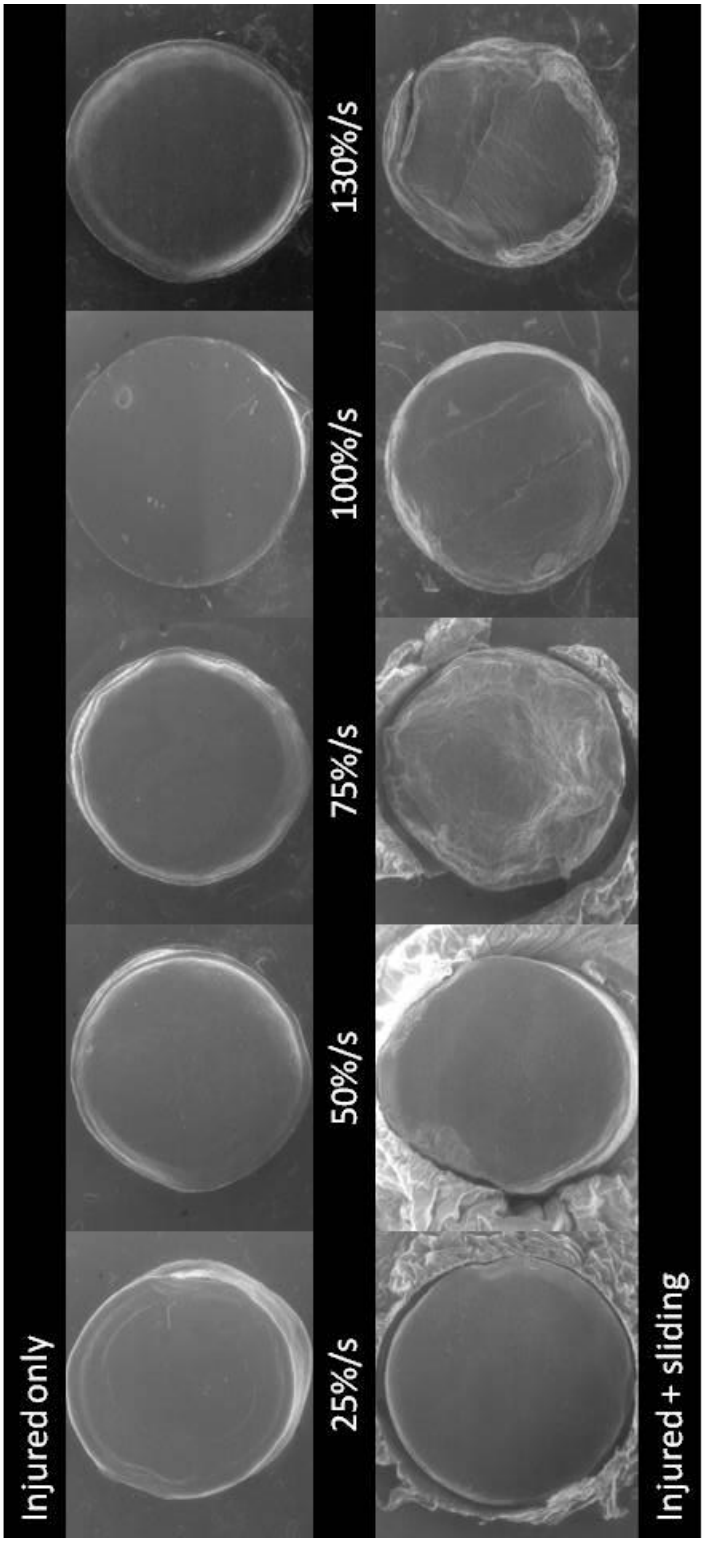

Figure 2.2 A) Representative ESEM images of injured and not sheared cartilage surfaces shows unblemished superficial zones. B) Representative ESEM images of injured and friction sheared cartilage shows variation in surface roughening and damage at high strain rates. Note the large areas that appear undamaged

surface appearance after impaction at the varied strain rates and shear loading due to friction testing while the top panel shows samples that were simply impacted and not sheared. Samples injured at low strain rates and sheared (bottom left) appeared undamaged and healthy but as injury strain rate increased past 50%/s large surface disruptions became apparent. At 75%/s there is widespread surface fibrillation, and at 100%/s and 130%/s there are visible cracks in the articular surface (bottom middle and right). A characteristic of this surface damage at high strain rates is its extreme variability both between and within samples. Shown here are representative images of the damage; in some cases surfaces were completely disrupted and in others large areas or entire surfaces appeared unblemished. The visible damage of these impacted and sheared samples are in stark contrast to tissue that was merely impacted without further shearing worn (upper panel). Every one of these imaged samples showed a consistently smooth appearance independent of the strain rate applied and largely indistinguishable from healthy tissue.

Surface disruption was quantified by profilometry measurements (Figure 2.3). Average surface roughness (Sa) of injured plus shear samples increased with injury strain rate (median of 1.84 μm at 25%/s to 3.16 μm at 130%/s) (Figure 2.3A). To illustrate the extreme variability in surface roughness all data are presented in a box and whisker plot. For healthy cartilage (0%/s) median Sa was 1.84 μm with a maximum value of 3.21 μm. At maximum injury strain rate (130%/s) fully half the roughness measurements fell within the range of healthy cartilage but with roughened patches that were markedly higher: the 75^{th} and 90^{th} percentile were 6.74 μm and 9.45 μm, or 213 to 299% higher than the median for that category. The roughest value was 12.01 μm, or ~600% higher than the smoothest surface in that category. This variation occurred both between and within different cartilage plugs. Profilometry measurements of injured only (no

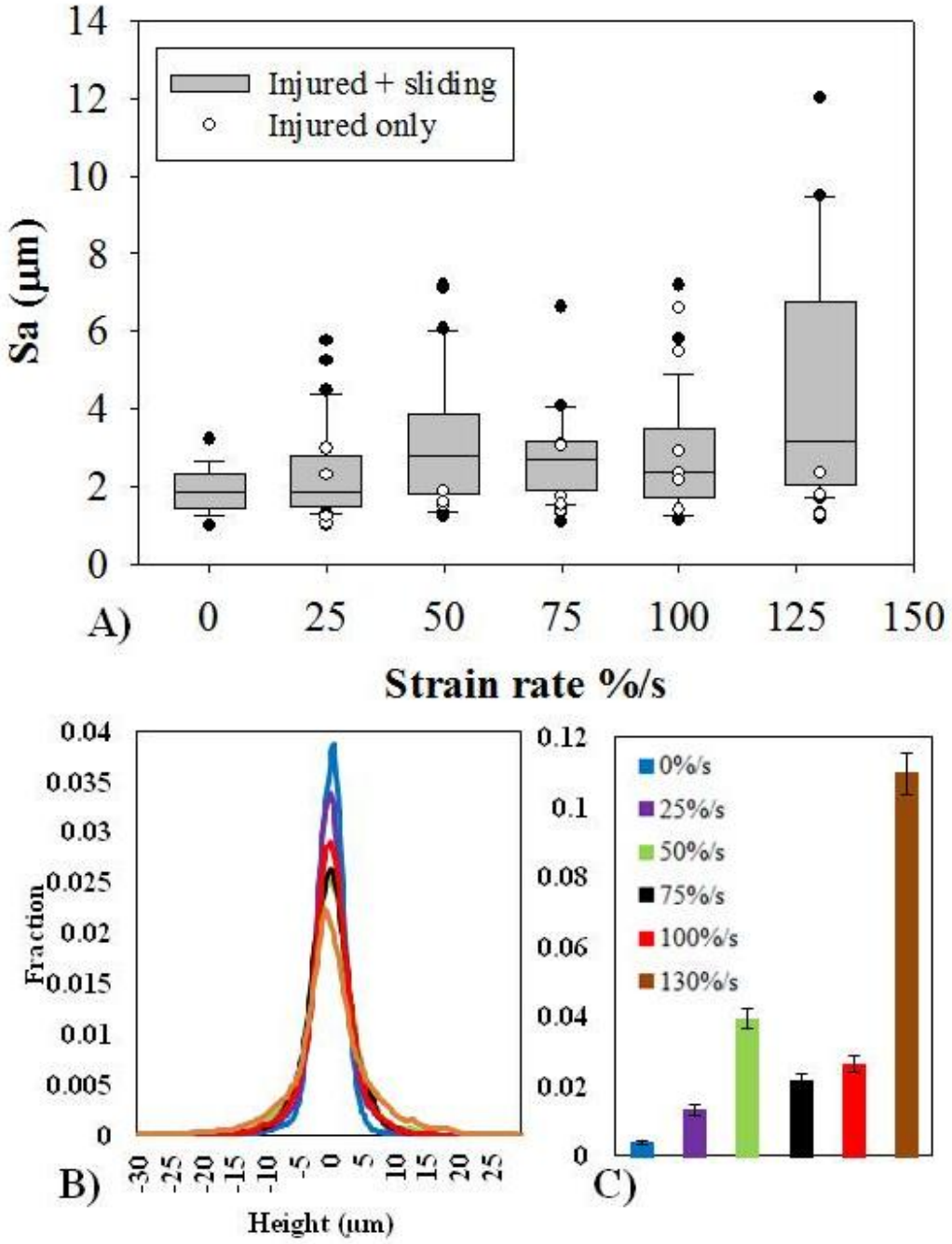

Figure 2.3 A) Variation of surface roughness of peak stress constant injured + sliding samples shows overall increase in roughness with strain rate indicated by the box and whisker plot with closed circles. Cartilage that was injured and not sheared (open circles) are within the nominal range. B) Probability density function of the surface height of each treatment group, with fraction on the y axis corresponding to each height on the x axis. C) Fraction of surface greater or less than 10 µm for each treatment group.

shear) samples (shown by the white circles) reflected the ESEM results; nearly every Sa value was in the control range (~1-3 μm). To further illustrate the differences in surface characteristics a probability density function was generated, pooling the scanned surface height (on the x axis) of each pixel of each sample taken for each treatment group (Figure 2.3B). The y axis shows the fraction of pixels at the corresponding height. Surfaces are generally Gaussian in distribution with a minimal spread in the data for control cartilage and maximum spread for 130%/s samples. The total fraction of the articular surface ± 10 μm corresponding to the most fibrillated, raised and pitted, deep areas is also shown (Figure 2.3C). Starting at 50%/s injury rate the fraction of most raised/pitted cartilage increase to above 5 times that of control, to more than 10% of the entire articular surface at 130%/s injury rate.

Lubricin protects cartilage from damage after injury

To investigate the possibility of protecting cartilage from degenerative changes we measured the coefficient of friction and surface roughness in the presence and absence of lubricin and HA. Lubricin, but not HA alone, was able to protect the surface following injury. We measured μeq in various lubricant baths for cartilage samples injured at 50%/s (Figure 2.4A). These baths are PBS, 5 μg/ml recombinant human lubricin (rh-lubricin), equine synovial fluid (ESF), intact-lubricin HA (ILHA) which was unaltered cartilage in a HA bath, and extracted-lubricin HA (ELHA) with lubricin native to the cartilage extracted by an NaCl protocol [52]. In all cases μeq did not depend on injury state. The lowest μeq was in ESF with a μeq of 0.13 ± 0.03 for injured and 0.16 ± 0.09 for control. Highest μeq were in the two cases where there was no boundary lubricant (0.33 ± 0.08 in PBS and 0.31 ± 0.1 in ELHA). Injured lubricin and ILHA showed intermediate μeq values.

The injured cartilage surfaces showed slightly higher surface roughness compared to freeswelling for all lubricants (Figure 2.4B). Again, this difference was significant in the two cases where lubricin was absent (2.77 ± 0.73 vs. 1.81 ± 0.51 in PBS and 3.24 ± 1.41 vs. 1.97 ± 0.58 in ELHA). It was also significantly higher compared to the other lubricants; ESF, lubricin and ILHA inhibited this increase in surface roughness while ELHA and PBS did not.

Both μeq and Sa responded to lubricin in a dose dependent manner (Figure 2.5A, 2.5B). The dashed lines represent a 4-variable sigmoidal model fit to the data, with $r^2 = 0.9309$ and $EC_{50} = 0.101$ for μeq and $r^2 = 0.942$ and $EC_{50} = 0.193$ for Sa. This dose dependence

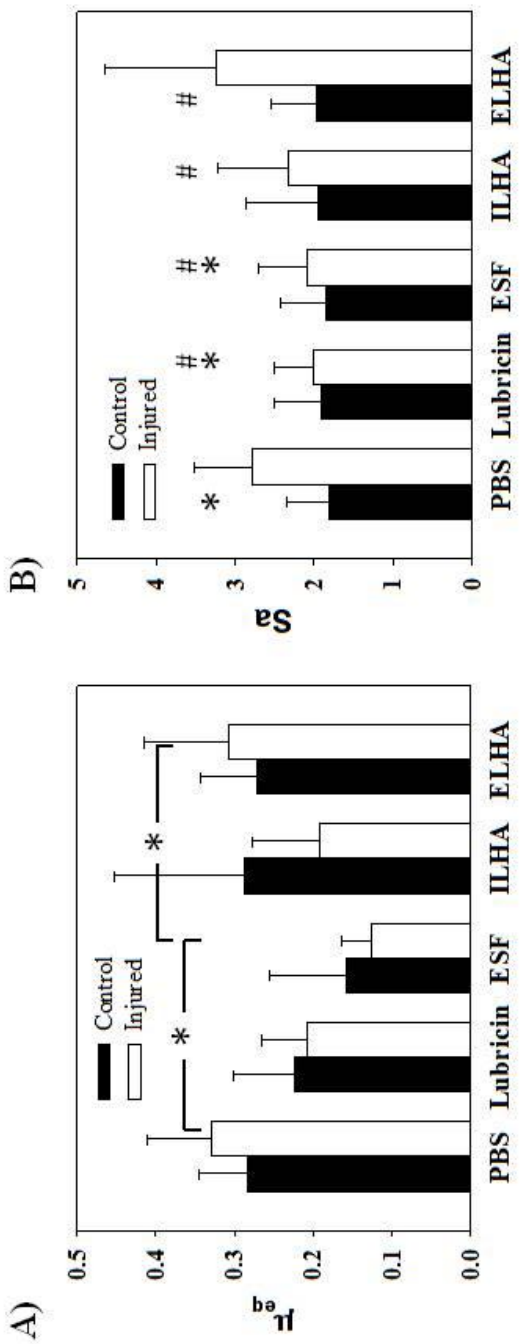

Figure 2.4 A) μeq for control and for cartilage injured at 50%/s in various lubricant baths. B) Sa for uninjured and injured cartilage. * Different from injured PBS, # Different from ELHA with no lubricin present in system ($p < 0.05$).

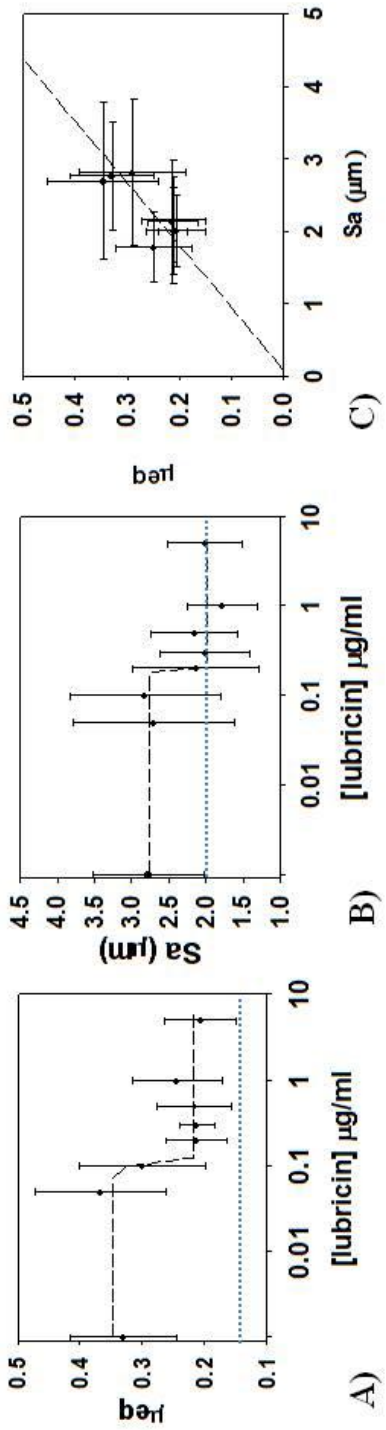

Figure 2.5 A) 4-parameter sigmoidal fit of µeq to [rh-lubricin] B) 4-parameter sigmoidal fit of Sa to [rh-lubricin]. C) µeq vs. Sa with linear fit.

dropped μeq from 0.35 to 0.22 and Sa from 2.76 to 1.99, or essentially the control value as shown by the dotted line. The relationship between μeq and Sa for all the lubricant baths was also determined with a linear correlation value of 0.67 (Figure 2.5C).

2.4 DISCUSSION

Injurious compression of articular cartilage is associated with disease development but the pathway by which this phenomenon occurs is still largely unknown. Studies of in vivo animal models have demonstrated that high-impact loads to the knee joint can induce cartilage degradation[97], although the changes occurring at the articular surface remain largely unexplored. In these models cartilage degradation can occur due to action of inflammatory mediators and catabolic enzymes, as well as direct mechanical damage. These changes can be abated by intra-articular injection of lubricant but the mechanism of this protection is unclear. This study demonstrated that a single compressive injury altered the mechanical properties of cartilage explants in a manner that was dependent on the strain rate of the injury. Further, these changes were only observed when cartilage was both compressed and sheared, and could be largely prevented by the addition of boundary, but not bulk, lubricants. As such, these data suggest a strong role for mechanical damage in the initiation of surface fibrillation of cartilage after injury.

Mechanical changes to cartilage injured in vitro have been previously reported[83], with bulk results showing that stiffness is decreased and water content increased with strain rate. In the current study, there was a positive linear correlation between strain rate and μeq. For the case where the peak stress varied along with strain rate the increase in μeq was less pronounced than when peak stress was high but held constant for varying strain rates. There is some disagreement in the literature as to the importance of peak stress on cartilage damage; some researchers have shown that the peak stress damage "threshold" is 25 MPa for rabbit patellofemoral cartilage

while others have reported that stresses as low as 5 MPa caused changes at the molecular level in the extracellular matrix of canine cartilage stemming from impact damage[37]. Conversely, previous in vitro single impact studies of both bovine and human cartilage have shown no link between peak stress and GAG release[28, 101]. The current study supports the latter observation, and indicates that it is true for articular surface response as well. Another possibility is that the maximum peak stress of 18 MPa used was below the wide "damage threshold" for stress. The fact that several samples shattered and were completely destroyed upon impact gives credence to the observation that peak stress is not as important a variable as strain rate.

The second major observation of this study was the striking focal surface disruption that occurred to the cartilage surface after both compressive injury and shear loading. The fissuring pattern of the surfaces under high strain rates is consistent with the crack damage previously reported under high impact loading[36, 81]. This surface damage was both extensive and also very inconsistent with some samples that appeared completely unaffected and others that were grossly altered. Changes in cartilage properties due to tissue location cannot account for these discrepant responses as plug site was randomized at cartilage harvest. Additionally, there was focal surface roughening of the cartilage even within small areas on the same sample. This non-uniform scatter of the surface damage is reflected both in the roughness measurements and the damage seen in the ESEM images. Collectively these results suggest a scenario in which a traumatic tissue insult loosens the collagen network in cartilage, making it more susceptible to roughening induced by shear motion at the tissue surface.

This widespread surface damage occurred on a very short time scale and was initiated entirely by mechanical input. Following the injurious compaction, samples were tested for only an hour for less than 50 cycles, but at the highest strain rate half the surface areas sampled were

already above the nominal range of roughness. As the samples were frozen prior to friction testing cell response did not contribute to fibrillation and fissuring, but patterns visible after an hour of testing are consistent with damage to impacted bovine cartilage after one to four days of tissue culture [36].

In vitro cartilage impaction results in abnormal lubricin expression[70], and the absence of bound lubricin results in high μeq for cartilage[52]. This effect is characteristic of both the post-traumatic and OA disease state[96]. In the two cases in which lubricin were absent from the system, that is for PBS and extracted-lubricin HA, μeq and Sa of injured cartilage were significantly higher while a rh-lubricin bath resulted in values similar to that of ESF. HA alone did not act as a boundary lubricant: when native lubricin was extracted from the surface of injured cartilage, HA failed to protect the surface from surface damage.

A current area of investigation is whether there is some synergistic effect between lubricin and HA. Wong et al. results indicate that synovial fluid function as reflected by intra-tissue cartilage shear deformation during tibio-femoral cartilage articulation is impaired by acute injury, while tribosupplementation with HA partially restores SF function [137]. The results of another study suggest that lubricin and HA contribute individually and in combination to the effective boundary lubrication of articular cartilage [113]. In contrast, a recent rat tribosupplementation study with injectable HA and lubricin indicated that lubricin with or without HA reduced radiographic and histologic indicators of cartilage damage, but that this effect was not HA dependent, nor did HA further reduce damage [128]. The current study supports the later result; in vitro there is no protection derived from HA alone nor further benefit to its interaction with rh-lubricin.

The chondroprotective effect of lubricin was dose dependent for both friction coefficient and surface roughness. All lubricin concentrations larger than 0.2 μg/ml generated maximum lubricating and minimum roughness values. In the case of Sa, the maximum dose used here of 5 μg/ml inhibited surface roughening in a manner similar to ESF, returning a nominal value of 2.0 μm. This drop is particularly notable as the concentrations used here are quite low; the human physiological concentration of lubricin is 100 – 600 μg/ml[112]. In addition, EC_{50} for lubrication observed here was significantly lower than, on the order of a magnitude, that measured for healthy cartilage after lubricin extraction[52]. This difference suggests that either compressive injury or the presence of native lubricin on the articular surface alters the lubricating action of rh-lubricin. Correlating μeq and Sa indicates that Sa can account for approximately 67% of the difference of μeq, reflecting the observation that Sa drops to control values with increasing lubricin concentration but μeq does not. Recent work shows a link between counterface roughness and kinetic coefficient of friction in human tissue[98]; the current study is an early attempt to quantify it.

In summary, this study demonstrated a solely mechanical mechanism of fibrillation following joint injury. This fibrillation depended on the strain rate of loading combined with subsequent shearing, and significantly altered surface morphology and friction coefficient on cartilage explants in vitro. This damage to the articular surface could also be halted by mechanical means, by the presence of healthy recombinant human lubricin added to the system, the extent of which depended on the concentration of lubricin added. Collectively, these data suggest that tribosupplementation via boundary lubricant replenishment of cartilage post-injury may be therapeutically important in preventing further tissue damage and the pathogenesis of a chronic disease such as OA.

2.5 MATERIALS AND METHODS

Cartilage harvest and lubricant preparation

Full thickness 3 mm diameter cylinders of articular cartilage were cored from the patellofemoral groove of 1-2 week old cows and the top 0.7 mm retained for testing with the superficial zone carefully maintained intact. Following harvest the resulting disks were cultured for 48 hours in media containing 1% ITS and Dulbecco's modified Eagle's medium.

Four different lubricant baths were used for these studies: phosphate buffered saline, (PBS, Invitrogen, Carlsbad, CA) with no boundary lubricant properties, recombinant human lubricin (rh-lubricin, Pfizer Research, Cambridge, MA) concentrations between 0.5 and 5 μg/ml, hyaluronic acid (HA, Hylartin V, Pfizer, NY) and equine synovial fluid (ESF). ESF was obtained at Cornell University Veterinary School using guidelines approved by the Cornell University Institutional Animal Care and Use Committee. ESF was sterilely aspirated from equine joints immediately following euthanasia. Aspirates free of blood and contaminants were pooled, aliquoted, and stored at -20ºC. Just prior to friction testing aliquots were thawed in a water bath at 37ºC and vortexed.

Sample injury and preparation

Following the 48 hours of equilibration cartilage plugs were subjected to unconfined injurious compression at a range of strain rates using a custom-designed loading apparatus [119]. Individual cartilage explants were placed in a well at the center of a polysulfone chamber. The mechanical injury protocol consisted of a single ramp compression of the cartilage thickness of the sample followed by immediate removal of compression at the same rate for a range of strain rates between 0-200%/s. Explants were compressed to half of their original height over a period

of less than two seconds, and compression was removed over the following equivalent time period.

Injury occurred via two different protocols, both designed to vary the strain rate applied to the cartilage. Group 1 samples were compressed to 50% their original thickness with varying ramp times. This loading resulted in strain rates varying between 25%/s and 200%/s. For these samples measurements of peak stress values during the loading protocol showed values roughly constant at approximately 18 MPa for all conditions. This group is referred to as "peak stress constant". All Group 2 samples were injured with a loading ramp time of 0.5 s, but the maximum amount to which the samples were compressed varied. This loading resulted in peak stresses of approximately 2 MPa for the lowest strain rate group (25%/s) up to 20 MPa for the highest strain rate group (130%/s), and are referred to as the "peak strain varied" group. Uninjured "freeswelling" control explants were placed into the chamber but were not compressed. Following injury samples were flash frozen until friction testing.

Friction testing

Cartilage cores were thawed in PBS at 37ºC just prior to friction testing. To remove native lubricin from the cartilage surface four samples of the peak strain varied group underwent 1.5 M NaCl lubricin extraction by 40 min of NaCl soak followed by 40 minutes of PBS equilibration as previously described[52].

Friction testing occurred under boundary mode conditions for young bovine cartilage (relative velocity = 0.33 mm/s, normal strain = 40%) [48]. Boundary mode friction refers to very low entraining speeds and high contact force between the articulating surfaces. The injured and free swelling control samples were tested in a custom friction apparatus previously described [49]. The linearly oscillating friction apparatus placed a normal strain on the tissue and controlled the

relative speed between samples and an articulating glass surface. The polished glass surface is very smooth and is a commonly used friction surface. A custom biaxial load cell simultaneously measured the normal and frictional shear loads on the sample. We calculated resulting equilibrium friction coefficient (μ_{eq}) as the ratio of the normal load to the shear load when the tissue had fully relaxed from the applied normal strain, measured after 60 min of equilibration. During friction testing cartilage samples were hydrated and submerged in a liquid bath. To examine the effect of strain rate of the cartilage surface samples from all groups and all strain rates were tested in PBS. To examine the interaction between lubricant and injury samples that were injured at 50%/s were tested in one of the four different lubricant baths of PBS, ESF, rh-lubricin, or HA. Four to six samples were tested for each condition of strain rate and lubricant.

Profilometry analysis

Immediately following friction testing surface roughness (Sa) was characterized by laser profilometry. A MicroXAM 3D was used to obtain three-dimensional non contact optical surface profiling measurements. Three to five measurements each of area 849 X 631 μm were taken per sample, randomly scattered over the surface. Cartilage surfaces were gently dabbed with a KimWipe to remove surface liquid that would distort the optical measurements. Care was taken to ensure no rubbing to disrupt the superficial layer. Scans were carried out as quickly as possible to minimize distortion due to tissue dehydration. Samples were then fixed in formalin.

ESEM

Environmental Scanning Electron Microscopy (ESEM) was used to macroscopically image cartilage surfaces (Quanta 600, FEI). Samples were rinsed with ethanol and placed directly in the vacuum chamber without further surface preparation. Magnifications shown are 70X.

Statistics

Data presented are sample means +/- standard deviation. Roughness data for peak stress varied samples are displayed as in a box and whisker plot. The significance ($p<0.05$) of lubricant and injury state was determined by 2-way ANOVA with Tukey post-hoc test.

CHAPTER 3

3 PREVENTION OF EARLY ARTICULAR CARTILAGE SURFACE DAMAGE AND FRICTIONAL CHANGES IN A RAT MODEL OF OA BY INTRA-ARTICULAR TREATMENT WITH RECOMBINANT LUBRICIN[2]

3.1 Abstract

Meniscus transection in rats results in a time dependent increase in cartilage damage which can be inhibited by intra-articular injection of recombinant human lubricin. Frictional properties are important to the proper function of articular joints but little information concerning them are available for this animal model of OA, particularly at the early stages of disease. The goal of the current study therefore is to assess the early response of friction and surface properties of cartilage exposed to this type of injury. Healthy 2-3 month male Lewis rats underwent transection of the medial collateral ligament and meniscus and the underlying cartilage was evaluated at one week and three weeks post surgery, and at three weeks following two weeks of intra-articular lubricin treatment. The frictional properties of osteochondral plugs from the tibial plateau were measured in a cartilage-on-glass system in a range of speeds, and then analyzed by

[2] To be submitted to the Journal of Orthopaedic Research with author list : Natalie Galley (Cornell), M Rivera-Bermudez (Pfizer Research), T Blanchet (Pfizer Research)[2], C Flannery (Pfizer Research), L Bonassar (Cornell)

profilometry for surface characteristics. Boundary mode coefficient of friction was lowest for the treatment group, and lubricin injection decreased cartilage roughness compared to untreated joints. Early intervention by recombinant lubricin injection may be an effective treatment for halting the initiation of OA following joint injury.

3.2 Introduction

Acute trauma to the soft tissues of the knee is a risk factor for the development of osteoarthritis (OA) with one out of two patients developing symptomatic OA within 20 years of injury[12]. The development of secondary OA in the injured joints is caused both by damage sustained during the initial trauma and by long term changes resulting from the event. Contributing factors include joint instability and altered joint loading[88, 111] due to changes in joint alignment or ligament laxity, enzymatic tissue degradation[42], and a lack of lubrication[32]. A host of other changes in cartilage take place following injury including glycosoaminoglycan loss[28, 102], collagen denaturation[21, 132], increased water content[83], decreased stiffness[90] and cell apoptosis[132].

Alterations in surface friction may also contribute to the onset of disease following injury[31]. The agent largely responsible for boundary lubrication in articular joints is lubricin[69]. Lubricin, a product of the gene proteoglycan 4 (PRG4), is a major component of synovial fluid and is expressed by both chondrocytes and synoviocytes[108, 115] and in cartilage is localized to the articular surface. Lubricin reduces coefficient of friction in many systems when coefficient of friction is at its highest due to high pressure and slow speeds between the surfaces in contact[66]. In the absence of lubricin the articular surface is vulnerable to frictional damage, as shown by patients with camptodactyly-arthropathy- coxa vara-pericarditis syndrome who have dysfunctional mutations in PRG4 and develop joint failure[92].

Inflammation likely also plays a role in post-traumatic OA. Acute joint trauma stimulates a flare of cytokines and growth factors including MMPs, IL-1, IL-6, and TNF-α[31, 87], which all influence chondrocyte metabolism and lubricin expression[31, 41, 71]. Increased lubricin biosynthesis appears to be an early transient response of surface layer cartilage to injurious compression for the first 48 hours[70]. However, this response may be short-lived. Deficient levels of lubricin have been measured in the synovial fluid of animal models[34, 127] and of human patients[32, 64]. In a guinea pig model of OA lubricin levels remained depressed 12 months after ACL transection[136] and clinically, lubricin levels in injury patients were decreased soon after injury and rose to those in the contralateral controls over the same 12 month time period[32].

Frictional properties are important to the proper function of articular joints; studies show that changes in frictional properties are related to OA progress[96]. The depletion of lubricin in the injured joint has implications on the chondroprotection of the injured tissue, as lowered lubricin levels are associated with increased whole joint coefficient of friction[33, 34]. This increase places the patient at risk because the decrease in lubricin levels in the early stages increases wear-induced damage.

Direct intra-articular supplementation of lubricin close to the traumatic event may offer an opportunity to preserve cartilage by re-establishing a protective covering of lubricin. The presence of healthy synovial fluid or recombinant human lubricin[46, 65] has proven effective at protecting injured cartilage surfaces from degradation. This benefit has been observed in two rat models of OA where either the medial collateral ligament and meniscus, or the anterior cruciate ligament was transected[40, 65]. Disease-modifying effects were noted using 2 or 3 lubricin injections per week, with marked improvements in lesion size and histological indices. The extent to which the cartilage frictional properties are affected by intra-articular injection of

lubricin in these animal models of OA is not fully understood, particularly at the early stages of disease. Therefore the goal of the current study is to assess the effect of intra-articular lubricant injection in a rat meniscectomy model on cartilage friction coefficient and surface properties.

3.3 Materials and Methods

Surgery and dosing: Healthy 2-3 month male Lewis rats weighing ~300 g underwent surgery in procedures approved by Bolder BioPATH's Institutional Animal Care and Use Committee. Following a skin incision over the medial aspect of the right knee the medial collateral ligament was transected and a single full thickness cut through the medial meniscus made to simulate a complete tear as described previously[40], abbreviated MNX. Right knees only were injured and left knees were left intact as controls.

Intra-articular injection began one week after surgery with three doses a week administered each week for two consecutive weeks. Lubricin used was a recombinant lubricin mutant approximately one third the length of full-length PRG4 produced by Chinese hamster ovary (CHO) cells, LUB:1[40], which has previously been observed to lubricate a cartilage-on-glass system[49]. The lubricin treatment group received a 40 µl LUB:1 injection at a concentration of 500 µg/ml in PBS into the affected joint, denoted treatment group "3 wk lub" (Figure 3.1A). Surgically injured animals that were not injected were evaluated at 1 week (1 wk) and 3 weeks (3 wk) post surgery. Additionally, a buffer treatment group was injected with 40 µl of PBS with the same dosing regimen as the lubricin group (Appendix A). The contralateral limbs at both 1 week and 3 weeks were pooled as controls (Con). At either one or three weeks post surgery animals were sacrificed and the knees removed and frozen.

Lubricants: Lubricants used for the friction studies were phosphate buffered saline (PBS) (Invitrogen, Carlsbad, CA) supplemented with a protease inhibitor cocktail (complete protease

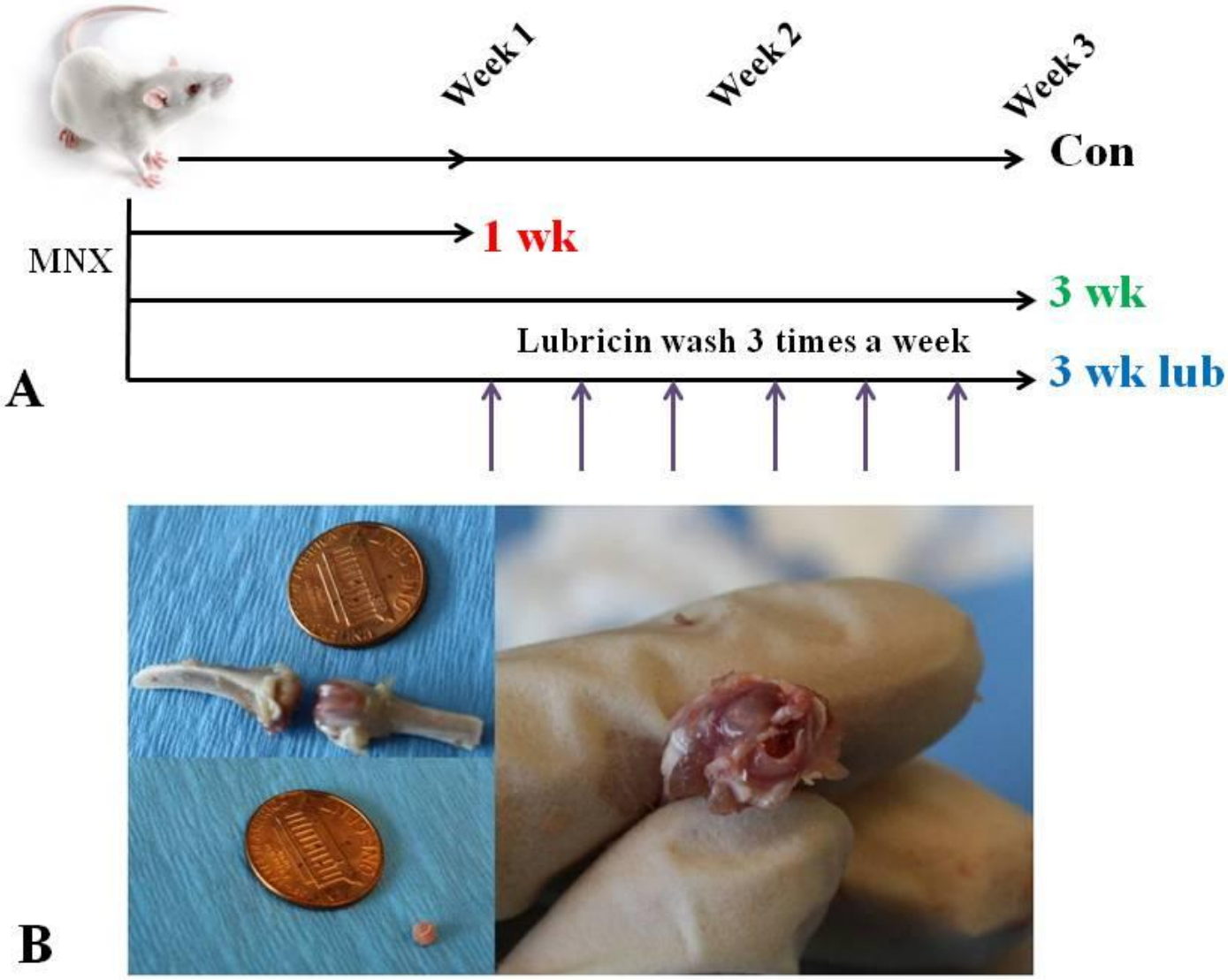

Figure 3.1 A) Osteochondral plugs were harvested from the medial tibial plateau of the left knee at 1 week and 3 weeks post meniscectomy as controls (Con). Osteochondral plugs were also harvested from the right knee at one week with no treatment (1 wk), at three weeks with no treatment (3 wk) and at three weeks with lubricin injections three times a week for the final two weeks (3 wk lub). B) Surgical pictures showing disarticulated joint with excised plug and explant location.

inhibitor cocktail; Roche Applied Science, Indianapolis, IN) and equine synovial fluid (ESF) as an ideal lubrication standard. ESF was aspirated from equine stifle joints as approved by the Cornell University Institutional Animal Care and Use Committee guidelines.

Friction testing: Immediately before testing, the knee joints were thawed in PBS in a water bath at 37ºC. The joints were then disarticulated and the menisci removed from the tibial plateau. A 3 mm osteochondral plug was punched from the medial tibial plateau with a biopsy punch and then cut down to 2-mm thick disks with the articular surface intact (Figure 3.1B).

Friction testing occurred under a range of speeds (relative velocity = 0.1 mm/s – 10 mm/s), and high normal strain in a custom friction apparatus that has been previously described [8]. The linearly oscillating friction apparatus placed a high normal strain on the tissue and controlled the relative speed between samples and a smooth articulating glass surface. A custom biaxial load cell simultaneously measured the resulting normal and frictional shear loads on the sample. The resulting equilibrium friction coefficient (μeq) was calculated as the ratio of the normal load to the shear load when the tissue has fully relaxed from the applied normal strain, taken at minimum 20 minutes following the applied strain. 20 minutes to equilibrium was determined from earlier pilot studies. Each plug was tested in PBS then removed and allowed to relax and equilibrate in PBS for minimum of 60 minutes before being reloaded and friction tested with ESF. Samples were rinsed in PBS prior to surface roughness testing.

Profilometry: Surface roughness was characterized by laser profilometry. A MicroXAM 3D was used to obtain three-dimensional optical surface profiling measurements. 2-3 measurements were taken for each sample with each scan covering an area of 849 μm X 631 μm. Cartilage surfaces were gently dabbed with a Kimwipe to remove optically distorting surface liquid while

ensuring no rubbing disrupted the superficial layer. Scans were carried out within five minutes to minimize tissue dehydration.

Statistics: To determine the effect of injury and treatment on the injured cartilage, the boundary mode coefficient of friction was evaluated. Boundary mode friction values for speeds less than 1 mm/s were pooled and then compared by two-way ANOVA with Fisher LSD post-hoc test to determine the effect of lubricant and treatment group. Differences in roughness were determined from one-way ANOVA with Fisher's LSD post-hoc test. Values shown are mean ± standard deviation, with sample size ≥ 9 for each treatment group.

3.4 Results

Friction coefficient: The friction coefficient of rat cartilage varied with speed in a manner consistent with previously reported cartilage tribological behavior[48]. In PBS μeq was the highest and largely invariant for speeds < 1 mm/s for each treatment group, consistent with boundary mode friction behavior (Figure 3.2A). All treatment groups had higher μeq values when friction tested in PBS compared to in ESF at all speeds (Figure 3.2B). 1 wk samples were higher than any other treatment group at all speeds in the absence of a boundary lubricant (Figure 3.2A), but there was no difference between treatment groups lubricated by ESF (Figure 3.2B).

The pooled μeq measurements for speeds < 1 mm/s (considered boundary mode) were evaluated (Figure 3.3). When tested in PBS, 1 wk samples had the highest μeq of 0.43 ± 0.11, approximately 20% higher than Con at 0.36 ± 0.10 (Figure 3.3A). For the lubricin treated cartilage μeq was similar at 0.35 ± 0.10 and lower than both the 3 wk and 1 wk non-treatment groups ($p = 0.023$ and $p < 0.001$ respectively). No difference was found between groups when tested in ESF (Figure 3.3B).

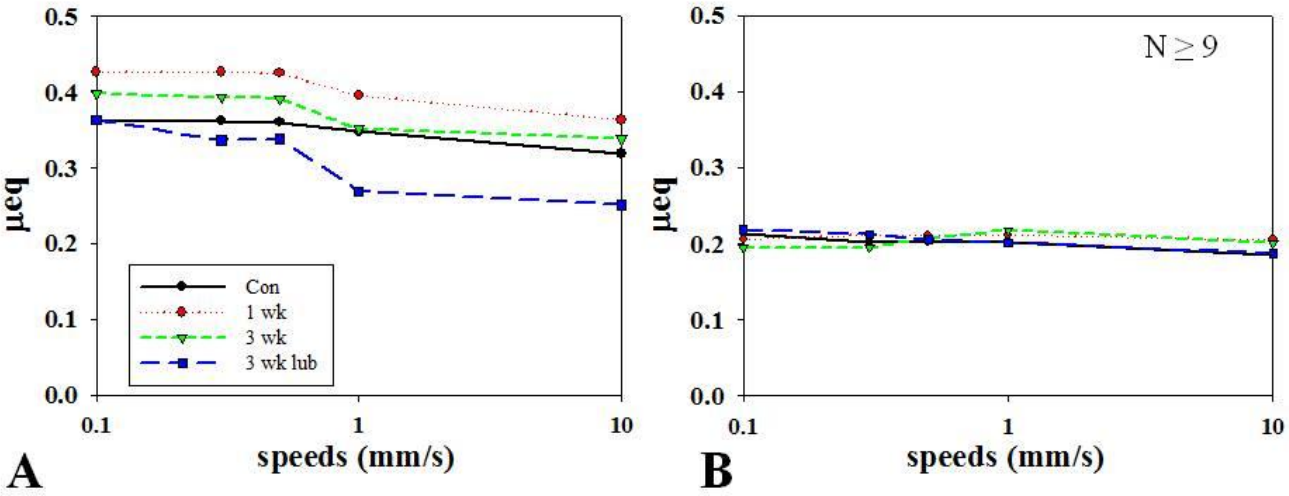

Figure 3.2 Coefficient of friction for all animal treatment groups as a function of speed measured in A) PBS and B) ESF.

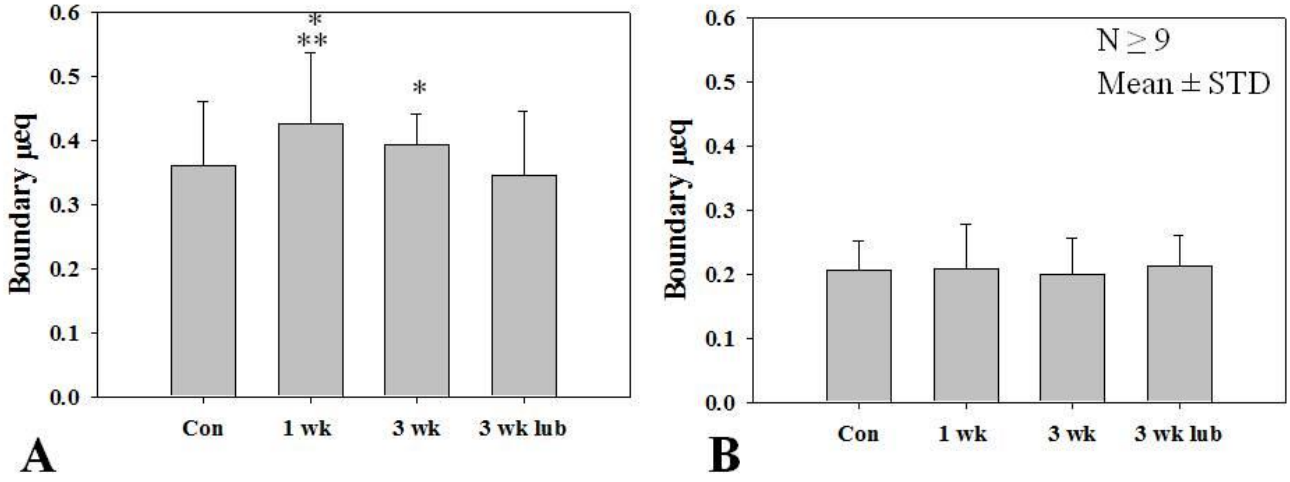

Figure 3.3 Boundary mode coefficient of friction for all animal treatment groups tested in A) PBS and B) ESF. Data are means ± standard deviation. *Different from 3 wk lub **Different from Con by two-way ANOVA ($p < 0.05$)

Roughness: Representative profilometry 3-D surface scans show differences in the cartilage surface (Figure 3.4). Con samples were generally smooth in appearance (Figure 3.4A), as were treated 3 wk lub samples (Figure 3.4C). Non-lubricin treatment groups show a more pitted, uneven surface with noticeable fibrillation (Figure 3.4B, 3.4D). Note that the maximum range for the 3 wk sample shown (Figure 3.4D) extends up past 40 μm compared to 20 μm for the others.

The roughness of the rat cartilage samples varied greatly, both from sample to sample and in different regions on the same sample. To get a picture of the overall cartilage surface a combined probability density function was generated. The heights at each pixel for each scan were binned from -50 to 50 μm and then combined with all scans of the same group to give the distribution of the overall scanned surface of each treatment group (Figure 3.5A). The distribution was generally Gaussian in shape with trailing tails at either end. The most damaged, fibrillated regions corresponding to the raised fibrillated regions pictured in the profilometry images are at the right hand side of this curve. The fraction of cartilage surface area representing the top 20% in cartilage height (height > 30 μm) was calculated (Figure 3.5B). These most fibrillated regions represented less than 0.5% of Con cartilage and increased with time to 1.1% at 1 wk and 2.2% at 3 wk. Lubricin injection had the effect of lowering the fraction to 0.78% over the course of the treatment.

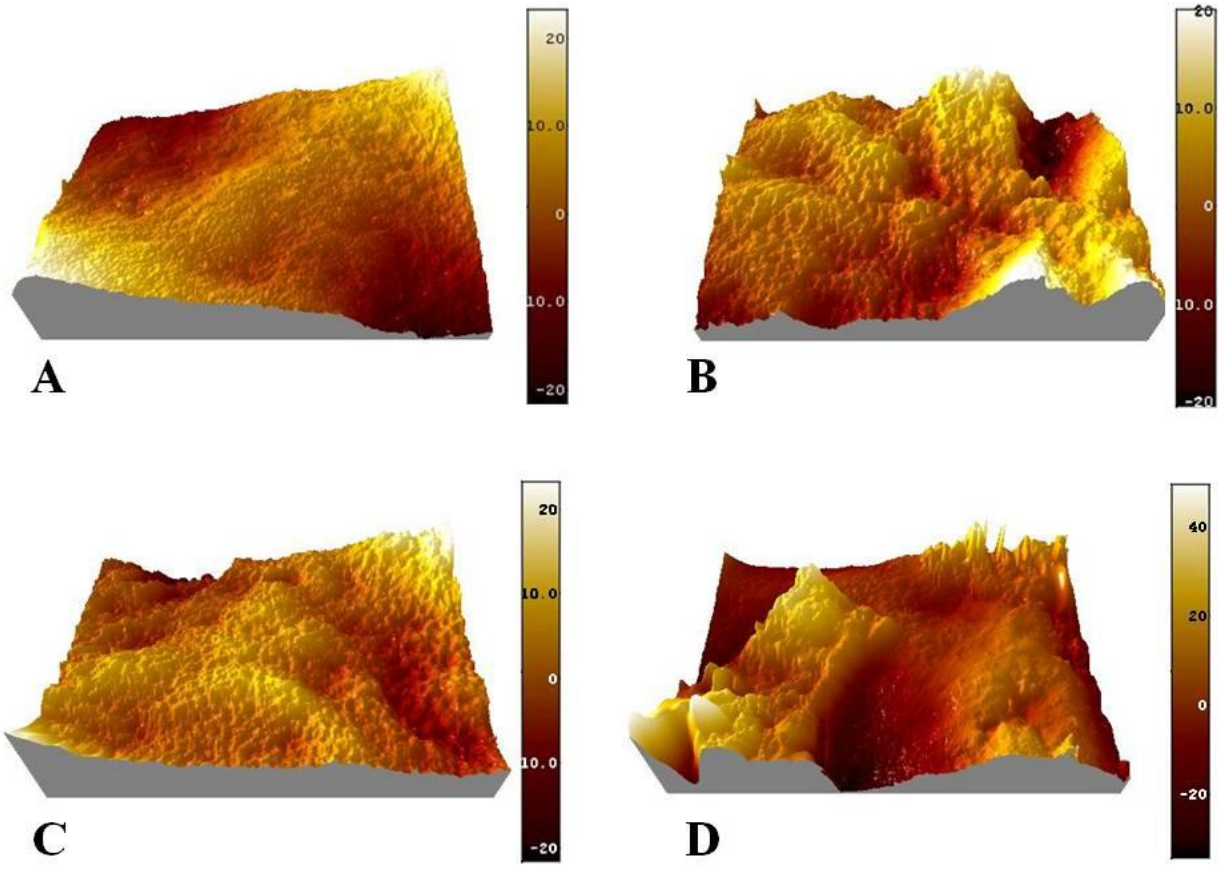

Figure 3.4 Representative profilometry images of rat cartilage surfaces. A) Control, B) 1 week post MNX, C) 3 weeks post MNX with lubricin treatment, D) 3 weeks post MNX with no treatment. Note that upper end of scale on D is 40 µm compared to 20 µm for the other groups.

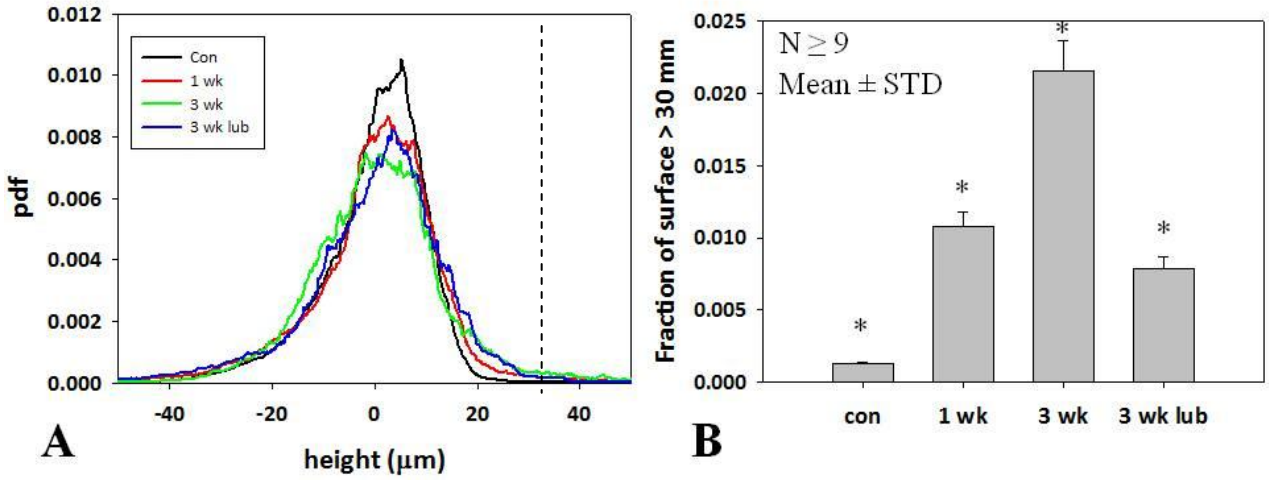

Figure 3.5 A) Probability density function of cartilage heights of all samples for each treatment group. B) Fraction of area of cartilage surfaces higher than 30 µm. Data are means ± standard deviation. *Different from all other groups by one-way ANOVA ($p < 0.05$)

3.5 Discussion

The progress of degeneration and disease that begins with injury to an articular joint is well-documented but still poorly understood. Animal models of injury via transection of the soft tissues of the knee have shown cartilage degeneration with changes in either synovial fluid or cartilage-bound lubricin. In the present study, we have shown that some of the pre-OA degenerative changes following this type of injury can be mitigated by intra-articular supplementation with lubricin.

In order to increase lubricin yields a recombinant human lubricin with a truncated mucin domain has been developed[40]. This construct, LUB:1, eliminates many of the repeating KEPAPTT sequences which facilitates its expression from CHO cells. LUB:1 contains approximately one-third the number of wild-type KEPAPTT-like sequence elements located within the mucin-like domain as well as the functional N-terminal domain which facilitates aggregation and the C-terminal domain that enables binding to cartilage.

Local administration of LUB:1 was effective in preventing cartilage degeneration during post-injury OA progression. Knee joints from rats treated with LUB:1 displayed significantly reduced cartilage roughening. The incidence of the most damaged areas of fibrillation of injured and untreated joints increased dramatically with time following meniscectomy but intra-articular lubricin treatment mitigated this effect. Cartilage treated with lubricin was less roughened than at the untreated state only two weeks prior, indicating that exogenous injected lubricin may in fact aid in cartilage repair. The imaged surface renderings in this study are similar to healthy human and bovine cartilage previously imaged by ESEM and AFM[25] and rat cartilage captured by AFM[23].

LUB:1 injection also had an effect on cartilage lubrication with a lower maximum μ for treated compared to untreated animals, both for the time-matched controls and for samples measured at the time point two weeks prior. Friction coefficient showed remarkable sensitivity to joint injury. At the early 1 week time point lesions are known to be relatively shallow and localized[60] but here μeq increased ~20%. The highly altered μeq suggests that friction testing is an extremely sensitive mechanical assay to early cartilage degeneration. The decrease in μeq at 3 weeks is counter to previously reported OA friction measurement trends[96] which show an increase in friction with disease progression in advanced stages of OA. This effect suggests that early OA frictional response does not follow that of the more advanced disease state, or may be due to the change in inflammatory response immediately following surgery.

Both μeq and average surface roughness (Appendix A) in this study are higher than those reported for larger animal models using the same cartilage-on-glass system[48]. One explanation is the relative skeletal maturity of the animals, adult rat vs. neonatal bovine. Another possibility is species difference, however previously reported rat μ values have been both significantly lower in an antigen-induced arthritis rat model[33] compared to reported rabbit μ values using the same whole-joint apparatus[34] and similar to those of porcine cartilage in an AFM study[23]. Thus the effect of species differentiation remains unclear.

There are several limitations to this study due to the nature of the samples tested. The tibial plateau of the rat is an uneven surface with varying geometry, thus the 3 mm osteochondral plugs removed from the joint were not perfectly even right cylinders ideally suited to the measurements taken here. This may have affected both the friction and profilometry measurements.

In this study we investigated the effect of intra-articular lubricant injection in a rat meniscectomy model on cartilage friction coefficient and surface properties. The present results indicate that lubricin is a disease-modifying supplement that may mitigate the pathogenesis following knee injury leading to OA. Tribosupplementation via intra-articular lubricin injection could be considered as a supplement or replacement for traditional viscosupplementation. Additional larger animal studies examining both the longer-term effects as well as the possibility of earlier intervention are required to explore the full extent of the benefits of lubricin injection.

CHAPTER 4

4 EFFECT OF SURFACE PROTEGLYCAN DEPLETION ON THE FRICTIONAL PROPERTIES OF ARTICULAR CARTILAGE[3]

4.1 Introduction

The equilibrium frictional response of articular cartilage can be understood in the context of classic Stribeck lubrication behavior[58]. This theory includes the effect of fluid viscosity, relative speed and contact force to predict the friction coefficient. There are three distinct lubrication modes, boundary, mixed, and hydrodynamic modes. Hydrodynamic mode occurs under a combination of low enough contact force and/or high relative speeds of the two surfaces and/or highly viscous lubricating fluid. Boundary mode occurs under high relative contact force combined with low speeds, and/or low lubricant viscosity. In boundary mode friction coefficient (μ) and potential for damage and wear are highest. In boundary lubrication any fluid film between the friction surfaces is thinner than the substrates' surface roughness and solid-solid contact occurs across discontinuous asperities. Load is carried by this small-area solid-solid contact without support by hydrodynamic pressure.

Cartilage is known to follow Stribeck behavior with the boundary and mixed mode lubrication applicable to articular cartilage in vitro[48]. In current application, the poroelastic effect

[3] To be submitted to ASME Journal of Biomechanical Engineering with author list: NK Galley, LJ Bonassar

of cartilage is taken into account in several ways. One is by examining the friction coefficient of cartilage under the assumption that the hydrodynamic layer is always present and will dominate lubrication effects[80]. Another is by studying friction coefficient when the tissue has relaxed and allowed all subsequent induced fluid movement to come to equilibrium[48]. As such, it is clear that the permeability of the tissue through which the tissue is squeezing will impact the ease with which the cartilage can support a μ-lowering lubricant layer. However at present current methods do not take into account the porosity of the tissue.

Osteoarthritis (OA) significantly increases the permeability of articular cartilage[8]. One commonly used model of OA is that of disease initiating at the articular surface and then propagating down through the tissue to the osteochondral boundary. It is thus reasonable to model OA progression as an ever-thickening layer of tissue with altered properties of lowered modulus and increased permeability.

The effect of a permeable surface layer is known in other areas of lubrication study. For example in civil engineering road design a permeable friction course[4] is a known technique of depositing a porous layer on top of a road in order to enhance drainage. The result is increased friction due to a shift from hydrodynamic lubrication to boundary lubrication mode.

We propose that a similar mechanism exists in cartilage. Specifically, we hypothesize that changing the permeability of the cartilage surface will change the operating conditions at which cartilage undergoes transitions in lubrication mode. To remove proteoglycans and increase permeability enzymatic digestion via trypsin degradation was used as described previously [7]. Trypsin digestion is known to remove GAG from the tissue; the quantity of GAGs removal from the tissue depends on the time the tissue is exposed to the enzyme. This GAG removal results in changes to both permeability and modulus. We hypothesize that these changes also result in a

reduced ability for digested cartilage to support a surface hydrodynamic layer, effectively reducing the number of force/speed combinations that operate under mixed or hydrodynamic mode. As such, the goal of the current study is to assess the effect of surface proteoglycan depletion on the changes in cartilage friction coefficient of healthy bovine cartilage using Stribeck surface analysis. This analysis is both experimental and numerical (see Appendix B).

4.2 Materials and Methods

Healthy tissue from the patellofemoral groove of neonatal calves was used. Joints of 1-3 day old calves were obtained from a local abattoir. The knees were disarticulated, and the full patellofemoral grove removed from the underlying bone and frozen. Prior to testing the cartilage was thawed in a water bath at 37ºC while immersed in a solution of phosphate buffered saline (PBS) (Invitrogen, Carlsbad, CA) supplemented with a protease inhibitor cocktail (complete protease inhibitor cocktail; Roche Applied Science, Indianapolis, IN). 6 mm cartilage plugs were excised with a biopsy punch with the articular surface kept intact and then cut down to 2 mm thickness.

Full thickness 6 mm diameter cylinders of articular cartilage were cut from the patellofemoral groove of 1-2 week old cows with the superficial zone left intact. Cores were submerged in 1.5 M NaCl solution for 20 minutes to extract the naturally occurring boundary lubricant lubricin from the surface[72] and eliminate any effect of trypsin on the presence of surface lubricants, and then equilibrated for 20 min in PBS supplemented with protease inhibitor.

To control enzymatic exposure to the non-articular cartilage surfaces the excised plugs were first encased in epoxy resin on all other sides and then submerged in 50 μg/ml trypsin solution in PBS. Cartilage plugs were immersed for 30 min, 1 hr, 2 hr, and 4 hr as well as undigested controls (Con). At the end of digestion each sample was washed in PBS.

The friction behavior of the treated and untreated cartilage was characterized by a custom oscillating tribometer[50]. To fully map the friction behavior of the cartilage samples a full Stribeck analysis was done[48]. Cartilage samples were loaded and then axially strained to 10%. After a period of 40 minutes to allow the samples to come to equilibrium[44] a range of speeds from 0.1 mm/s to 20 mm/s was applied between the relaxed cartilage and a smooth glass counterface. These stress-relaxation followed by speeds sweep steps were then continued up to 40% strain.

Histological sections were also prepared from the center of each cartilage plug . Following minimum 48 of fixation in buffered formalin full thickness paraffin-embedded sections were stained with safranin-O and fast green. Photographs of the histological sections were taken and analyzed with image software to manually determine the depth of GAG depletion.

The surface roughness of the samples was also characterized using laser profilometry. 5 measurements were taken for each sample with each scan covering an area of 849 X 631 μm.

4.3 Results

Data shown are means with n = 4 for each testing condition. The GAG depletion as a result of trypsin exposure is shown by histology (Figure 4.1). The depth of the depleted surface layer varied linearly with exposure time (Figure 4.2).

Both control and trypsinized cartilage showed Stribeck behavior that is consistent with cartilaginous tissues (Figure 4.3). Maximum μ corresponding with boundary mode is rendered in red. For 0 hr control cartilage this region is relatively contained (Figure 4.3A) as it is for 30 min exposure (Figure 4.3B), but both 2 hr and 4 hr trypsin exposure increased the boundary region dramatically. The transition from boundary to mixed mode occurred at a wider range of articulating conditions for the highly trypsinized cartilage compared to control.

0 min 30 min 60 min 120 min 240 min

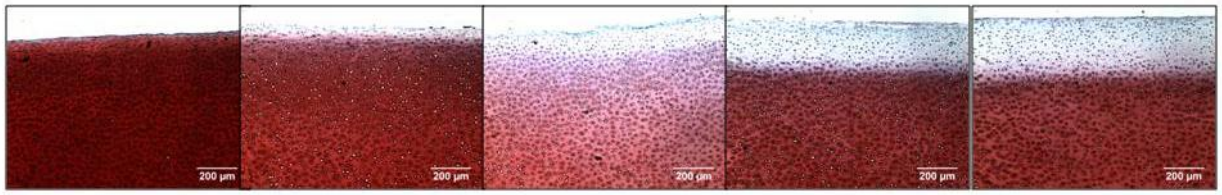

Figure 4.1 Safranin-O staining of cartilage exposed to 50 µg/ml trypsin for from left to right: 0 min, 30 min, 1 hr, 2hr, 4hr. Bar is 200µm

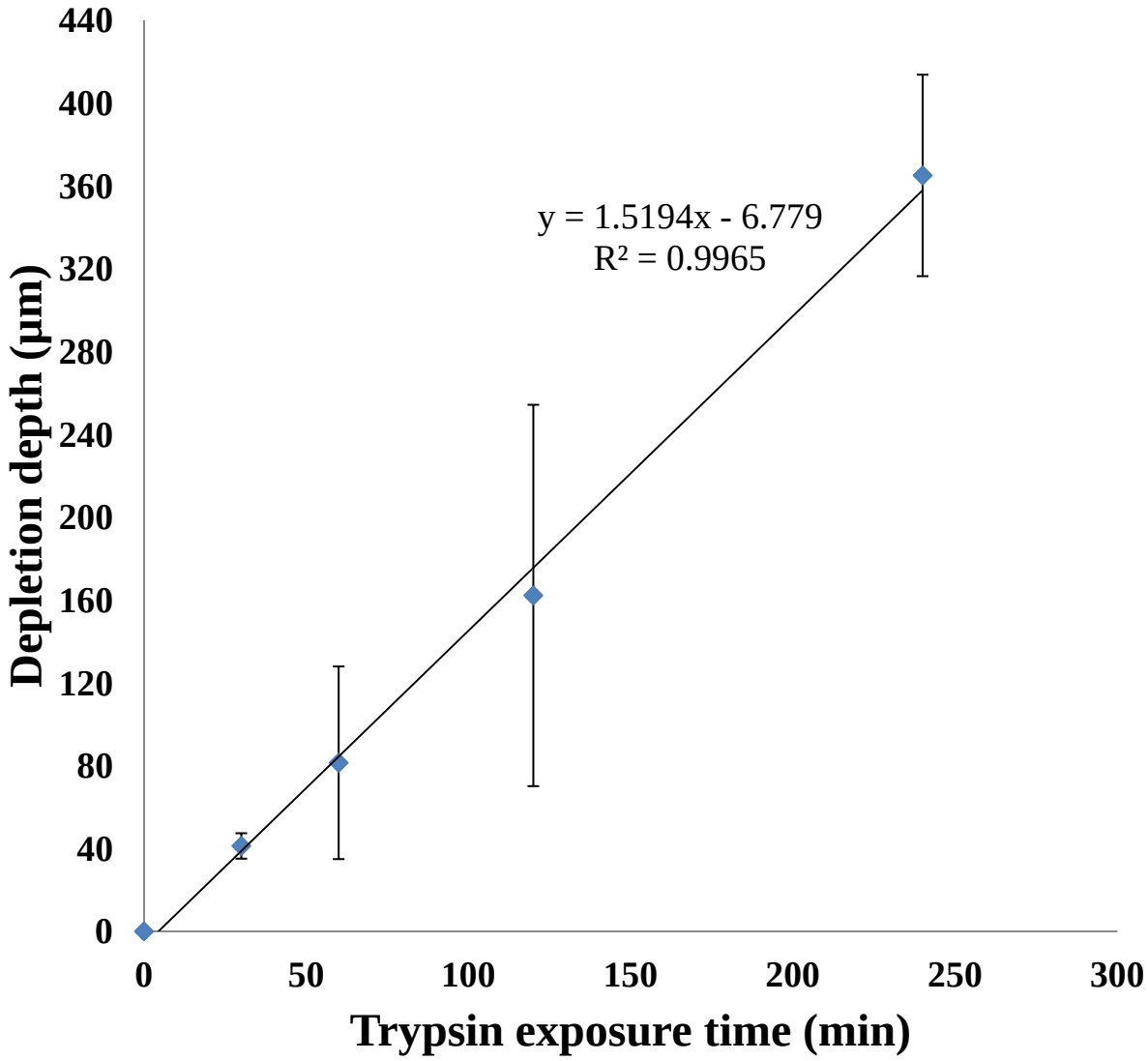

Figure 4.2 GAG depletion depth increases linearly with trypsin exposure time. Data are means ± standard deviation. Line is linear fit, with good agreement.

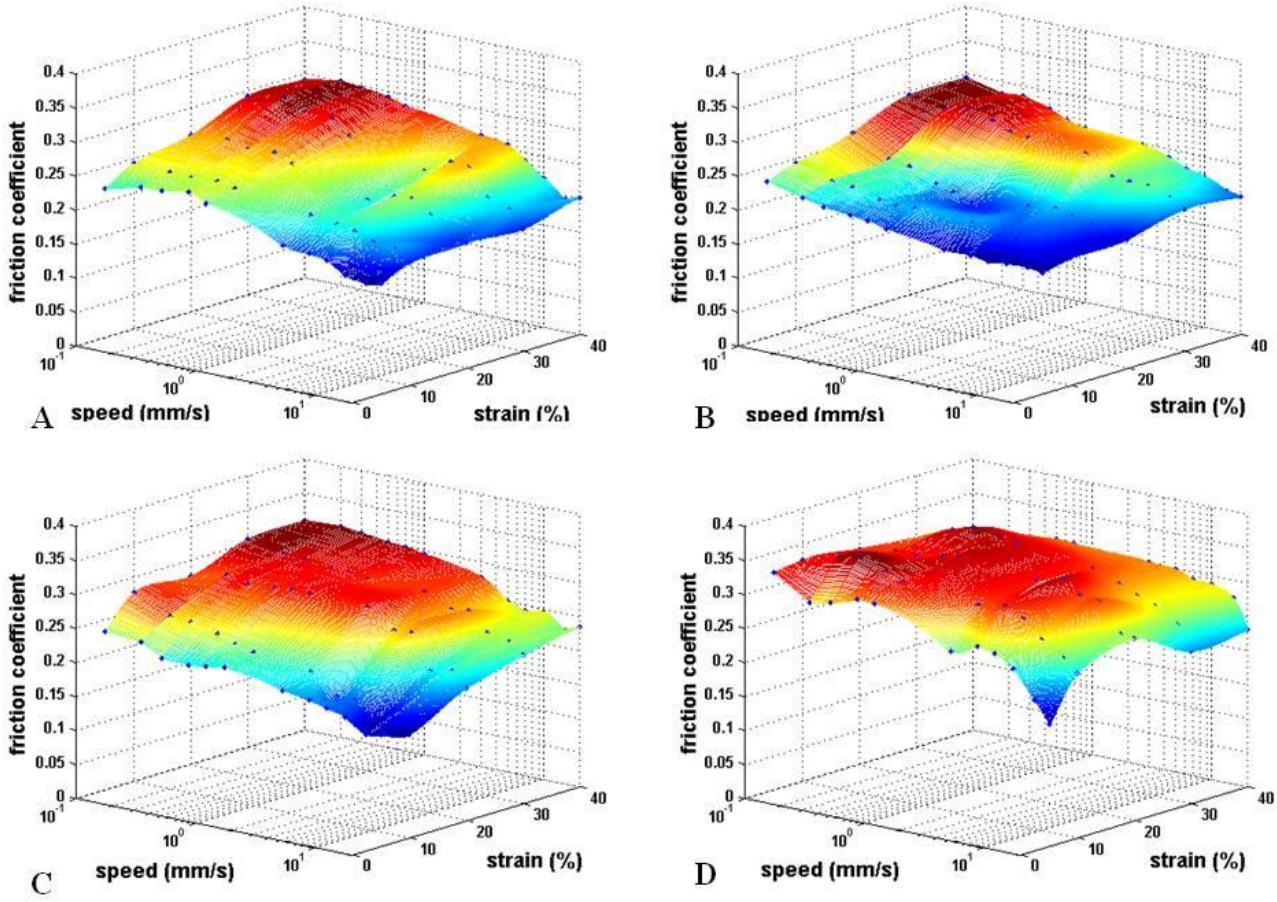

Figure 4.3 Stribeck surfaces (speeds 0.1 – 20mm/s, strain 10-40%) of articular cartilage exposed to trypsin degradation for A) 0 min, B) 30 min, C) 2 hr, D) 4 hr.

To more closely examine the effect of speed on lubrication mode, the μeq at high strain with varying speeds is shown (Figure 4.4). At maximum strain (40%) both trypsinized and control cartilage show μeq ~ 0.30. μeq begins decreasing as speed increases to 1 mm/s for Con but 4 hr trypsinized samples remain almost constant until close to 10 mm/s. At 10 mm/s Con samples have dropped to 74% of their maximum value while trypsin samples remain at 95% of their maximum μeq.

The relationship between this μeq drop and trypsin exposure time is shown in Figure 4.5. The transition speed from Figure 4.4 is plotted against the depletion depth from Figure 4.2 (for both the measured depletion depth and the predicted depletion depth of the linear fit to the depletion depth) as is quadratic ($R^2 = 0.9974$).

4.4 Discussion

In this study the effect of trypsin degradation on the friction behavior of articular cartilage was examined. Boundary mode friction coefficient was unchanged by trypsin treatment, suggesting that ECM components removed by trypsin (e.g. proteoglycans) do not act as lubricants. This observation is in contrast to other studies that suggest that proteoglycans and their subunits act as lubricants[5]. The data presented here indicate that the primary effect of trypsin-induced proteoglycan depletion was to shift the transition between mixed and boundary modes to higher speed and lower strains.

The removal of proteoglycans from the cartilage is known to increase the permeability the porosity of the tissue[7]. This increased permeability inhibits the ability of the tissue to support a lubricating fluid layer, effectively reducing the number of speed/strain combinations that can produce mixed mode. This effect is demonstrated by the larger range of articulating strains and

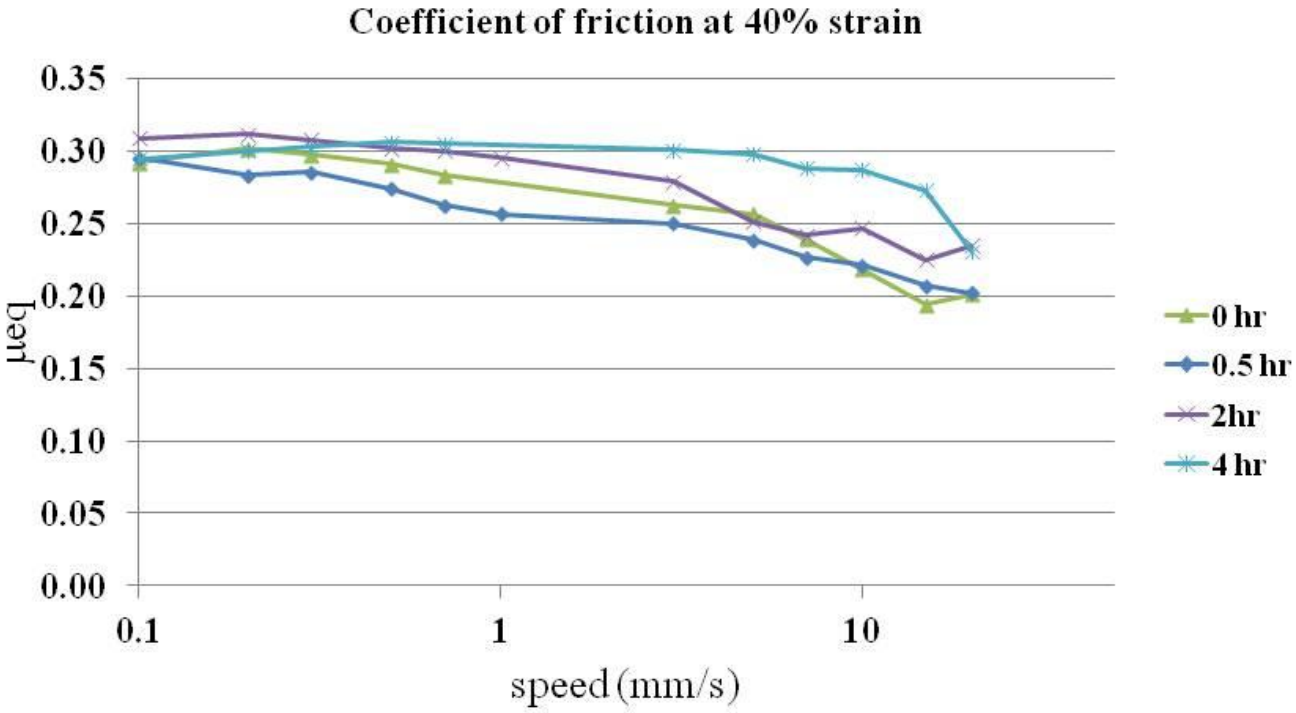

Figure 4.4 Coefficient of friction for trypsinized cartilage as a function of speed under maximum strain.

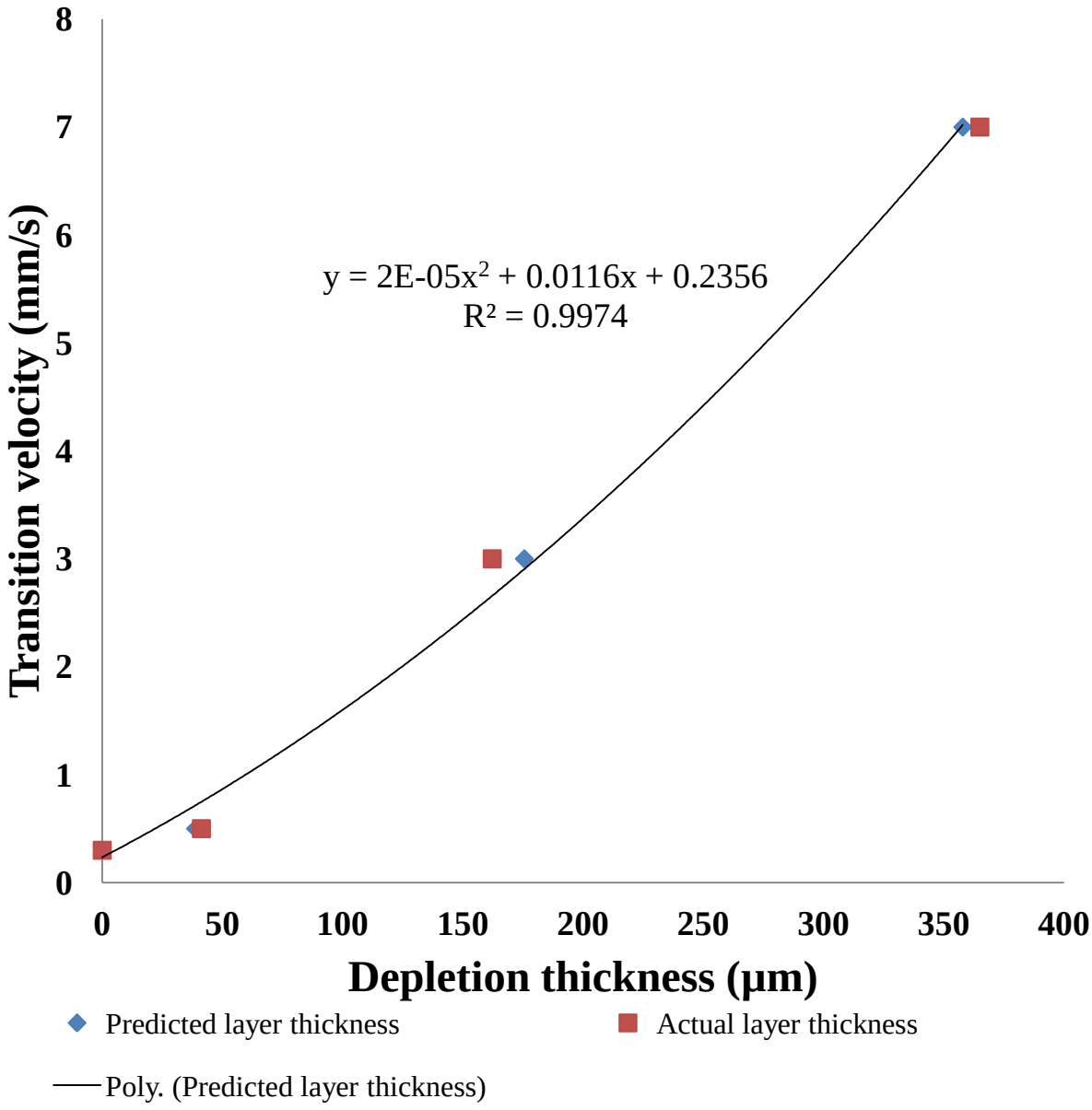

Figure 4.5 Transition velocity from boundary to mixed mode for actual measured depletion thickness compared to linear prediction. Both increase quadratically with GAG depletion thickness. Line is a second order fit to the predicted layer thickness, with good agreement.

speeds over which trypsinized samples appear to operate in boundary mode compared to healthy cartilage.

Increased permeability by trypsin degradation effectively shifts the transition from boundary to mixed mode to include more speeds and strains. The highly quadratic behavior of the transition velocity to depletion thickness strongly suggests that permeable effects are dominant in this case. We therefore suggest that the primary effect of trypsin digestion is to shift the transition points between lubrication modes.

This has several clinical implications. First, it elucidates a possible pathway of mechanical OA development. As the surface layer of the diseased tissue's properties change, it becomes more difficult for the cartilage to support a protective fluid layer. This translates to a larger fraction of the time spent in boundary mode compared to in the healthy state, corresponding to higher risk for the tissue. Thus this mechanism of surface damage is self-propagating.

In the design of tissue-engineered cartilaginous tissues one of the desired design criteria of implantable scaffolds is high permeability to allow tissue ingrowth into the implant. This ingrowth has been shown to result in increased functionality with time[47]. However it puts the native tissue apposing the implant at risk at early stages while the implant is still highly permeable and has yet to develop native-like properties.

Both these scenarios highlight the need for an effective boundary lubricant during disease progress. Tribosupplementation with a boundary lubricant such as lubricin can mitigate some of this damage by lowering the coefficient of friction under maximum coefficient of friction conditions. This also underscores the ineffectiveness of hyaluronic acid (HA) as a viscosupplement. Viscosupplements are not chondroprotective in the boundary mode, since in

boundary mode the friction properties are independent of bulk fluid properties. Tribosupplementation may be the answer to halting the progression of OA.

CHAPTER 5

5 FRICTIONAL PROPERTIES OF THE MENISCUS IMPROVE AFTER SCAFFOLD-AUGMENTED REPAIR OF PARTIAL MENISCECTOMY: A PILOT STUDY

First published as: Galley NK, Gleghorn JP, Rodeo S, Warren RF, Maher SA, Bonassar LJ. Frictional Properties of the Meniscus Improve After Scaffold-augmented Repair of Partial Meniscectomy: A Pilot Study. Clin Orthop Relat Res. 2011;469(10):2817-2823. Reprinted with permission from Springer Copyright Clearance Center.

5.1 Abstract

To prevent further degeneration it is desirable to fill a meniscal defect with a supportive scaffold that mimics the mechanics of native tissue. Degradable porous scaffolds have been used, but little information is available on the mechanical behavior of the tissue that fills the site of implantation. To determine the frictional behavior of native and engineered meniscal replacement tissue from in vivo implantation over time. We evaluated boundary and mixed-mode friction coefficients of tissue generated in porous polyurethane scaffolds used to augment the repair of the meniscus of 13 skeletally mature sheep after partial meniscectomy. Implants were removed for evaluation at 3, 6, and 12 months. The friction coefficient, aggregate modulus, and hydraulic permeability were evaluated for tissue harvested from native meniscus adjacent to the implants, native meniscus from the intact contralateral knee, and repair tissue from the site of the scaffold implantation. The equilibrium friction coefficient (μ_{eq}) was measured in the presence of a lubricant bath of either phosphate-buffered saline (PBS) or equine synovial fluid (ESF).

Boundary μ_{eq} in PBS of engineered meniscus improved with time and was similar to native tissue after 6 months. ESF enhanced lubrication for all samples at all time points demonstrating the efficacy of ESF as a joint lubricant for repair tissue as well as native meniscus. Modulus increased and permeability decreased with implantation, likely as a result of tissue ingrowth. Promoting tissue ingrowth into porous scaffolds is a potential strategy for improving friction performance in meniscal repair.

5.2 Introduction

Menisci play important mechanical roles in the knee, including load transmission, energy dissipation, and joint congruity and stability[1]. Partial meniscectomy is a common surgical treatment among the over 1 million meniscal procedures performed each year[75]; however, loss of even part of the meniscus can destabilize the knee and predispose the joint to long-term degenerative changes and osteoarthritis[14, 22, 111].

The degree of joint degeneration after meniscectomy is reportedly related to the amount of meniscus removed[24], making it beneficial to save as much tissue as possible. Replacing resected tissue with a support material may further improve outcome; contact area is increased and contact pressure decreased with a replacement scaffold in place when compared with a partially meniscectomized knee[11].

Various replacement materials currently in use attempt to mimic the mechanical function of cartilaginous tissues and allow the patient improved use of the joint. Specifically, polymeric materials provide a favorable cellular environment for tissue ingrowth[131] in addition to distributing load[11]. Porous polyurethane foams in particular are of interest as a meniscal replacement because the porosity of the foam scaffold facilitates tissue ingrowth[131]. Previous

studies showed promising results in the regeneration of tissue in meniscal lesions in dogs using a degradable porous polymer scaffold[57], [130].

For both native meniscus and engineered meniscal replacements, frictional properties are particularly important because the meniscus continually slides against articular cartilage during the gait cycle[94]. The resulting coefficient of friction (μ) can vary widely from 0.015 to 0.28 for native cartilage[16], [48], partly as a result of the tissue's biphasic behavior. Biphasic time-dependent response to loading is a characteristic of cartilaginous tissues[45], [48]; when compressed, the load is initially supported by hydrostatic pressure but as fluid pressurization diminishes, support is increasingly carried by the solid surfaces[80]. The frictional behavior observed at this point depends on several factors, including fluid viscosity, relative speed, and normal force [48]. When slow speeds and high contact forces exist, the result is boundary mode friction, in which μ and thus potential for damage and wear are highest. Boundary mode contrasts to mixed mode in which a fluid layer is partially supported between the solid surfaces and helps to carry the load, diminishing overall μ.

Acting as a load-bearing surface is an important role for polyurethane foam replacements, like for native tissue. Meniscus μ has been examined as part of whole-joint friction investigations[94], but the frictional behavior of meniscal tissue has not been widely studied to date. The frictional properties of porous polyurethane foam/cartilage articulating surfaces has recently been investigated[49], but the mechanical behavior of the resultant meniscal tissues after in vivo integration is unknown.

We used on ovine partial meniscectomy model to assess the mechanical behavior of meniscal repair tissue. Specifically, the goals of this study were (1) to determine whether the equilibrium friction properties of native meniscus are well described by Stibeck behavior across a range of

articulating conditions (2) to determine if synovial fluid effectively lubricates repair meniscal tissue, (3) to determine the effect of implantation time on frictional behavior, and (4) to determine the effect on mechanical properties due to tissue ingrowth into a porous polyurethane foam.

5.3 Materials and Methods

The right lateral menisci of 13 healthy, skeletally mature Columbia X Rambouillet sheep were subjected to partial resection (Figure 5.1). We performed an arthrotomy to expose the meniscus and a wedge of meniscus to within 1 mm of the capsule was removed by a longitudinal cut connecting two radial cuts in the midanterior and posterior horns. The removed meniscal tissue was used as a template to size the replacement polyurethane material. We replaced the defect site with fitted 80% biodegradable aliphatic polyurethane with pore sizes of less than 400 μm (ActifitTM; Orteq Ltd, Cambridge, UK)[49], [130]. The scaffold used to fill the defect had a C-shaped geometry with a cross sectional wedge shape, and a peripheral thickness of 8 mm thinning to a 2 mm central thickness. The implant was approximately 2 mm thicker than the native meniscus to better mimic the mechanical characteristics of the native tissue. The implant was sutured to adjacent meniscal tissue and capsule in a horizontal mattress fashion using one cranial, lateral, and caudal suture with No. 3-0 Ethibond sutures (Ethicon, Somerville, NJ). The lateral collateral ligament and bone block were reattached with a stainless steel bone screw. Right knees only were implanted and left knees were left intact as age-matched controls. Animals were not immobilized after surgery.

In this pilot study six animals were euthanized after 3 months, three after 6 months, and four after 12 months. Sheep were anesthetized via intravenous injection of 1.8 mg/kg ketamine, 0.2 mg/kg xylazine, and 0.2 mg/kg acepromazine. Postoperative pain was managed via

intramuscular injection of 0.3 mg/kg buprenorphine administered twice per day for three days. At the termination of the study, animals were euthanized via overdose of 390 mg/kg of sodium pentobarbital. All animal studies were approved by the Institutional Animal Care and Use Committees at the Hospital for Special Surgery and Colorado State University.

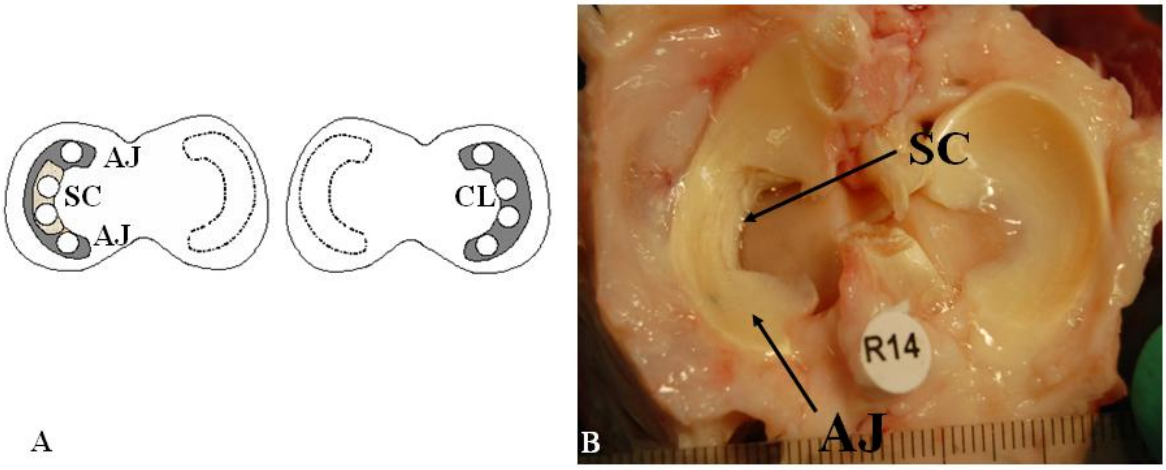

Figure 5.1 (A) Diagram of explant/implant locations in right and left knees: SC = scaffold region; AJ = native meniscal tissue adjacent to the implanted scaffold; CL = native meniscus from the contralateral intact knee. Lightly shaded region denotes region of scaffold placement. Open circles are explanted tissue locations taken from menisci with dark shading. (B) Twelve-month operated knee before explant removal. AJ and SC sites indicated with SC region showing integration with surrounding tissue

We removed both knees at the midfemur and midtibia. Knees were dissected down to the joint capsule, both menisci of both knees removed, and 13 4-mm cores taken with a biopsy punch. We divided samples into three groups based on location: meniscal samples cored from the regenerated tissue of the scaffold region (SC), from native meniscal tissue from the anterior and posterior horns adjacent to the implanted scaffold region of the right knee (AJ), and native meniscus from the contralateral intact knee (CL) (Figure 5.1). Cores were flash-frozen in liquid nitrogen and stored at -20º C until testing. Immediately before testing, we thawed samples in a hydrating bath of phosphate-buffered saline (PBS) (Invitrogen, Carlsbad, CA) supplemented with a protease inhibitor cocktail (complete protease inhibitor cocktail; Roche Applied Science, Indianapolis, IN) and cut to 2-mm thickness.

During testing, we submerged tissue samples in a lubricant bath of either PBS with protease inhibitor or equine synovial fluid (ESF). Bovine and equine synovial fluid lubricate bovine cartilage similarly[48] and the relative abundance of synovial fluid in the equine joint (several millimeters compared with trace amounts in ovine and bovine joints) make it particularly attractive as a lubricant. ESF was aspirated from the leg joints of four skeletally mature, healthy horses immediately after euthanasia (College of Veterinary Medicine, Cornell University, Ithaca, NY). Contaminant and blood-free aspirates were pooled and stored at -20º C. Before friction testing, we thawed ESF aliquots in a water bath at 37°C.

The scaffold constructs and native tissue controls were tested in a custom friction apparatus previously described[49]. Briefly, the linearly oscillating friction apparatus placed a normal strain on the tissue and regulated the relative speed between samples and a counterface. In this study, we used smooth polished glass as a counterface. A custom biaxial load cell simultaneously measured the normal and frictional shear loads on the sample. The resulting equilibrium friction

coefficient (μ_{eq}, the ratio of the normal load to the shear load when the engineered sample has fully relaxed from the applied normal strain) was calculated through a custom MATLAB (Natick, MA) code.

We created a Stribeck surface[48] to determine the entraining speeds and normal strains that produce boundary and mixed lubrication modes for native meniscus. Because lubricant greatly affects the transitions between lubrication modes, this was performed as follows for meniscus both lubricated with PBS and with ESF. Samples were loaded in the apparatus while submerged in a PBS bath. We applied a normal strain of 10% and the samples were allowed to equilibrate for 40 minutes. This time was to permit the normal stress to come to equilibrium and was determined from preliminary studies. We then oscillated the meniscal samples against the counterface glass in a series of 10 entraining speeds. A further step increase of 10% strain was applied and the equilibration-oscillation process repeated up to a maximum of 40% strain. The resulting region of speed/strain space that yielded maximal μ was considered boundary lubrication.

For all explants, we measured μ_{eq} over a range of speeds from 0.2 mm/s to 30 mm/s and normal strains from 10% to 40%. Samples were removed from the apparatus and allowed to relax for 40 minutes while submerged in PBS. We then repeated the strain and oscillation sequence with the samples in an ESF bath.

We determined boundary and mixed mode μ_{eq} relative to native meniscus. From the Stribeck curve for native meniscus in PBS, a representative value for boundary mode was selected at 40% strain, 0.2-mm/s entraining speed, and mixed mode at 10% strain and a speed of 10 mm/s. All samples were measured at these conditions. The equilibrium stress relaxation profile resulting from the unconfined compression in 10% strain step increments were fit to a poroelastic model[76]

and used to calculate equilibrium modulus (H_A) and permeability (κ) as described previously[50], from the normal loads recorded during the unconfined compression equilibrium relaxation period. For comparison purposes, lubrication properties of the unimplanted scaffold are included; their measurement has been previously described[49].

All data are presented as mean ± SD. We determined the effect of lubricant, location, and implantation time on μ_{eq} using a series of two-factor analysis of variance with Tukey's honestly significant difference post hoc test. Comparison of H_A and κ was done by one- factor analysis of variance. All analyses were carried out using SigmaStat (SPSS Inc, Chicago, IL).

5.4 Results

Native meniscus tissue lubricated by PBS and by ESF exhibited frictional behavior well described by Stribeck surfaces. Normal force exerted by both native and engineered tissue changed with time in typical stress-relaxation behavior (Figure 5.2); native tissue and 6-month explants showed similar characteristics with similar final load, whereas 3-month explants reached equilibrium much faster than native values. The boundary mode regime is visible in the small region of maximum μ_{eq} and the larger mixed lubrication mode where μ_{eq} is varying (Figure 5.3A). Comparatively, μ_{eq} for explanted SC were overall higher both in PBS and ESF (Figure 5.3B). The zone of maximal μ_{eq} indicating boundary lubrication mode extended over a much larger strain-speed space than the native meniscus.

μ_{eq} measured in boundary mode conditions for almost all samples and time points was lower in ESF compared with PBS (Figure 5.4). Native meniscus was more effectively lubricated by ESF with a boundary mode μ_{eq} approximately 30% of its PBS μ_{eq} at 3 months. For native meniscus mixed mode lubricating conditions (Figure 5.5), μ_{eq} showed similar but less pronounced trends than

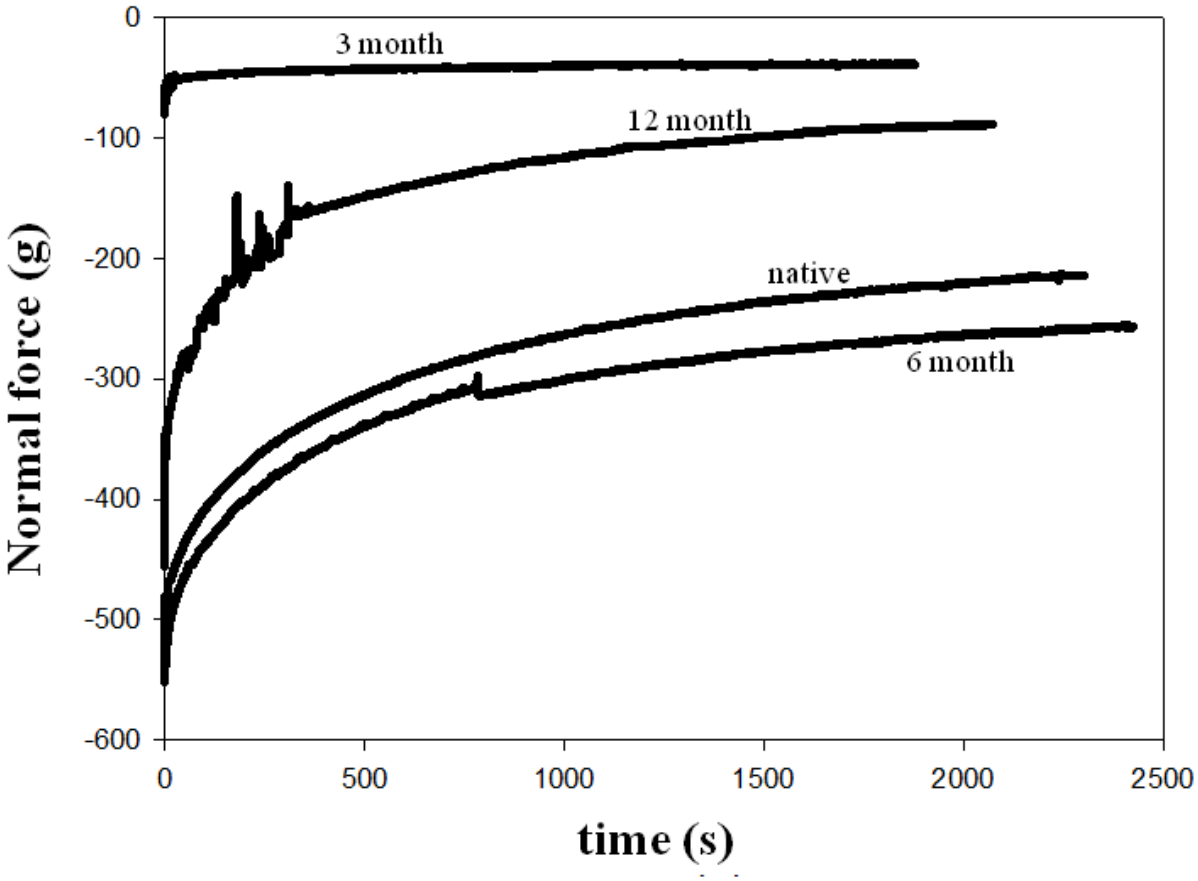

Figure 5.2 Normal force as a function of time for 3-, 6-, and 12-month explants and native meniscus. Repair tissue shows cartilage relaxation behavior, with much higher equilibrium values and longer time to equilibrium values for explanted tissue

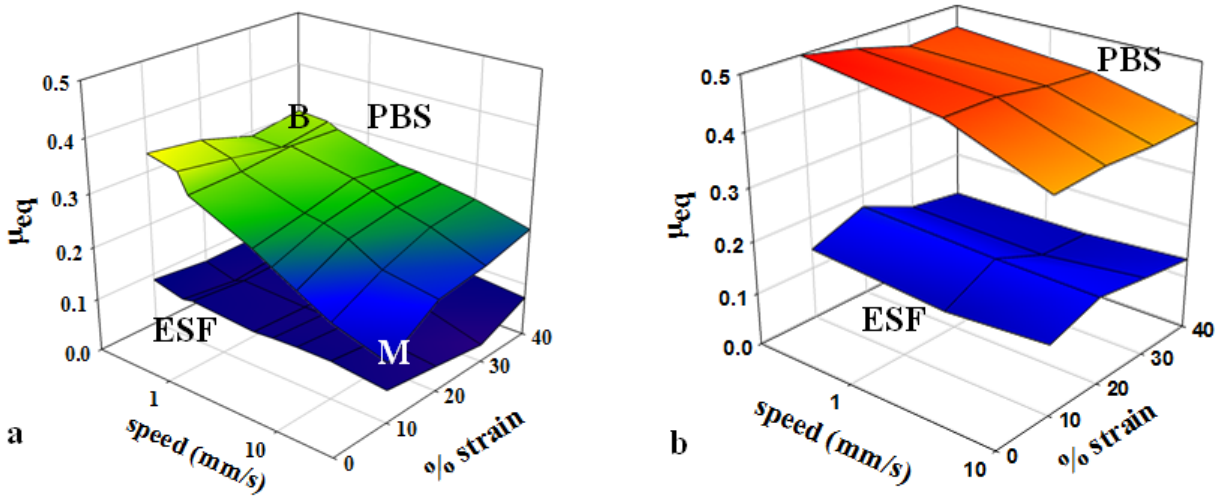

Figure 5.3 Stribeck curves in phosphate-buffered saline (PBS) (upper surface) and equine synovial fluid (ESF) (lower surface) for (a) native meniscus and (b) 3-month scaffold explants. B indicates speed/strain used to compare boundary mode and M mixed mode. Native and engineered meniscus show Stribeck behavior with higher μ_{eq} for PBS compared to ESF and transitions from boundary to mixed mode

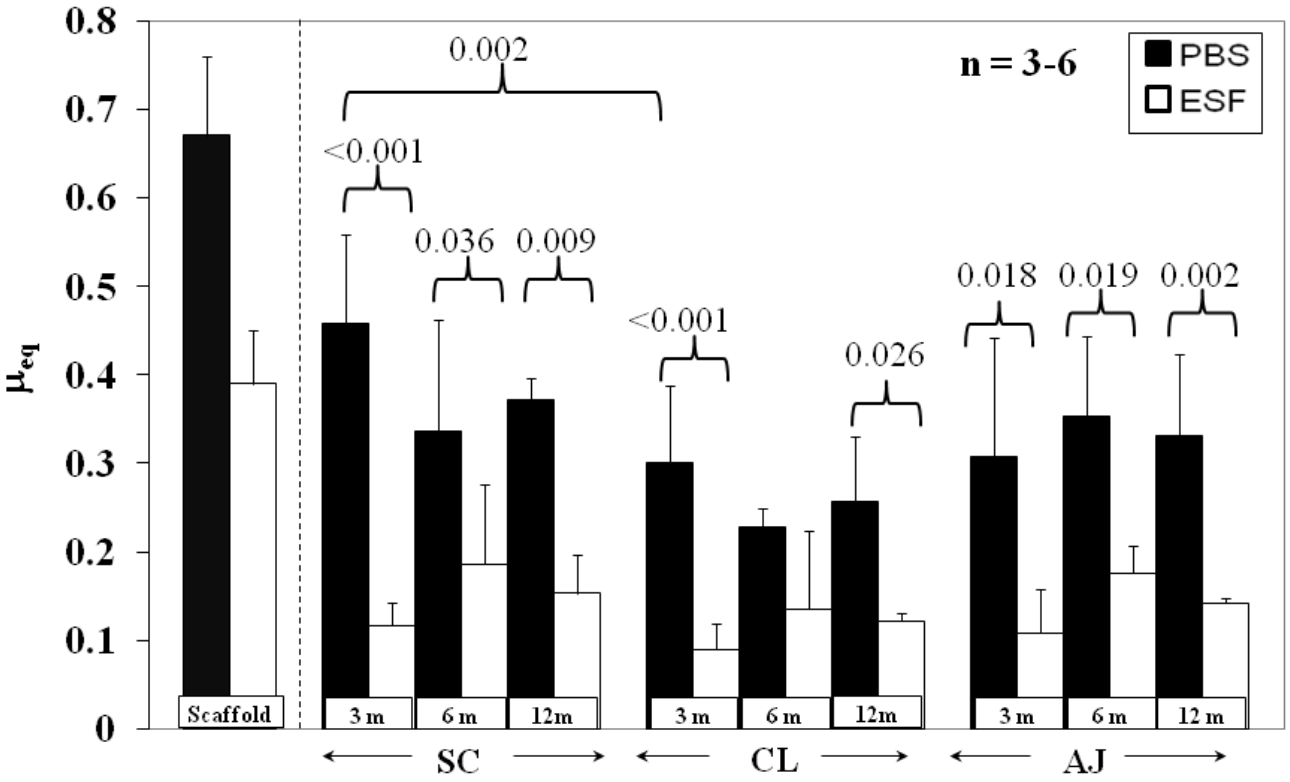

Figure 5.4 μ_{eq} for native and engineered cartilage explants at all time points measured at ε = 40%, v = 0.2 mm/s, equivalent to boundary mode lubrication in native meniscus. Mean ± SD. Scaffold refers to unimplanted scaffold taken from Gleghorn et al. [49]. PBS = phosphate-buffered saline; ESF = equine synovial fluid; SC = scaffold region; AJ = native meniscal tissue adjacent to the implanted scaffold; CL = native meniscus from the contralateral intact knee. Boundary μ_{eq} changes with time and is significantly lower for ESF compared to PBS.

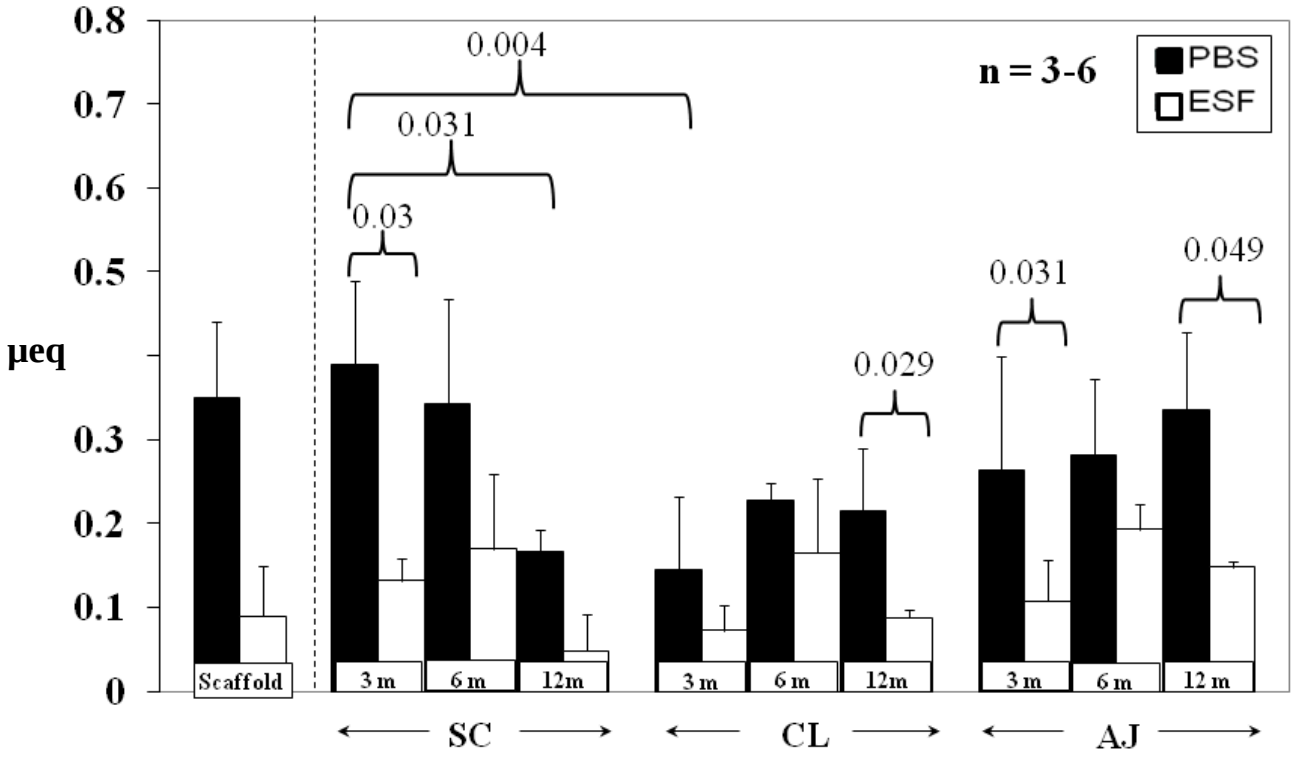

Figure 5.5 μ_{eq} for native and engineered cartilage explants at all time points measured at ε = 10%, v = 10 mm/s, equivalent to mixed mode lubrication in native meniscus. Mean ± SD. Scaffold refers to unimplanted scaffold, taken from Gleghorn et al. [49]. PBS = phosphate-buffered saline; ESF = equine synovial fluid; SC = scaffold region; AJ = native meniscal tissue adjacent to the implanted scaffold; CL = native meniscus from the contralateral intact knee. Mixed μ_{eq} is generally lower for ESF compared to PBS

in boundary mode conditions. μ_{eq} in PBS was higher than in ESF for several times and locations, e.g. SC at 3 months ($p = 0.03$) and CL at 12 months ($p = 0.029$).

μ_{eq} also changed with implantation time. For SC explants in PBS, boundary μ_{eq} decreased ($p = 0.006$) with time, dropping to 0.46 ± 0.06 at 3 months and subsequently to 0.34 ± 0.13 at 6 months (Figure 5.4). At both 6 and 12 months, μ_{eq} of SC implants was approximately 0.35 in PBS. By 3 months, μ_{eq} had decreased ($p = 0.007$) to 0.12 ± 0.03 in ESF, a 69% drop from 0.39 at 0 months. At 6 and 12 months, μ_{eq} of SC implants was approximately 0.15 in ESF. Starting at 6 months, there was no difference ($p = 0.877$) between SC μ_{eq} values in either ESF or PBS for any subsequent time point nor were these two values different ($p < 0.001$) from either native tissue location. In mixed mode μ_{eq} of SC samples in PBS dropped from 3 to 12 months ($p = 0.031$) and was also higher than for CL 3 month samples ($p = 0.004$) (Figure 5.5). All native CL and AJ tissue was not different.

Tissue infiltrated the replacement scaffold as evidenced histologically by hematoxylin eosin staining (Figure 5.6). At two weeks post operation little extracellular matrix is visible (animal died from unrelated causes), while at 3 and 12 months significant staining is apparent. At 3 months, H_A was 132 ± 25 kPa, changing to 387 ± 260 kPa at 6 months and 192 ± 90 kPa at 12 months (Table 1). Native meniscus was 466 ± 191 kPa, measured in CL samples. Permeability trend was higher for SC compared with CL samples, 1.01×10^{-14} to 2.56×10^{-14} m^4/Ns for SC at 40% strain compared with 2.71×10^{-15} m^4/Ns in native meniscus, however due to high variability in these samples no statistically significant difference was found. Relaxation times (μ_{eq}) varied between 21 and 334 seconds for SC samples with strains of 10% to 40%.

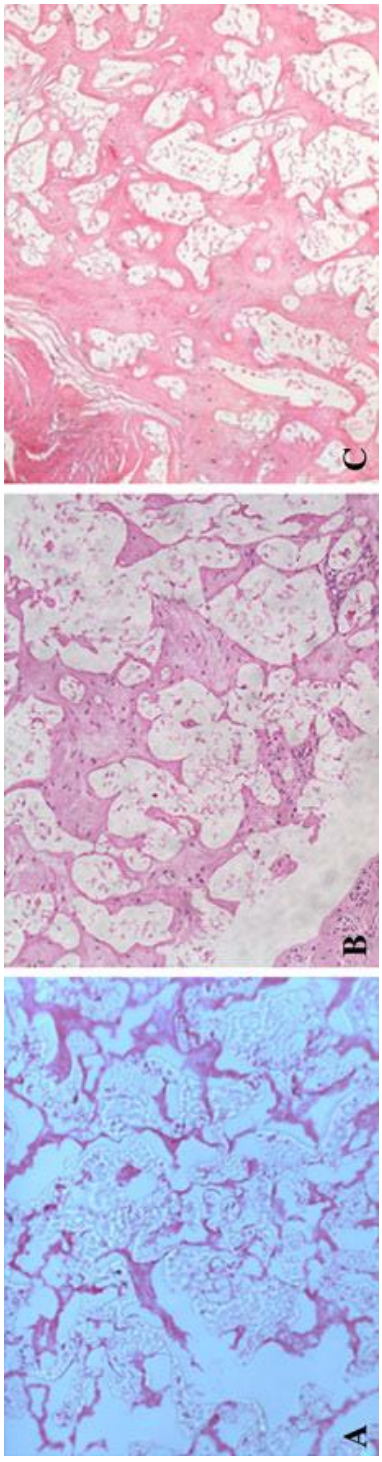

Figure 5.6 H.E. staining of SC samples at a) 2 weeks, b) 3 months, and 12 months. Progressive tissue ingrowth occurs over the course of 1 year in vivo

Mechanical Property	3 month (n = 4)	6 month (n = 3)	12 month (n =4)	Native (n = 9)
H_A (kPa)	132 ± 25	387 ± 260	192 ± 90	466 ± 191
k (10% strain)	3.38E-14 ± 1.52E-14	2.66E-14 ± 1.83E-15	1.20E-13 ± 3.87E-14	3.05E-14 ± 2.86E-15
k (20% strain)	1.91E-14 ± 8.92E-15	1.44E-14 ± 1.17E-14	5.43E-14 ± 4.31E-14	8.83E-15 ± 6.26E-15
k (30% strain)	1.50E-14 ± 4.36E-15	1.50E-14 ± 1.27E-14	4.29E-14 ± 3.58E-14	3.66E-15 ± 2.37E-15
k (40% strain)	1.42E-14 ± 1.45E-14	1.01E-14 ± 7.61E-15	2.56E-14 ± 2.46E-14	2.71E-15 ± 2.29E-15

Table 2 Mechanical properties of meniscal scaffold with implantation time. Compressive modulus (HA) and hydraulic permeability (k) of meniscal repair tissue at 3, 6, and 12 months compared to native meniscal tissue from the contralateral knee

5.5 Discussion

A complete knowledge of the mechanical behavior of a scaffold when implanted into a defect is essential in predicting its ability to protect the surrounding tissues from further degradation. With meniscal replacement design, understanding the tribologic behavior of the meniscus and meniscal replacements is necessary to effectively design scaffolds for implantation. We therefore sought to quantify the friction behavior of both native and engineered meniscal repair tissue that resulted from implantation in vivo. The goals of this study were to determine if Stribeck surface analysis can characterize the frictional behavior of native meniscus, assess if replacement material can be lubricated by synovial fluid, and determine if friction and mechanical characteristics of the engineered scaffold change with time and tissue ingrowth into scaffolds implanted in meniscal defects in sheep over the course of 1 year.

We caution readers of limitations of our study. The primary limitation is the low power used in this small number large-animal study. As a result we may be underreporting the significant changes that occurred to the meniscal implants in vivo.

Native meniscus tissue lubricated by PBS and by ESF exhibited frictional behavior well described by Stribeck surfaces, which have been used to visualize cartilage lubrication modes in native cartilage[48] and porous materials used in cartilage replacement[49]. In the case of solid tribologic materials a relationship between porosity and friction has already been shown[56]. Similarly, in this study the frictional properties of the resultant tissues change with the porosity and permeability changes caused by ingrowth into the meniscal scaffold. The higher porosity and pore size of polyurethane foams compared with cartilaginous tissues presumably limit its ability to maintain a pressurized fluid film at the meniscal surface. This is shown in the region of maximal μ_{eq} boundary mode friction that is broader for SC samples at 3 months than native

tissue (Figure 5.3B). Three-month SC Stribeck surfaces are different from both unimplanted foam[49] and native meniscus (Figure 5.3). This may indicate that the early repair tissue has an intermediate permeability and can sustain a lubricating fluid film over different tribologic conditions. Tissue explanted at 3 months showed a response to loading that was different from both later time points or native meniscus (Figure 5.2), reaching equilibrium much more quickly. This is in accordance with the high permeability and the higher μ_{eq} in both conditions corresponding to native mixed (Figure 5.5) and boundary (Figure 5.4) modes at this time point.

Several studies show synovial fluid is a more effective lubricant than saline on cartilage[16, 17, 44, 45, 113, 114] and for some engineered tissues[50]. Our data are in agreement: ESF enhanced lubrication for all tissues at all times. Lower μ_{eq} in ESF than PBS indicates the efficacy of ESF as a boundary lubricant for repair tissue as well as native meniscus. Partial meniscal replacement with a porous polyurethane scaffold reportedly restores mean contact pressures to those of the intact knee and improves peak contact pressures and mean contact area relative to a partially meniscectomized knee while under physiological loading[11]. The similarity of μ_{eq} of CL and AJ samples in this study is in agreement with this; the frictional behavior of the native meniscus adjacent to the implants was not adversely affected by scaffold placement.

In this study, the μ_{eq} of native meniscus boundary mode conditions of engineered meniscus improved with time and was similar to native tissue after 6 months (Figure 5.4). Tissue ingrowth into the scaffold may also have caused a drop in μ_{eq} as a result of the extracellular matrix produced by infiltrating cells that may enable binding and localization of lubricating biomolecules. Interaction between matrix and synovial fluid components would account for the precipitous drop in boundary μ_{eq} in ESF after 3 months. A likely candidate is lubricin, a glycoprotein found in the synovial fluid that binds to the surface of cartilage in articular joints[62,

[72, 113] and is the best predictor of lubricating function in engineered cartilage[50]. It has been proposed that lubricin serves as the primary boundary lubricant in articular joint lubrication and possibly acts synergistically with hyaluronic acid[6, 19, 43, 66, 69, 113]. Trends in mixed-mode frictional properties of both native and replacement meniscal tissue were generally similar to their boundary mode behavior. Overall mixed μ_{eq} was lower than boundary μ_{eq}, as expected.

In addition to affecting the mechanical properties, the mechanical properties of the repair tissue were likely influenced by the tissue ingrowth which occurs in this material[103, 130, 131]. This could affect the properties in at least two ways. First, infiltration of the artificial scaffold would have the effect of decreasing porosity and pore size, which would result in decreasing permeability. This is supported by the change in the characteristic high permeability and fast relaxation times (μ_{eq} less than 30 seconds up to 40% strain[49]) of unimplanted polyurethane foams that were absent in the implanted scaffolds; at 6 months, relaxation times were 95, 125, 184, and 323 seconds at 10%, 20%, 30%, and 40% strains, respectively. The values we recorded well match previously reported μ values for sheep[74], and this corresponds to decreases in κ of up to 28%. Tissue ingrowth is also indicated by changes in aggregate modulus; at 6 months, H_A had increased to 387 MPa and was 192 at 12 months, which, although lower than 6 months, was still an improvement over the value at 3 months (Table 1). With implantation, scaffold properties (Table 1) and structure (Figure 5.6) had changed to become more cartilage-like. The decrease in κ with increasing strain in the engineered menisci is consistent with patterns of poroelastic behavior exhibited by various types of cartilage.

This study of a year-long in vivo meniscal implant has provided a more complete understanding of the frictional response of meniscal repair tissue. The high friction coefficient of polyurethane scaffolds changed with implantation, decreasing to near native values after 6 to 12

months in vivo. Our observations suggest that by promoting tissue ingrowth into porous scaffolds, meniscal repair tissue can attain similar frictional properties to native meniscus.

CHAPTER 6

6 CONCLUSIONS

Alterations to the tissue and synovial fluid due to disease or injury can include changes in viscosity, composition, modulus, and surface features which all may influence the lubrication of the tissue due to differences in the ability to sustain fluid films and to lubricant-cartilage interactions. The studies here elucidate the importance of synovial fluid components and tissue structure in cartilage tribology as well as identify lubrication mechanisms of cartilage in various states of disease progression and injury.

This dissertation presents investigations of the boundary mode friction coefficient of injured cartilage and the role of lubricin in mediating and repairing surface damage. Chapter 2 investigated the role of lubricin in preventing surface damage of mechanically injured cartilage when introduced as an in vitro lubricant. Chapter 3 detailed the chondroprotective role of lubricin when injected intra-articularly in vivo to treat mechanically damaged cartilage. Chapter 4 examined changes in friction behavior of enzymatically damaged cartilage and Chapter 5 looked at a possible repair strategy for injured meniscus.

Chapter 2 documented friction changes to injuriously compressed cartilage. The most significant outcome of this chapter was the identification of a purely mechanical mechanism of OA initiation following mechanical injury, which could be prevented by the introduction of exogenous lubricin. An important experimental finding was a confirmation that neither axial compression nor friction associated with cartilage shear alone are capable of causing fibrillation and damage, but rather it is the combination of both these forces that is necessary. This axial impaction has a strain rate threshold before it becomes degenerative, and the subsequent damage

is highly focal and inhomogeneous. This damage was preventable if lubricin was introduced, at a minimum concentration that we determined, but was not preventable of lubricin was absent from the system. These data offer an improvement in our basic understanding of OA initiation following cartilage injury.

The study in Chapter 3 demonstrated that an rh-lubricin mutant lowers cartilage coefficient in an in vivo model of cartilage injury. The results show that introduction of lubricin following mechanical injury in vivo prevents the increase in boundary mode friction that otherwise occurs. In addition, lubricin injection reduced the amount of surface damage to the cartilage. This study builds on previous work in this animal model that shows that the introduction of exogenous LUB:1 is chondroprotective[40], and shows that its use improves mechanical function of injured cartilage.

A link between cartilage permeability and tribological function was proposed in Chapter 4. Rather than increasing the boundary mode friction value, GAG loss from the upper surface caused by trypsin degradation drastically increased the amount of time that cartilage was in the boundary mode. This effect has direct implications to injured tissue. These findings suggest 1) that controlling permeability of engineered tissues may be critical for proper lubricating function and 2) that the production of matrix that is capable of localizing lubricin may be essential to proper functioning of these constructs due to the increased boundary mode friction experienced by the tissue.

The studies in Chapter 5 demonstrate a repair model of damaged cartilaginous tissues. The major finding of this study is that permeable scaffolds are able to achieve native tissue-like properties with implantation time. This improvement is made possible by the repair tissues' ability to produce and localize lubricin.

This work focused on investigating the functional tribological implications on mechanical changes caused by injured cartilage. These studies confirm that boundary mode frictional properties are very prominent in the tribological environment of damaged cartilage (Chapter 4) and the combination of this boundary friction with joint insult together contribute to surface fibrillation (Chapter 2). This early surface damage can be prevented by exogenous recombinant lubricin (Chapters 2 and 3) in both its full length (Chapter 2) and truncated forms (Chapter 3) and which has the ability to alter the frictional properties of articular cartilage. In addition this protection is dose-dependent (Chapter 2) and may even have the ability to repair cartilage that has been roughened due to absence of either of these boundary lubricants in their healthy concentrations (Chapter 3). The repair of tribologically functional cartilaginous tissue occurs with tissue ingrowth that allows for the localization of lubricin to the surface layer (Chapter 5).

The major contribution of this work is the improvement of our understanding of how cartilage lubrication and injury are linked. This can be expressed in context of the Stribeck curve discussed in Chapter 1. Chapters 2, 3 and 5 discuss disruptions to the cartilage that have the effect of shifting the value of the boundary mode coefficient of friction up and down, shown in blue in Figure 6.1. Mechanical injury causes a host of changes in the joint, including depleting the surface layer of chondroprotective lubricin on the articular surface[70]. In injury Chapters 2 and 3 we see that the injury shifts the flat part of the curve upwards, increasing maximum μeq. The result is increased shear on the damaged tissue, and subsequently increased wear and damage. Conversely, introduction of a lubricant shifts the flat part of the curve downwards, shown in Chapters 2, 3, and 5 in different animal models. In Chapter 3 we demonstrate that this shift can restore the boundary μeq to its original value.

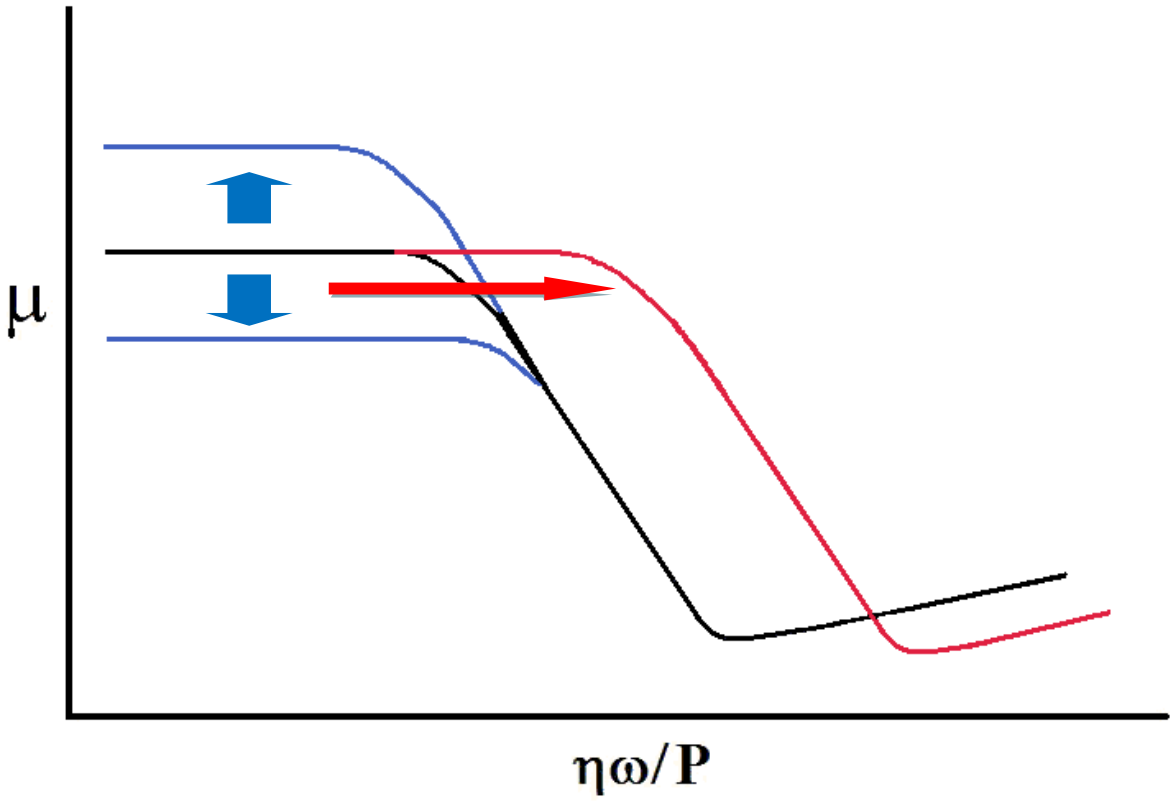

Figure 6.1 Schematic of a Stribeck curve illustrating the shifts in cartilage lubrication behavior caused by injury.

Chapter 4 suggests a completely different effect on the Stribeck curve due to disruption of the proteoglycan network of the cartilage. Rather than shifting the value of boundary μeq, this disruption shifts the range of conditions that produce this maximal value, indicated in red in Figure 6.l. Increased permeability due to protein digestion makes it more difficult for the cartilage to support the necessary fluid film that otherwise protects the cartilage. This lack of fluid film increases the likelihood that the affected cartilage is experiencing boundary tribological conditions, and subsequently increased wear and damage.

This later mechanism of increased boundary mode occurrence is distinct from that of increased boundary mode value, but likely interconnected. High μeq and surface roughening are linked (Chapter 2) and the high μeq will eventually increase surface roughness and consequently in turn the value of boundary μeq. Thus the changes due to increased boundary mode exposure will eventually cause a further increase in boundary mode value.

6.1 Study limitations

The studies in this dissertation do have several limitations that should be considered when interpreting their results. First, concerning the in vitro work, one must of course be careful in applying the results of a carefully controlled explant study to the complicated in vivo environment where multiple factors contribute to the mechanism of lubrication.

Like many other cartilage lubrication studies, one limitation of the studies of this dissertation is the use of immature bovine cartilage. This tissue has a pristine surface and has seen little use, and may not be directly translatable to human cartilage. Future work should examine if the results shown in this dissertation are applicable to human tissue.

Cartilage degradation and damage propagation is a multifaceted process, and while the mechanics of its lubrication as relates to the upper zone only is discussed here, there are other

factors that should be considered. The changes in bulk properties following cartilage impaction such as variations in modulus and water content[83] are indications of the sub surface damage that is also unfolding. While these effects are not investigated here, it is reasonable to assume that influence on the articular surface and frictional response of the tissue is considerable and not to be neglected in a full understanding of mechanics of cartilage damage.

Also to be considered is the effect of damage on chondrocytes. Cartilage injury has been shown to cause apoptosis[132], and recent work has shown that lack of boundary lubrication is implicated in cell death as well[135], where a link between apoptosis and lubricin staining intensity was found, indicating a role of lubricin in preventing apoptosis.

6.2 Future directions

There are many unanswered questions in the field of cartilage lubrication that this dissertation did not address. With respect to the in vivo work there are many questions remaining about the efficacy of intra-articular lubricin injection. Here we showed that three times a week injection of LUB1 a week after injury was able to partially recover the smoothness of the articular surface and to completely recover the boundary friction coefficient. However we do not know how these variables change in the longer term, nor which is the most effective lubricin concentration or dosage frequency.

Patients typically seek treatment 1 week following joint injury, which is the beginning of the treatment cycle in the study here. Future studies should examine if lubricin injection is beneficial if treatment is not sought for two, four, six weeks or longer. In addition to determining the cut-off time for clinical application, studies should examine the binding mechanism for lubricin. Much is still unclear concerning the how the molecule attaches, and a valuable contribution to

the literature would be determining if lubricin will attach to cartilage already in later stages of osteoarthritic development and if not how it can be induced to do so.

In contrast to seeing how late lubricin can be injected into the joint and still see improvement an interesting question to be asked is whether you can prevent surface roughening completely by introducing exogenous lubricin immediately following the cartilage insult. The results from Chapter 2 where this was done in vitro indicate that this may be the case and a future study should determine if this is possible in vivo as well.

The interaction between lubricin and HA was touched upon in Chapter 2, but many questions remain. HA has been implicated in boundary lubrication and based upon the complexity of cartilage lubrication and the joint environment one could expect that HA and other SF molecules can enhance or inhibit lubricin boundary lubrication. Future studies should map out the full cartilage behavior of these molecules independently and together.

APPENDICES

A. SUPPLEMENTAL RAT DATA

The roughness values and distribution of both injured and control rat cartilage were very different compared to the previously documented immature bovine cartilage. Shown here are additional rat roughness analyses from Chapter 3.

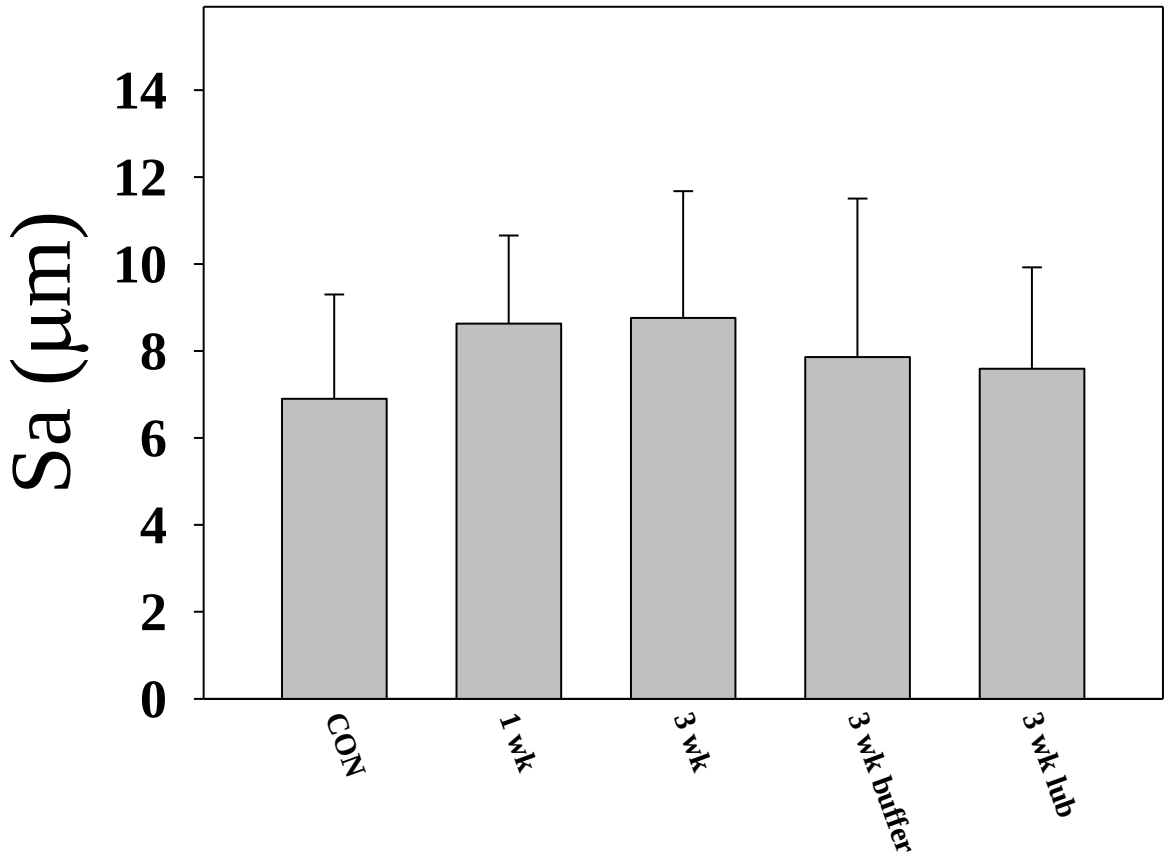

Figure A 1 Average roughness (Sa) for the various rat treatment groups, control, injured with no treatment evaluated at 1 week (1wk) and at 3 weeks (3 wk), with PBS buffer injection treatment (3 wk buffer) and lubricin injection treatment (3 wk lub).

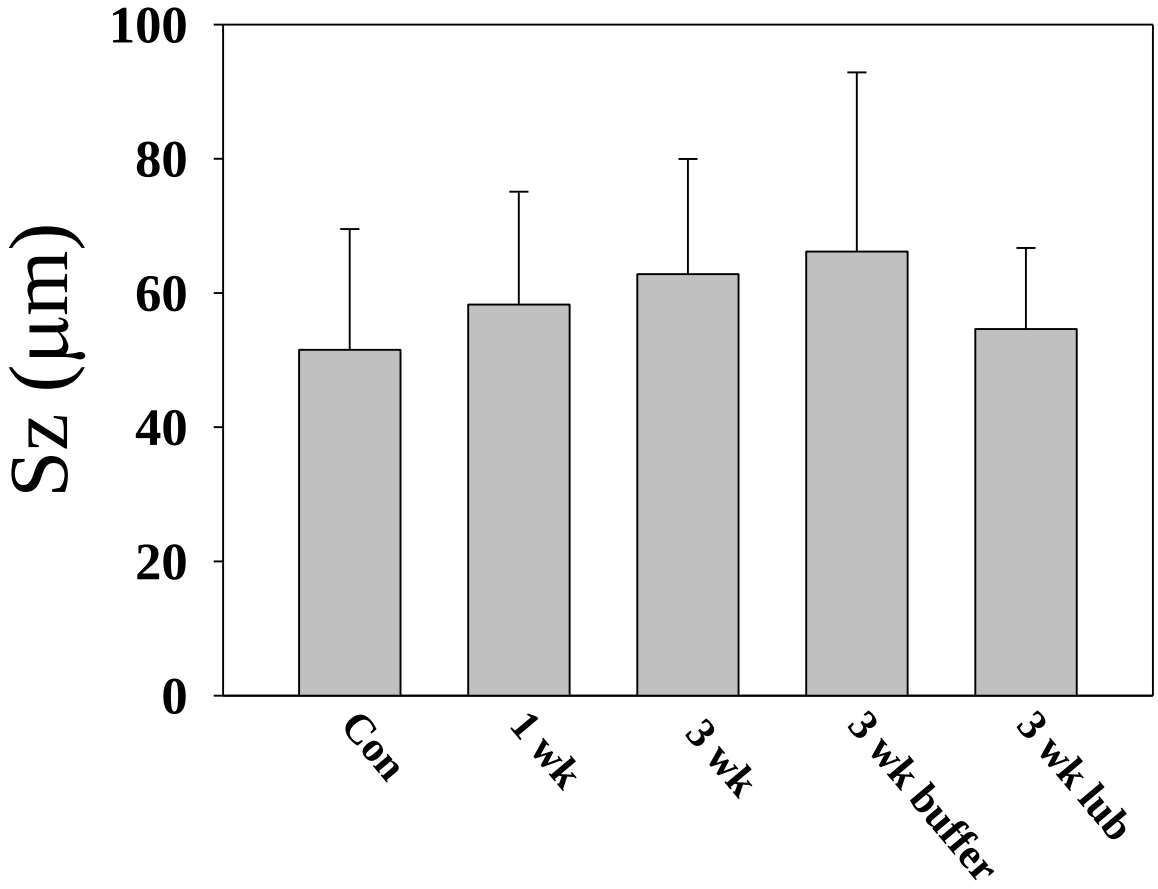

Figure A 2 5 point range of roughness (Sz) for the various rat treatment groups, control, injured with no treatment evaluated at 1 week (1wk) and at 3 weeks (3 wk), with PBS buffer injection treatment (3 wk buffer) and lubricin injection treatment (3 wk lub).

B. FINITE ELEMENT ANALYSIS OF ENZYMATICALLY DEGRATED CARTILAGE USING COMSOL

Finite element models of cartilage plugs undergoing uniaxial unconfined compression were created using COMSOL MULTIPHYSICS software (COMSOL, Burlington, MA). The model was of a two dimensional axisymmetric cartilage plug, 3 mm in radius and 2 mm thick. The model was used to estimate the mechanical environment resulting from an applied uniaxial unconfined step strain followed by stress relaxation. A ramped step load Heaviside function was applied, corresponding to a 10% step function as applied experimentally.

To model the fluid- solid interaction in the cartilage, a time dependant coupled pore pressure/effective stress analysis was implemented using the structural mechanics and chemical engineering modules of COMSOL[2]. In the structural mechanics engineering module the solid mechanics governing equations were used and combined with Darcy's law in the chemical engineering module. The governing equation for transient Darcy flow was set to depend on fluid density, solid fraction, and fluid velocity, which was dependent on the solid permeability, fluid viscosity, and pressure gradient. Scaffold solid deformation depended on the normal, shear stresses, and strains imposed on the models as a result of the load. The plane strain deformation was coupled to Darcy flow using a source term.

To replicate the effect of enzymatic digestion a two-layered axisymmetric construct was implemented, with differing properties between the two layers and continuity at the interface. The total height of the construct was held constant at 2 mm, with the height of the top layer changed to represent differing trypsin exposure times, according to Figure 4.2. The boundary conditions allowed displacement to occur freely at the top loaded surface and along the radial direction, but were fixed along the axial direction at the bottom surface. The tissue solid material

was assumed to be homogeneous and isotropic with strain dependent permeability and a porosity of 70%, a Poisson's ratio of 0.125 and an average solid density of 7850 Kg/m^3. The scaffolds were hydrated with fluid with density of 1000 Kg/m^3.

For the bottom layer representing healthy cartilage, modulus was 700 kPa, a hydraulic permeability of 7.6 $e10^{-15}$ m^4/N s. Trypsin degradation was assumed to completely deplete the proteoglycans in the affected cartilage volume, resulting in modulus reduced by an order of magnitude and a permeability increased by a factor of 15^7. Values are summarized in Table 2. The finite element simulations were run for 3000 s, at which time steady state was achieved. Representative images of the deformed cartilage multi-layer plugs are shown in Figure A1.

	Bottom layer – Healthy cartilage	Top layer – digested cartilage[2]
E (kPa)	700	70
ν	0.125	0.125
α (1/K)	$1.2\ e^{-5}$	$1.2\ e^{-5}$
ρ (kg/m^3)	7850	7850
ε (kg/m^3)	0.7	0.7
κ (m^2)	7.63^{-15}	1.14^{-13}

Table A 1 COMSOL mechanical and fluid parameters of cartilage layers

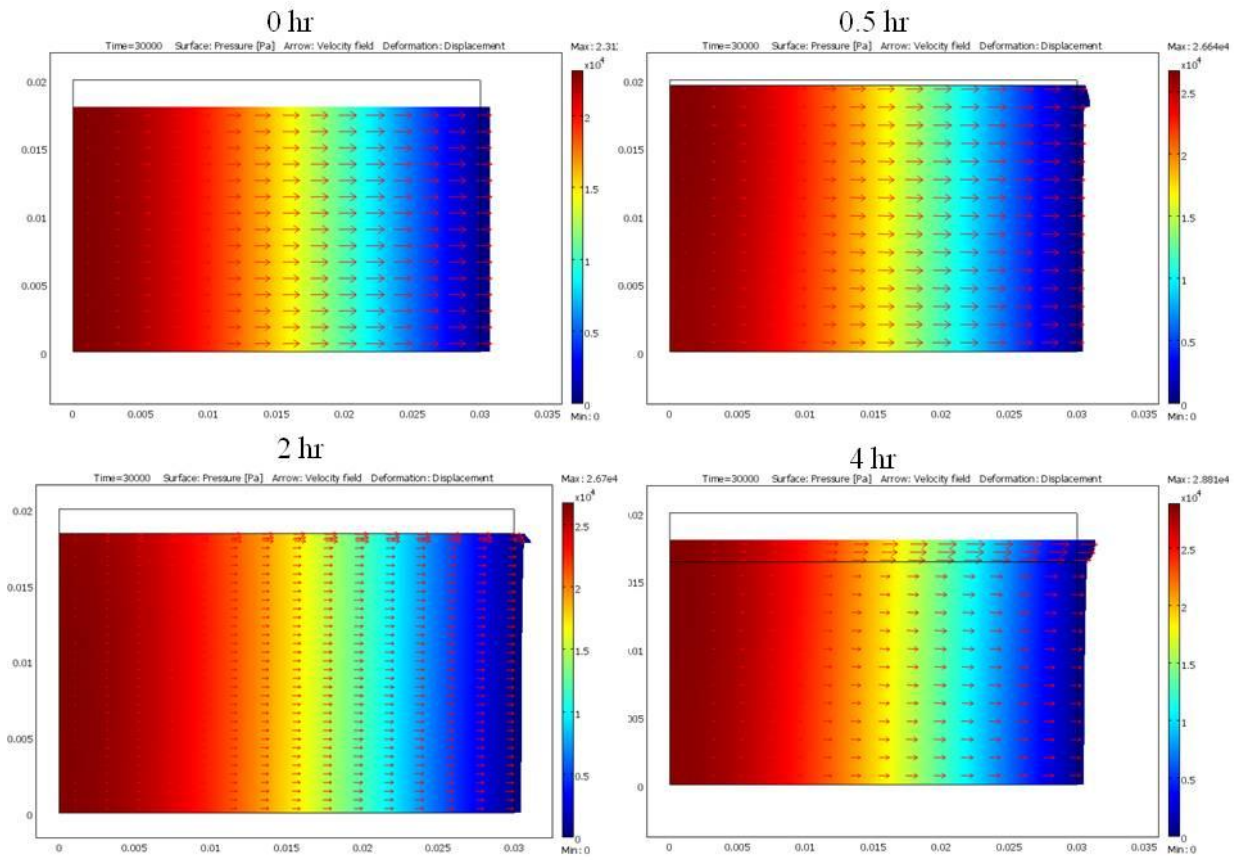

Figure A 3 COMSOL finite element results of pressure (color field) and fluid velocity (red arrows) at steady-state.

C. IONIC ENVIRONMENT AFFECTS THE AGGREGATION AND LUBRICATION BEHAVIOR OF RECOMBINANT HUMAN LUBRICIN

Introduction

Lubricin, also known as superficial zone protein and PRG4 is a secreted, water soluble, mucinous glycoprotein found in synovial fluid that is primarily responsible for boundary lubrication of articular cartilage. Structurally lubricin (~240kDa) has C- and N- domains and is amphiphilic with a hydrophilic central mucin-like domain that is negatively charged and heavily glycosylated, while the end domains are hydrophobic and positively charged[19].

Lubricin's behavior is a result of its multiple functional domains. The N and C terminals are believed to play a role in aggregation in surface binding, respectively[72]. This characteristic is a critical property of a boundary lubricant when the contacting surfaces are under high force yet the lubricant must remain adhered to the surface. The central mucin domain is responsible for the lubrication properties of the protein[67]. A recombinant form of human lubricin has been developed that is structurally identical to native lubricin but with a truncated central lubricating region. This derivative known as LUB:1 has been shown to decrease lesion size in osteoarthritic rats[40].

Lubricin is known to bind to a variety of substrates, but the lubricin-cartilage interaction and the molecule's configuration on the cartilage surface are not yet fully understood. Although we know lubricin binds and lubricates both negatively and positively charged and hydrophobic and hydrophilic substrates[138] with varying ability, very little is known about how the protein's aggregation and surface conformation affect its ability to lubricate tissue. We hypothesize that ionic environment affects LUB:1's aggregation behavior, which will affect its lubrication ability.

Therefore the goals of the current study are to use AFM to examine the aggregation of LUB:1 under different ionic conditions and to examine their effect on frictional performance.

Methods

Full thickness 6 mm diameter cylinders of articular cartilage were cut from the patellofemoral groove of 1-2 week old cows with the superficial zone left intact. Friction testing occurred at relative velocity = 0.3 mm/s and normal strain = 25% in a custom friction apparatus. In brief, the linearly oscillating friction apparatus placed a normal strain on the tissue and controlled the relative speed between samples and an articulating glass surface. A custom biaxial load cell simultaneously measured the resulting normal and frictional shear loads on the sample. The resulting equilibrium friction coefficient (μ_{eq}) was calculated as the ratio of the normal load to the shear load when the tissue has fully relaxed from the applied normal strain. μ_{eq} was measured after 30 min of stress relaxation. During friction testing tissue samples were submerged in varying LUB:1 concentrations in PBS, 200 mM NaCl, or 200 mM arginine, with the enhanced ionization expected to interfere with aggregation.

Silicon chips were plasma cleaned to enhance bonding between the silicon oxide layer and lubricin. 100 µL of 3-aminopropyltriethoxysilane (APTES) was deposited and then incubated at 80ºC for 90 minutes to induce the negatively charged molecule to adhere to the substrate. 10µL of LUB:1 of varying concentration was deposited and then incubated at room temperature for up to 20 minutes and then rinsed. Atomic Force Microscopy (AFM) images were taken (at ambient temperature and humidity) in dry tapping mode at a scan rate of 1Hz, cantilever oscillation driven 5% offset from resonance, and maximum 512 pixel resolution.

Results

Friction data shown are means with N = 4 for each buffer at each concentration. A four parameter sigmoidal function was fit to each curve as shown by the solid lines (Figure 1A-C) which fit the PBS friction data well (R^2 = 0.900, Figure 1D) and NaCl and arginine less well (R^2 = 0.755 and 0.575 respectively). At low LUB:1concentrations max μ_{eq} was ~0.20, while the transition to min μ_{eq} indicated by EC_{50} was ~9 μg/ml for PBS and ~2.8 μg/ml for NaCl and arginine.

AFM images show lubricin molecules on a silicon substrate (Figure 3). Buffer type had an effect on conformation, with LUB1 in PBS appearing in large clumped aggregates while in 200 mM NaCl and 200 mM arginine LUB1 appears much more dispersed and globular.

Discussion

This study demonstrated that ionic environment regulates the aggregation and lubricating efficiency of lubricin mutants. LUB:1 in PBS lubricin coated the silicon surface unevenly and formed large aggregates. In 200 mM NaCl and 200 mM arginine individual LUB:1 strands could be identified, particularly in arginine, and the absorbed protein appeared more evenly distributed and lacked the large scale clumped features seen in PBS.

LUB:1 lubricated native articular cartilage in the presence of PBS, arginine, and NaCl with overall similar dose responses, however the LUB:1 concentration required to affect the drop in μ_{eq} was less than a third in the solutions that inhibited aggregation and produced even coatings of the molecule. These results are the first to show that changes in aggregation behavior induced by ionic environment affect the lubricating ability of lubricin mutants.

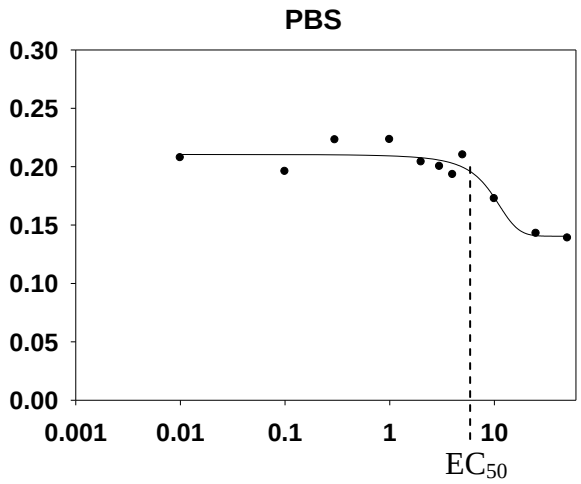

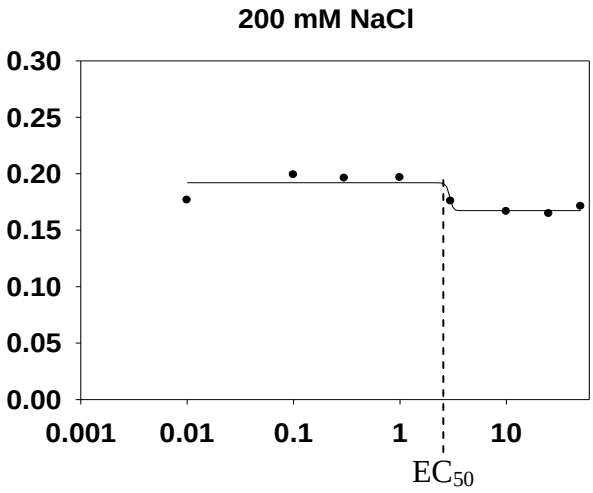

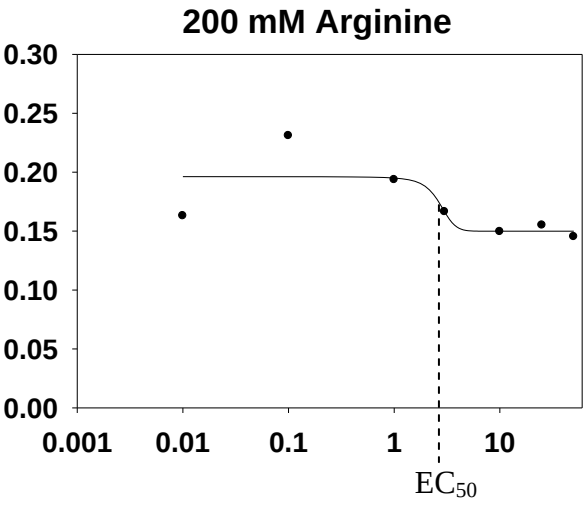

f = min + (max-min)/(1+10^((logEC50-x)*Hillslope))

	R^2	Min	Max	$logEC_{50}$
PBS	**0.900**	**0.14**	**0.21**	**9.36**
NaCl	**0.755**	**0.17**	**0.19**	**2.93**
Arg	**0.575**	**0.15**	**0.20**	**2.70**

Figure A 4 μ_{eq} vs. LUB1 (μg/ml) concentration for LUB1 in a) PBS, b) NaCl and c) arginine. Solid line is four parameter sigmoidal fit and dotted lines are EC_{50}. d) Coefficients of four-parameter sigmoidal fits for the three buffers.

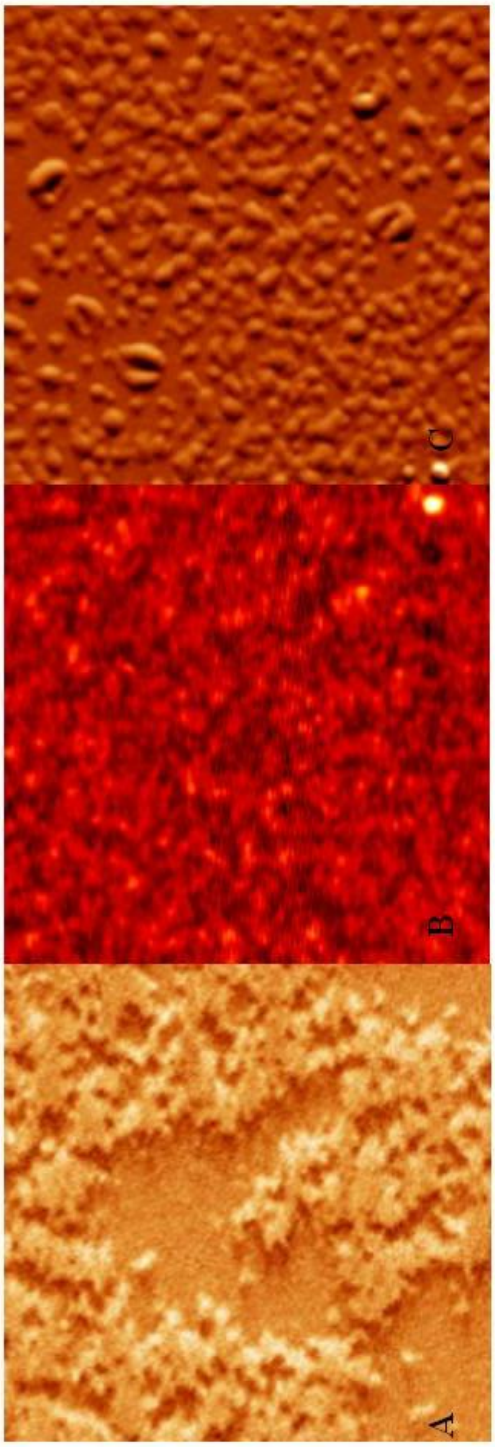

Figure A 5 1 μm ×1 μm AFM images of LUB1 (a) in PBS, (b) in NaCl, and (c) in arginine.

D. PROFILOMERY DATA AND OPERATION FOR CARTILAGINOUS TISSUES

Standard operating procedure to take profilometry pictures of articular cartilage:

Pre-imaging prep

1. Ensure cartilage has any synovial fluid or other agent removed by rinsing in PBS and allowing to equilibrate in PBS minimum 20 minutes
2. Prep profilometry kit including:
    a. samples
    b. tweezers
    c. Petri dish for holding sample during imaging
    d. gloves
    e. KimWipes
3. Log into CCMR Coral Remote and reserve profilometer
4. In Bard basement profilometry room turn on: computer, monitors, translation stage, TV visual, microscope, and light source
5. Open Win XAM software, SPIP imaging opens automatically

Sample preparation in microscope room

1. Load cartilage recipe "nataliecartilage.rcp" containing optimized imaging parameters for cartilage
2. Remove cartilage sample from PBS bath and place articular side up on a KimWipe, allowing fluid to soak into the tissue
3. With another KimWipe GENTLY pat the articular surface, taking extreme care NOT to rub the articular surface
4. Place on Petri dish and place under objective
5. Wait a few seconds to allow surface liquid to evaporate

Focusing profilometer

1. On scope, close F-stop and increase the light to maximum. On imaging screen a red polyhedron will appear against a black background
2. Shift the Z of the scope until
    a. Light is a focused dot on the cartilage surface
    b. The streaks of light that will expand and contract into the polyhedron as you translate the Z focuses into the polyhedron itself as much as possible and not the black background
3. Increase the F-stop until the red polyhedron expands to fill the entire screen. Continue just until filled, not beyond
4. Decrease light until a few red lines/dot remain and no longer fills the entire screen

Imaging

1. Level the cartilage by turning the X and Y tilt knobs
2. Use the translation lever to move around the cartilage surface
3. Hit "Acquire"

4. Image will automatically be rendered in SPIP, which contains surface roughness and other analysis tools
5. Carry out as many scans as required, but within 5 minutes. If longer imaging time is necessary, allow the sample to rehydrate before drying it again and continuing scans.

The following pages present, in order, examples of healthy neonatal bovine cartilage and of the polished glass counterface used in friction testing, a table of cartilage roughness values from the current literature, and a gallery of sample healthy bovine cartilage images taken using the above procedure.

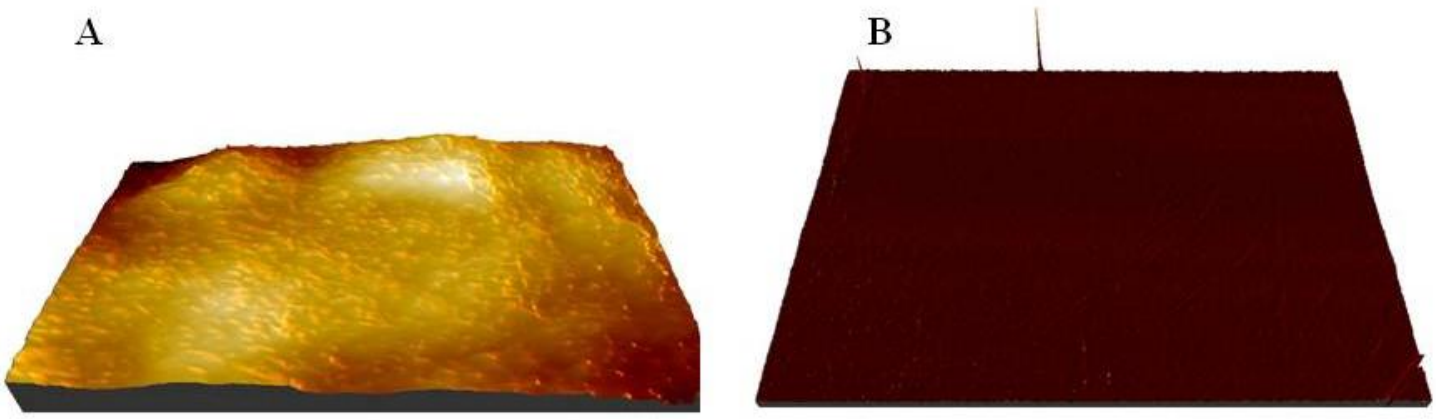

Figure A 6 Profilometry images of A) healthy bovine cartilage and B) polished glass.

Average roughness of articular surface of healthy native cartilage		
Roughness	**Study**	**Measurement technique**
1.6 μm	Forster 1999[45]	Stylus profilometry
0.8 μm	Forster 1999[45]	Laser profilometry
1.06 μm	Graindorge 2006[54]	Laser profilometry
0.46 μm	Park 2004[100]	Atomic force microscopy
0.20 – 0.325 μm	Coles 2008[23]	Atomic force microscopy
0.7 – 2.0 μm	Current work	Laser profilometry

Table A 2 Sample roughness values of healthy native articular cartilage from the current literature

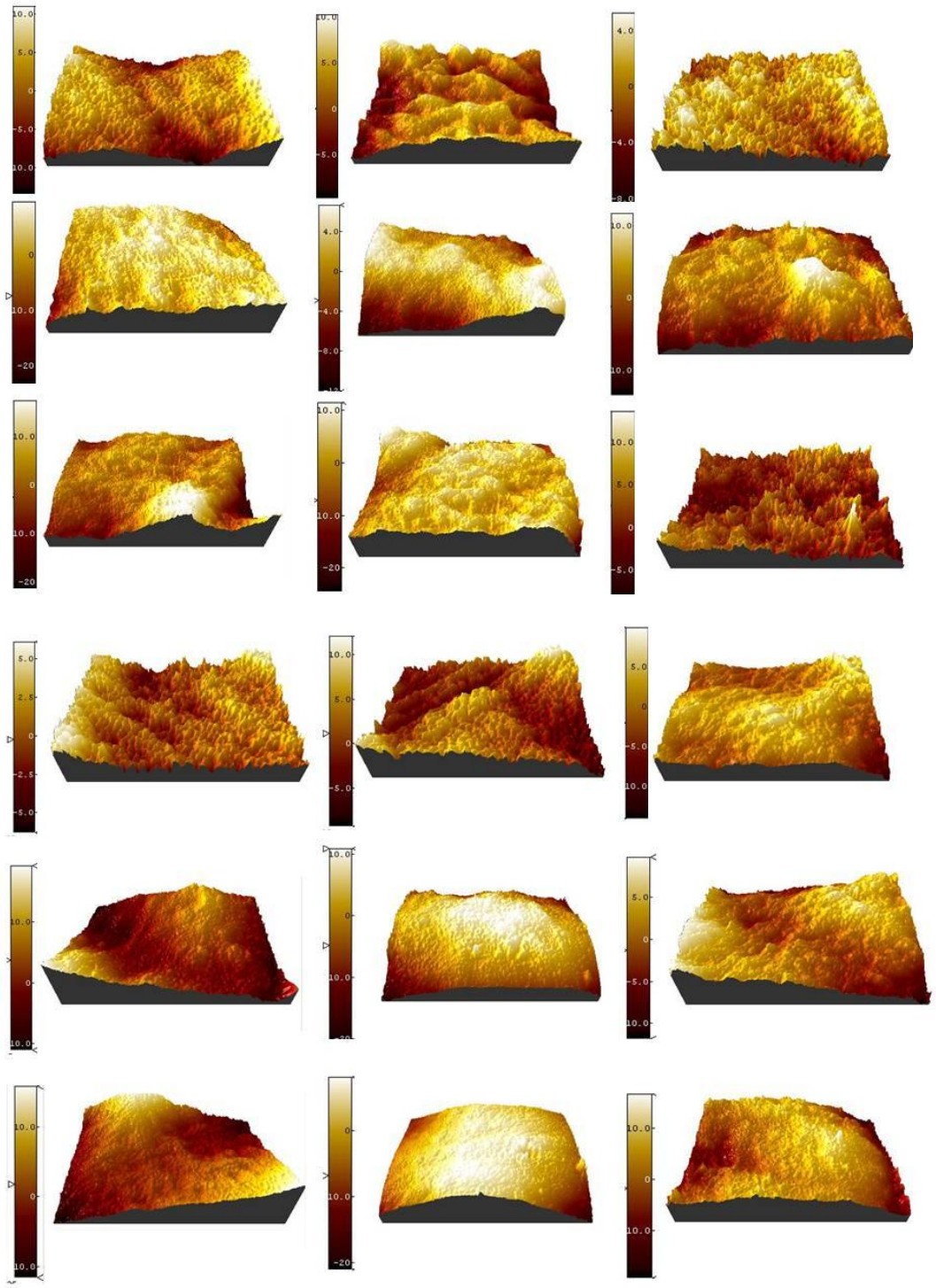

Figure A 7 3D profilometry images of healthy bovine cartilage

REFERENCES

1. Ahmed A, Burke D. In-vitro measurement of static pressure distribution in synovial joints—Part I: Tibial surface of the knee. *J Biomech Eng.* 1983;105:216-225.
2. Babalola OM, Bonassar LJ. Parametric finite element analysis of physical stimuli resulting from mechanical stimulation of tissue engineered cartilage. *J Biomech Eng.* 2009;131(6):061014.
3. Barnett CH. Measurement and interpretation of synovial fluid viscosities. *Ann Rheum Dis.* 1958;17(2):229-233.
4. Barrett M. Effects of a Permeable Friction Course on Highway Runoff. *J Irrig Drain Eng.* 2008;134:646-651.
5. Basalo IM, Chen FH, Hung CT, Ateshian GA. Frictional response of bovine articular cartilage under creep loading following proteoglycan digestion with chondroitinase ABC. *J Biomech Eng.* 2006;128(1):131-134.
6. Bell CJ, Ingham E, Fisher J. Influence of hyaluronic acid on the time-dependent friction response of articular cartilage under different conditions. *Proc Inst Mech Eng H.* 2006;220(1):23-31.
7. Bonassar LJ, Frank EH, Murray JC, Paguio CG, Moore VL, Lark MW, Sandy JD, Wu JJ, Eyre DR, Grodzinsky AJ. Changes in cartilage composition and physical properties due to stromelysin degradation. *Arthritis Rheum.* 1995;38(2):173-183.
8. Boschetti F, Peretti GM. Tensile and compressive properties of healthy and osteoarthritic human articular cartilage. *Biorheology.* 2008;45(3-4):337-344.
9. Brandt KD, Smith GN, Jr., Simon LS. Intraarticular injection of hyaluronan as treatment for knee osteoarthritis: what is the evidence? *Arthritis Rheum.* 2000;43(6):1192-1203.

10. Brandt KD, Smith GN, Simon LS. Intraarticular injection of hyaluronan as treatment for knee osteoarthritis. *Arthritis & Rheumatism.* 2000;43(6):1192-1203.

11. Brophy RH, Cottrell J, Rodeo SA, Wright TM, Warren RF, Maher SA. Implantation of a synthetic meniscal scaffold improves joint contact mechanics in a partial meniscectomy cadaver model. *J Biomed Mater Res A.* 2010;92A(3):1154-1167.

12. Buckwalter JA. Sports, joint injury, and posttraumatic osteoarthritis. *J Orthop Sports Phys Ther.* 2003;33(10):578-588.

13. Buckwalter JA, Brown T. Joint Injury, Repair and Remodeling. *Clinical Orthopaedics and Related Research.* 2004;423:7-16.

14. Burks RT, Metcalf MH, Metcalf RW. Fifteen-year follow-up of arthroscopic partial meniscectomy. *Arthroscopy.* 1997;13(6):673-679.

15. Buschmann MD, Grodzinsky AJ. A molecular model of proteoglycan-associated electrostatic forces in cartilage mechanics. *J Biomech Eng.* 1995;117(2):179-192.

16. Caligaris M, Ateshian GA. Effects of sustained interstitial fluid pressurization under migrating contact area, and boundary lubrication by synovial fluid, on cartilage friction. *Osteoarthritis Cartilage.* 2008;16:1220-1227.

17. Caligaris M, Canal CE, Ahmad CS, Gardner TR, Ateshian GA. Investigation of the frictional response of osteoarthritic human tibiofemoral joints and the potential beneficial tribological effect of healthy synovial fluid. *Osteoarthritis Cartilage.* 2009;17(10):1327-1332.

18. Chan SM, Neu CP, Duraine G, Komvopoulos K, Reddi AH. Atomic force microscope investigation of the boundary-lubricant layer in articular cartilage. *Osteoarthritis Cartilage.* 2010;18(7):956-963.

19. Chang DP, Abu-Lail NI, Guilak F, Jay GD, Zauscher S. Conformational mechanics, adsorption, and normal force interactions of lubricin and hyaluronic acid on model surfaces. *Langmuir.* 2008;24(4):1183-1193.

20. Chang SC, Hoang B, Thomas JT, Vukicevic S, Luyten FP, Ryba NJ, Kozak CA, Reddi AH, Moos M, Jr. Cartilage-derived morphogenetic proteins. New members of the transforming growth factor-beta superfamily predominantly expressed in long bones during human embryonic development. *J Biol Chem.* 1994;269(45):28227-28234.

21. Chen CT, Bhargava M, Lin PM, Torzilli PA. Time, stress, and location dependent chondrocyte death and collagen damage in cyclically loaded articular cartilage. *J Orthop Res.* 2003;21(5):888-898.

22. Christoforakis J, Pradhan R, Sanchez-Ballester J, Hunt N, Strachan RK. Is there an association between articular cartilage changes and degenerative meniscus tears? *Arthroscopy.* 2005;21:1366-1369.

23. Coles JM, Blum JJ, Jay GD, Darling EM, Guilak F, Zauscher S. In situ friction measurement on murine cartilage by atomic force microscopy. *J Biomech.* 2008;41(3):541-548.

24. Cox JS, Nye CE, Schaefer WW, Woodstein IJ. The Degenerative Effects of Partial and Total Resection of the Medial Meniscus in Dogs' Knees. *Clin Orthop Relat Res.* 1975;109:178-183.

25. Crocketta R, Roosa S, Rossbacha P, Dorab C, Bornb W, Troxler H. Imaging of the surface of human and bovine articular cartilage with ESEM and AFM. *Tribology Letters.* 2005;19(4):311-317.

26. Dahl LB, Dahl IM, Engstrom-Laurent A, Granath K. Concentration and molecular weight of sodium hyaluronate in synovial fluid from patients with rheumatoid arthritis and other arthropathies. *Ann Rheum Dis.* 1985;44(12):817-822.

27. Darling EM, Athanasiou KA. Retaining zonal chondrocyte phenotype by means of novel growth environments. *Tissue Eng.* 2005;11(3-4):395-403.

28. DiMicco MA, Patwari P, Siparsky PN, Kumar S, Pratta MA, Lark MW, Kim YJ, Grodzinsky AJ. Mechanisms and kinetics of glycosaminoglycan release following in vitro cartilage injury. *Arthritis Rheum.* 2004;50(3):840-848.

29. Eisenberg SR, Grodzinsky AJ. Swelling of articular cartilage and other connective tissues: electromechanochemical forces. *J Orthop Res.* 1985;3(2):148-159.

30. Elsaid K, Jay G, Warman ML, Rhee DK, Chichester CO. Association of Articular Cartilage Degradation and Loss of Boundary-Lubricating Ability of Synovial Fluid Following Injury and Inflammatory Arthritis. *Arthritis & Rheumatism.* 2005;52(6):1746-1755.

31. Elsaid KA, Chichester CO. Review: Collagen markers in early arthritic diseases. *Clin Chim Acta.* 2006;365(1-2):68-77.

32. Elsaid KA, Fleming BC, Oksendahl HL, Machan JT, Fadale PD, Hulstyn MJ, Shalvoy R, Jay GD. Decreased lubricin concentrations and markers of joint inflammation in the synovial fluid of patients with anterior cruciate ligament injury. *Arthritis Rheum.* 2008;58(6):1707-1715.

33. Elsaid KA, Jay GD, Chichester CO. Reduced expression and proteolytic susceptibility of lubricin/superficial zone protein may explain early elevation in the coefficient of friction in the joints of rats with antigen-induced arthritis. *Arthritis Rheum.* 2007;56(1):108-116.

34. Elsaid KA, Jay GD, Warman ML, Rhee DK, Chichester CO. Association of articular cartilage degradation and loss of boundary-lubricating ability of synovial fluid following injury and inflammatory arthritis. *Arthritis Rheum.* 2005;52(6):1746-1755.

35. Englert C, McGowan KB, Klein TJ, Giurea A, Schumacher BL, Sah RL. Inhibition of integrative cartilage repair by proteoglycan 4 in synovial fluid. *Arthritis Rheum.* 2005;52(4):1091-1099.

36. Ewers BJ, Dvoracek-Driksna D, Orth MW, Haut RC. The extent of matrix damage and chondrocyte death in mechanically traumatized articular cartilage explants depends on rate of loading. *J Orthop Res.* 2001;19(5):779-784.

37. Farquhar T, Xia Y, Mann K, Bertram J, Burton-Wurster N, Jelinski L, Lust G. Swelling and fibronectin accumulation in articular cartilage explants after cyclical impact. *J Orthop Res.* 1996;14(3):417-423.

38. Feller J. Anterior cruciate ligament rupture: is osteoarthritis inevitable? *Br J Sports Med.* 2004;38(4):383-384.

39. Flannery C, Hughes C, Schumacher B, Tudor D, Aydelotte MB, Kuettner KE, Caterson B. Articular cartilage superficial zone protein (SZP) is homologous to megakaryocyte stimulating factor precursor and is a multifunctional proteoglycan with potential growth promoting, cytoprotective and lubricating properties in cartilage metabolism. *Biochem Biophys Res Commun* 1999;234:535–541.

40. Flannery C, Zollner R, Corcoran C, Jones A, Root A, Rivera-Bermúdez M, Blanchet T, Gleghorn J, Bonassar L, Bendele A, Morris E, Glasson S. Prevention of cartilage degeneration in a rat model of osteoarthritis by intraarticular treatment with recombinant lubricin. *Arthritis Rheum.* 2009;60(3):840-847.

41. Flannery CR, Hughes CE, Schumacher BL, Tudor D, Aydelotte MB, Kuettner KE, Caterson B. Articular cartilage superficial zone protein (SZP) is homologous to megakaryocyte stimulating factor precursor and Is a multifunctional proteoglycan with potential growth-promoting, cytoprotective, and lubricating properties in cartilage metabolism. *Biochem Biophys Res Commun.* 1999;254(3):535-541.

42. Fleming BC, Hulstyn MJ, Oksendahl HL, Fadale PD. Ligament Injury, Reconstruction and Osteoarthritis. *Curr Opin Orthop.* 2005;16(5):354-362.

43. Forsey RW, Fisher J, Thompson J, Stone MH, Bell C, Ingham E. The effect of hyaluronic acid and phospholipid based lubricants on friction within a human cartilage damage model. *Biomaterials.* 2006;27(26):4581-4590.

44. Forster H, Fisher J. The influence of loading time and lubricant on the friction of articular cartilage. *Proc Inst Mech Eng H.* 1996;210(2):109-119.

45. Forster H, Fisher J. The influence of continuous sliding and subsequent surface wear on the friction of articular cartilage. *Proc Inst Mech Eng H* 1999;213:329-345.

46. Galley N, Chen S, Frank E, Flannery C, Grodzinsky A, Bonassar L. Role of Lubricant in Articular Cartilage Surface Damage and Frictional Changes After Injurious Compression. Paper presented at: Orthopaedic Research Society, 2010; New Orleans.

47. Galley NK, Gleghorn JP, Rodeo S, Warren RF, Maher SA, Bonassar LJ. Frictional Properties of the Meniscus Improve After Scaffold-augmented Repair of Partial Meniscectomy: A Pilot Study. *Clin Orthop Relat Res.* 2011;469(10):2817-2823.

48. Gleghorn JP, Bonassar LJ. Lubrication mode analysis of articular cartilage using Stribeck Surfaces. *J Biomech.* 2008;41(9):1910-1918.

49. Gleghorn JP, Doty SB, Warren RF, Wright TM, Maher SA, Bonassar LJ. Analysis of Frictional Behavior and Changes in Morphology Resulting from Cartilage Articulation with Porous Poyurethane Foams. *J Orthop Res.* 2010.

50. Gleghorn JP, Jones AR, Flannery CR, Bonassar LJ. Boundary mode frictional properties of engineered cartilaginous tissues. *Eur Cell Mater.* 2007;14:20-28; discussion 28-29.

51. Gleghorn JP, Jones AR, Flannery CR, Bonassar LJ. Alteration of articular cartilage frictional properties by transforming growth factor beta, interleukin-1beta, and oncostatin M. *Arthritis Rheum.* 2009;60(2):440-449.

52. Gleghorn JP, Jones ARC, Flannery CR, Bonassar LJ. Boundary Mode Lubrication of Articular Cartilage by Recombinant Human Lubricin. *J Orthop Res.* 2009;27(6):771-777.

53. Graindorge S, Ferrandex W, Ingham E, Jin Z, Twigg P, Fisher J. The role of the surface amorphous layer of articular cartilage in joint lubrication. *IMechE.* 2006;220:597-607.

54. Graindorge S, Ferrandez W, Ingham E, Jin Z, Twigg P, Fisher J. The role of the surface amorphous layer of articular cartilage in joint lubrication. *Proc Inst Mech Eng H.* 2006;220(5):597-607.

55. Greene GW, Banquy X, Lee DW, Lowrey DD, Yu J, Israelachvili JN. Adaptive mechanically controlled lubrication mechanism found in articular joints. *Proc Natl Acad Sci U S A.* 2011;108(13):5255-5259.

56. He Y, Winnubst L, Burggraaf AJ, Verweij H. Influence of Porosity on Friction and Wear of Tetragonal Zirconia Polycrystal. *J. Am. Ceram. Soc.* 1997;80(8):377-380.

57. Heijkants RGJC, van Calck RV, de Groot JH, Pennings AJ, Schouten AJ. Design, synthesis and properties of a degradable polyurethane scaffold for meniscus regeneration. *J Mater Sci Mater Med.* 2004;15:423-427.

58. Hersey MD. *Theory of Lubrication*. New York: Wiley; 1936.

59. Ikegawa S, Sano M, Koshizuka Y, Nakamura Y. Isolation, characterization and mapping of the mouse and human PRG4 (proteoglycan 4) genes. *Cytogenet Cell Genet.* 2000;90(3-4):291-297.

60. Janusz MJ, Bendele AM, Brown KK, Taiwo YO, Hsieh L, Heitmeyer SA. Induction of osteoarthritis in the rat by surgical tear of the meniscus: Inhibition of joint damage by a matrix metalloproteinase inhibitor. *Osteoarthritis Cartilage.* 2002;10(10):785-791.

61. Jay G. Lubricin and surfacing of articular joints. *Current Opinion in Orthopaedics.* 2004;15:355–359.

62. Jay GD. Lubricin and surfacing of articular joints. *Curr Opin Orthop.* 2004;15:355-359.

63. Jay GD, Britt DE, Cha CJ. Lubricin is a product of megakaryocyte stimulating factor gene expression by human synovial fibroblasts. *J Rheumatol.* 2000;27(3):594-600.

64. Jay GD, Elsaid KA, Zack J, Robinson K, Trespalacios F, Cha CJ, Chichester CO. Lubricating ability of aspirated synovial fluid from emergency department patients with knee joint synovitis. *J Rheumatol.* 2004;31(3):557-564.

65. Jay GD, Fleming BC, Watkins BA, McHugh KA, Anderson SC, Zhang LX, Teeple E, Waller KA, Elsaid KA. Prevention of cartilage degeneration and restoration of chondroprotection by lubricin tribosupplementation in the rat following anterior cruciate ligament transection. *Arthritis Rheum.* 2010;62(8):2382-2391.

66. Jay GD, Haberstroh K, Cha CJ. Comparison of the boundary-lubricating ability of bovine synovial fluid, lubricin, and Healon. *J Biomed Mater Res.* 1998;40(3):414-418.

67. Jay GD, Harris DA, Cha CJ. Boundary lubrication by lubricin is mediated by O-linked beta(1-3)Gal-GalNAc oligosaccharides. *Glycoconj J.* 2001;18(10):807-815.

68. Jay GD, Tantravahi U, Britt DE, Barrach HJ, Cha CJ. Homology of lubricin and superficial zone protein (SZP): products of megakaryocyte stimulating factor (MSF) gene expression by human synovial fibroblasts and articular chondrocytes localized to chromosome 1q25. *J Orthop Res.* 2001;19(4):677-687.

69. Jay GD, Torres JR, Warman ML, Laderer MC, Breuer KS. The role of lubricin in the mechanical behavior of synovial fluid. *Proc Natl Acad Sci U S A.* 2007;104(15):6194-6199.

70. Jones AR, Chen S, Chai DH, Stevens AL, Gleghorn JP, Bonassar LJ, Grodzinsky AJ, Flannery CR. Modulation of lubricin biosynthesis and tissue surface properties following cartilage mechanical injury. *Arthritis Rheum.* 2009;60(1):133-142.

71. Jones AR, Flannery CR. Bioregulation of lubricin expression by growth factors and cytokines. *Eur Cell Mater.* 2007;13:40-45; discussion 45.

72. Jones AR, Gleghorn JP, Hughes CE, Fitz LJ, Zollner R, Wainwright SD, Caterson B, Morris EA, Bonassar LJ, Flannery CR. Binding and localization of recombinant lubricin to articular cartilage surfaces. *J Orthop Res.* 2007;25(3):283-292.

73. Jones ARC, Chen S, Chai DH, Stevens AL, Gleghorn JP, Bonassar LJ, Grodzinsky AJ, Flannery CR. Modulation of Lubricin Biosynthesis and Tissue Surface Properties Following Cartilage Mechanical Injury. *Arthritis & Rheumatism.* 2009;60(1):133-142.

74. Joshi MD, Suh JK, Marui T, Woo SL. Interspecies variation of compressive biomechanical properties of the meniscus. *J Biomed Mater Res.* 1995;29(7):823-828.

75. Khetia EA, McKeon BP. Meniscal allografts: biomechanics and techniques. *Sports Med Arthrosc.* 2007;15(3):114-120.

76. Kim YJ, Bonassar LJ, Grodzinsky AJ. The role of cartilage streaming potential, fluid flow and pressure in the stimulation of chondrocyte biosynthesis during dynamic compression. *J Biomech.* 1995;28(9):1055-1066.

77. Kirwan JR, Rankin E. Intra-articular therapy in osteoarthritis. *Baillieres Clin Rheumatol.* 1997;11(4):769-794.

78. Klein TJ, Chaudhry M, Bae WC, Sah RL. Depth-dependent biomechanical and biochemical properties of fetal, newborn, and tissue-engineered articular cartilage. *J Biomech.* 2007;40(1):182-190.

79. Klein TJ, Schumacher BL, Schmidt TA, Li KW, Voegtline MS, Masuda K, Thonar EJ, Sah RL. Tissue engineering of stratified articular cartilage from chondrocyte subpopulations. *Osteoarthritis Cartilage.* 2003;11(8):595-602.

80. Krishnan R, Kopacz M, Ateshian GA. Experimental verification of the role of interstitial fluid pressurization in cartilage lubrication. *J Orthop Res.* 2004;22(3):565-570.

81. Krueger JA, Thisse P, Ewers BJ, Dvoracek-Driksna D, Orth MW, Haut RC. The extent and distribution of cell death and matrix damage in impacted chondral explants varies with the presence of underlying bone. *J Biomech Eng.* 2003;125(1):114-119.

82. Kumar P, Oka M, Toguchida J, Kobayashi M, Uchida E, Nakamura T, Tanaka K. Role of uppermost superficial surface layer of articular cartilage in the lubrication mechanism of joints. *J Anat.* 2001;199(Pt 3):241-250.

83. Kurz B, Jin M, Patwari P, Cheng DM, Lark MW, Grodzinsky AJ. Biosynthetic response and mechanical properties of articular cartilage after injurious compression. *J Orthop Res.* 2001;19(6):1140-1146.

84. Kurz B, Jin M, Patwari P, Cheng DM, Lark MW, Grodzinsky AJ. Biosynthetic response and mechanical properties of articular cartilage after injurious compression. *Journal of Orthopaedic Research.* 2001;19:1140-1146.

85. Kurz B, Lemke AK, Fay J, Pufe T, Grodzinsky AJ, Schunke M. Pathomechanisms of cartilage destruction by mechanical injury. *Ann Anat.* 2005;187(5-6):473-485.

86. LeBaron RG, Athanasiou KA. Ex vivo synthesis of articular cartilage. *Biomaterials.* 2000;21(24):2575-2587.

87. Lee JH, Fitzgerald JB, Dimicco MA, Grodzinsky AJ. Mechanical injury of cartilage explants causes specific time-dependent changes in chondrocyte gene expression. *Arthritis Rheum.* 2005;52(8):2386-2395.

88. Li G, Moses JM, Papannagari R, Pathare NP, DeFrate LE, Gill TJ. Anterior cruciate ligament deficiency alters the in vivo motion of the tibiofemoral cartilage contact points in both the anteroposterior and mediolateral directions. *J Bone Joint Surg Am.* 2006;88(8):1826-1834.

89. Loening AM, James IE, Levenston ME, Badger AM, Frank EH, Kurz B, Nuttal ME, Hung H-H, Blake SM, Grodzinsky AJ, Lark MW. Injurious mechanical compression of bovine articular cartilage induces chondrocyte apoptosis. *Archives of Biochemistry and Biophysics.* 2000;381(2):205-212.

90. Loening AM, James IE, Levenston ME, Badger AM, Frank EH, Kurz B, Nuttall ME, Hung HH, Blake SM, Grodzinsky AJ, Lark MW. Injurious mechanical compression of bovine articular cartilage induces chondrocyte apoptosis. Arch Biochem Biophys. 2000;381(2):205-212.

91. Lohmander LS, Roos H, Dahlberg L, Hoerrner LA, Lark MW. Temporal patterns of stromelysin-1, tissue inhibitor, and proteoglycan fragments in human knee joint fluid after injury to the cruciate ligament or meniscus. J Orthop Res. 1994;12(1):21-28.

92. Marcelino J, Carpten JD, Suwairi WM, Gutierrez OM, Schwartz S, Robbins C, Sood R, Makalowska I, Baxevanis A, Johnstone B, Laxer RM, Zemel L, Kim CA, Herd JK, Ihle J, Williams C, Johnson M, Raman V, Alonso LG, Brunoni D, Gerstein A, Papadopoulos N, Bahabri SA, Trent JM, Warman ML. CACP, encoding a secreted proteoglycan, is mutated in camptodactyly-arthropathy-coxa vara-pericarditis syndrome. Nat Genet. 1999;23(3):319-322.

93. Marshall KW. Intra-articular hyaluronan therapy. Curr Opin Rheumatol. 2000;12(5):468-474.

94. McCann L, Ingham E, Jin Z, Fisher J. Influence of the meniscus on friction and degradation of cartilage in the natural knee joint. Osteoarthritis Cartilage. 2009;17:995-1000.

95. Morrell KC, Hodge WA, Krebs DE, Mann RW. Corroboration of in vivo cartilage pressures with implications for synovial joint tribology and osteoarthritis causation. Proc Natl Acad Sci U S A. 2005;102(41):14819-14824.

96. Neu CP, Reddi AH, Komvopoulos K, Schmid TM, Di Cesare PE. Increased friction coefficient and superficial zone protein expression in patients with advanced osteoarthritis. Arthritis Rheum. 2010;62(9):2680-2687.

97. Newberry WN, Garcia JJ, Mackenzie CD, Decamp CE, Haut RC. Analysis of acute mechanical insult in an animal model of post-traumatic osteoarthrosis. J Biomech Eng. 1998;120(6):704-709.

98. Nguyen QT, Wong BL, Chun J, Yoon YC, Talke FE, Sah RL. Macroscopic assessment of cartilage shear: effects of counter-surface roughness, synovial fluid lubricant, and compression offset. J Biomech. 2010;43(9):1787-1793.

99. Niikura T, Reddi AH. Differential regulation of lubricin/superficial zone protein by transforming growth factor beta/bone morphogenetic protein superfamily members in articular chondrocytes and synoviocytes. Arthritis Rheum. 2007;56(7):2312-2321.

100. Park S, Costa KD, Ateshian GA. Microscale frictional response of bovine articular cartilage from atomic force microscopy. J Biomech. 2004;37(11):1679-1687.

101. Patwari P, Cheng DM, Cole AA, Kuettner KE, Grodzinsky AJ. Analysis of the relationship between peak stress and proteoglycan loss following injurious compression of human post-mortem knee and ankle cartilage. Biomech Model Mechanobiol. 2007;6(1-2):83-89.

102. Patwari P, Cook MN, DiMicco MA, Blake SM, James IE, Kumar S, Cole AA, Lark MW, Grodzinsky AJ. Proteoglycan degradation after injurious compression of bovine and human articular cartilage in vitro: interaction with exogenous cytokines. Arthritis Rheum. 2003;48(5):1292-1301.

103. Ramrattan NN, Heijkants RGJC, Tienen TGv, Schouten AJ, Veth RPH, Buma P. Assessment of Tissue Ingrowth Rates in Polyurethane Scaffolds for Tissue Engineering. Tissue Eng. 2005;11(7/8):1212-1223.

104. Reddi AH. Role of morphogenetic proteins in skeletal tissue engineering and regeneration. Nat Biotechnol. 1998;16(3):247-252.

105. Rees SG, Davies JR, Tudor D, Flannery CR, Hughes CE, Dent CM, Caterson B. Immunolocalisation and expression of proteoglycan 4 (cartilage superficial zone proteoglycan) in tendon. Matrix Biol. 2002;21(7):593-602.

106. Repo RU, Finlay JB. Survival of articular cartilage after controlled impact. J Bone Joint Surg Am. 1977;59(8):1068-1076.

107. Repo RU, Finlay JB. Survival of articular cartilage after controlled impact. J Bone Joint Surg Am. 1977;59:1068-1076.

108. Rhee DK, Marcelino J, Baker M, Gong Y, Smits P, Lefebvre V, Jay GD, Stewart M, Wang H, Warman ML, Carpten JD. The secreted glycoprotein lubricin protects cartilage surfaces and inhibits synovial cell overgrowth. J Clin Invest. 2005;115(3):622-631.

109. Roberts BJ, Unsworth A, Mia N. Modes of lubrication in human hip joints. Ann Rheum Dis. 1982;41:217-224.

110. Roos EM. Joint injury causes knee osteoarthritis in young adults. Curr Opin Rheumatol. 2005;17(2):195-200.

111. Roos H, Laurbn M, Adalberth T, Roos EM, Jonsson K, Lohmander S. Knee osteoarthritis after meniscectomy: prevalence of radiographic changes after twenty-one years, compared with matched controls. Arthritis Rheum. 1998;41:687–693.

112. Schmid TM, Lindley KM, Su J-L, Soloveychik V, Madsen L, Block J, Kuettner KE, Schumacher BL. Superficial zone protein (SZP) is an abundant glycoprotein in human synovial fluid with lubricating properties. In: Hascall VC, Kuettner KE, eds. The Many Faces of Osteoarthritis; 2002:159-161.

113. Schmidt TA, Gastelum NS, Nguyen QT, Schumacher BL, Sah RL. Boundary lubrication of articular cartilage: role of synovial fluid constituents. Arthritis Rheum. 2007;56(3):882-891.

114. Schmidt TA, Sah RL. Effect of synovial fluid on boundary lubrication of articular cartilage. Osteoarthritis Cartilage. 2007;15(1):35-47.

115. Schumacher BL, Block JA, Schmid TM, Aydelotte MB, Kuettner KE. A novel proteoglycan synthesized and secreted by chondrocytes of the superficial zone of articular cartilage. Arch Biochem Biophys. 1994;311(1):144-152.

116. Schumacher BL, Hughes CE, Kuettner KE, Caterson B, Aydelotte MB. Immunodetection and partial cDNA sequence of the proteoglycan, superficial zone protein, synthesized by cells lining synovial joints. J Orthop Res. 1999;17(1):110-120.

117. Schumacher BL, Schmidt TA, Voegtline MS, Chen AC, Sah RL. Proteoglycan 4 (PRG4) synthesis and immunolocalization in bovine meniscus. J Orthop Res. 2005;23(3):562-568.

118. Shine KM, Spector M. The presence and distribution of lubricin in the caprine intervertebral disc. J Orthop Res. 2008;26(10):1398-1406.

119. Stevens AL, Wishnok JS, White FM, Grodzinsky AJ, Tannenbaum SR. Mechanical injury and cytokines cause loss of cartilage integrity and upregulate proteins associated with catabolism, immunity, inflammation, and repair. Mol Cell Proteomics. 2009;8(7):1475-1489.

120. Sun Y, Berger EJ, Zhao C, An KN, Amadio PC, Jay G. Mapping lubricin in canine musculoskeletal tissues. Connect Tissue Res. 2006;47(4):215-221.

121. Swann DA, Hendren RB, Radin EL, Sotman SL, Duda EA. The lubricating activity of synovial fluid glycoproteins. Arthritis Rheum. 1981;24(1):22-30.

122. Swann DA, Silver FH, Slayter HS, Stafford W, Shore E. The molecular structure and lubricating activity of lubricin isolated from bovine and human synovial fluids. Biochem J. 1985;2225:195-201.

123. Swann DA, Silver FH, Slayter HS, Stafford W, Shore E. The molecular structure and lubricating activity of lubricin isolated from bovine and human synovial fluids. Biochem J. 1985;225(1):195-201.

124. Swann DA, Slayter HS, Silver FH. The molecular structure of lubricating glycoprotein-I, the boundary lubricant for articular cartilage. J Biol Chem. 1981;256(11):5921-5925.

125. Tadmor R, Chen N, Israelachvili JN. Thin film rheology and lubricity of hyaluronic acid solutions at a normal physiological concentration. J Biomed Mater Res. 2002;61(4):514-523.

126. Teeple E, Elsaid K, Jay G, Zhang L, Badger G, Akelman M, Bliss T, Fleming B. Intra-Articular Lubricin with and without Hyaluronic Acid Delays the Progression of Post-Traumatic Arthritis in the Anterior Cruciate Ligament Deficient Rat Knee. Paper presented at: Orthopaedic Research Society, 2010; New Orleans.

127. Teeple E, Elsaid KA, Fleming BC, Jay GD, Aslani K, Crisco JJ, Mechrefe AP. Coefficients of friction, lubricin, and cartilage damage in the anterior cruciate ligament-deficient guinea pig knee. J Orthop Res. 2008;26(2):231-237.

128. Teeple E, Elsaid KA, Jay GD, Zhang L, Badger GJ, Akelman M, Bliss TF, Fleming BC. Effects of supplemental intra-articular lubricin and hyaluronic acid on the progression of

posttraumatic arthritis in the anterior cruciate ligament-deficient rat knee. Am J Sports Med. 2011;39(1):164-172.

129. Tetlow LC, Adlam DJ, Woolley DE. Matrix metalloproteinase and proinflammatory cytokine production by chondrocytes of human osteoarthritic cartilage: associations with degenerative changes. Arthritis Rheum. 2001;44(3):585-594.

130. Tienen TG, Heijkants RGJC, de Groot JH, Schouten AJ, Pennings AJ, Veth RPH, Buma P. Meniscal Replacement in Dogs. Tissue Regeneration in Two Different Materials With Similar Properties. J Biomed Mater Res B Appl Biomater. 2006;76(2):389-396.

131. Tienen TGv, Heijkants RGJC, Buma P, Groot JHd, Pennings AJ, Veth RPH. Tissue ingrowth and degradation of two biodegradable porous polymers with different porosities and pore sizes. Biomaterials. 2002;23:1731-1738.

132. Torzilli PA, Grigiene R, Borrelli J, Jr., Helfet DL. Effect of impact load on articular cartilage: cell metabolism and viability, and matrix water content. J Biomech Eng. 1999;121(5):433-441.

133. Torzilli PA, Grigiene R, Borrelli JJ, Helfet DL. Effect of impact load on articular cartilage: cell metabolism and viability, and matrix water content. Journal of Biomechanical Engineering. 1999;121:433-441.

134. Waddell DD, Bert JM. The use of hyaluronan after arthroscopic surgery of the knee. Arthroscopy. 2010;26(1):105-111.

135. Waller K, Zhang LX, Elsaid KA, Fleming B, Aslani K, Jay GD. The Role of Lubricin and Boundary Lubrication in the Prevention of Chondrocyte Apoptosis. Biomedical Engineering Engineering Society Annual Meeting. Hardford, CN; 2011.

136. Wei L, Fleming BC, Sun X, Teeple E, Wu W, Jay GD, Elsaid KA, Luo J, Machan JT, Chen Q. Comparison of differential biomarkers of osteoarthritis with and without posttraumatic injury in the Hartley guinea pig model. J Orthop Res. 2010;28(7):900-906.

137. Wong BL, Kim SH, Antonacci JM, McIlwraith CW, Sah RL. Cartilage shear dynamics during tibio-femoral articulation: effect of acute joint injury and tribosupplementation on synovial fluid lubrication. Osteoarthritis Cartilage. 2010;18(3):464-471.

138. Zappone B, Ruths M, Greene GW, Jay GD, Israelachvili JN. Adsorption, lubrication, and wear of lubricin on model surfaces: polymer brush-like behavior of a glycoprotein. Biophys J. 2007;92(5):1693-1708.